

Physiological determinants of nitrogen dynamics in response to genotype by management interactions in US maize hybrids

by

Javier Antonio Fernandez

B.S., National University of the Northeast, 2016

AN ABSTRACT OF A DISSERTATION

submitted in partial fulfillment of the requirements for the degree

DOCTOR OF PHILOSOPHY

Department of Agronomy
College of Agriculture

KANSAS STATE UNIVERSITY
Manhattan, Kansas

2021

Abstract

In maize (*Zea mays* L.), the largest staple crop in the world, nitrogen (N) represents a major limiting factor for productivity. However, improving N use efficiency (NUE) is still one of the most critical research issues to achieve food security in a context affected by climate change. This dissertation is structured in six chapters (Chapter 1, Introduction, and Chapter 6, Conclusions) outlining the agronomic and physiological traits associated with a better N utilization in US maize hybrids across Genotype \times Environment \times Management ($G \times E \times M$) conditions, with emphasis on the implications of long-term genetic selection. Chapter 2 presents a comprehensive meta-analysis on a diverse dataset assembled from field studies from 1983 until 2018 to compare early- versus late-season N (applied after tenth-leaf) fertilization effects on yield and N recovery efficiency. Results provided evidence for the lack of a main effect of late N application on yields but suggest the existence of crop growth conditions prone to a greater reproductive N uptake where this practice might be suitable. Throughout multiple field trials, Chapter 3-5 advanced in our understanding of how long-term genetic improvement has modified N dynamics across $G \times M$ scenarios. Chapter 3 proposes a novel N by carbon (C) framework to analyze and define key morpho-physiological traits of breeding interest that allow modern maize plants to achieve higher productivity and NUE. Results show both an earlier stem N remobilization and a decline in grain N concentration are key drivers of N utilization efficiency in modern hybrids. Chapter 4 documents the underlying fluxes of post-flowering N allocation and translocation dynamics behind genetic improvement over time in field-grown corn. This research suggests that direct selection for yield has indirectly favored N allocation to leaves in modern genotypes resulting in an improved post-flowering C accumulation. Finally, Chapter 5 explores historical changes in the contribution of grain weight and its physiological

characteristics to maize genetic progress. This research evidences a significant contribution of increments in grain weight in US maize but concludes the trade-off between grain number and weight poses a challenge for future yield progress.

Physiological determinants of nitrogen dynamics in response to genotype by management interactions in US maize hybrids

by

Javier Antonio Fernandez

B.S., National University of the Northeast, 2016

A DISSERTATION

submitted in partial fulfillment of the requirements for the degree

DOCTOR OF PHILOSOPHY

Department of Agronomy
College of Agriculture

KANSAS STATE UNIVERSITY
Manhattan, Kansas

2021

Approved by:

Major Professor
Ignacio A. Ciampitti

Copyright

© Javier Fernandez 2021.

Abstract

In maize (*Zea mays* L.), the largest staple crop in the world, nitrogen (N) represents a major limiting factor for productivity. However, improving N use efficiency (NUE) is still one of the most critical research issues to achieve food security in a context affected by climate change. This dissertation is structured in six chapters (Chapter 1, Introduction, and Chapter 6, Conclusions) outlining the agronomic and physiological traits associated with a better N utilization in US maize hybrids across Genotype \times Environment \times Management ($G \times E \times M$) conditions, with emphasis on the implications of long-term genetic selection. Chapter 2 presents a comprehensive meta-analysis on a diverse dataset assembled from field studies from 1983 until 2018 to compare early- versus late-season N (applied after tenth-leaf) fertilization effects on yield and N recovery efficiency. Results provided evidence for the lack of a main effect of late N application on yields but suggest the existence of crop growth conditions prone to a greater reproductive N uptake where this practice might be suitable. Throughout multiple field trials, Chapter 3-5 advanced in our understanding of how long-term genetic improvement has modified N dynamics across $G \times M$ scenarios. Chapter 3 proposes a novel N by carbon (C) framework to analyze and define key morpho-physiological traits of breeding interest that allow modern maize plants to achieve higher productivity and NUE. Results show both an earlier stem N remobilization and a decline in grain N concentration are key drivers of N utilization efficiency in modern hybrids. Chapter 4 documents the underlying fluxes of post-flowering N allocation and translocation dynamics behind genetic improvement over time in field-grown corn. This research suggests that direct selection for yield has indirectly favored N allocation to leaves in modern genotypes resulting in an improved post-flowering C accumulation. Finally, Chapter 5 explores historical changes in the contribution of grain weight and its physiological

characteristics to maize genetic progress. This research evidences a significant contribution of increments in grain weight in US maize but concludes the trade-off between grain number and weight poses a challenge for future yield progress.

Table of Contents

List of Figures	xi
List of Tables	xviii
Acknowledgements	xx
Dedication	xxi
Chapter 1 - Introduction	1
Chapter 2 - Late-season nitrogen fertilization on maize yield: A meta-analysis	4
Abstract	4
Introduction	5
Materials and methods	7
Data	7
Calculations and parameters evaluated	8
Data analysis	9
Results	12
Descriptive statistics of crop variables: a comparison between E_N and L_N	12
Late season application of N neither increased maize yields nor N efficiency indexes	14
Yield and N recovery efficiency are dependent on N nutrition index and post-silking N uptake	16
Discussion	18
Effect of late season fertilizer N applications on maize yields and REN	18
Relationship between post-silking N uptake and late season fertilizer N applications	23
Conclusions	24
Chapter 3 - Integrating nitrogen and water-soluble carbohydrates dynamics in maize: A comparison of hybrids from different decades	32
Abstract	32
Introduction	33
Materials and methods	36
Field experiments	36
Measurements and laboratory analyses	38
Statistical analysis and calculations	40

Results.....	42
Yield, yield components, and N uptake	42
Dynamics of N and WSC in stems and leaves.....	44
Grain N demand related to N and WSC remobilization from stems and leaves.....	46
Discussion.....	47
Conclusions.....	51
Chapter 4 - Post-silking ¹⁵ N labelling reveals an enhanced nitrogen allocation to leaves in modern maize (<i>Zea mays</i>) genotypes	58
Abstract.....	58
Introduction.....	59
Materials and methods	62
Field experiments and phenotypic determinations	62
Isotopic labelled fertilizer application and calculation of ¹⁵ N plant traits	64
Statistical analyses and calculations	65
Results.....	69
Discussion.....	72
Coordination between exogenous- and endogenous-N dynamics with N use efficiency	73
Carbon fixation as affected by adjustments in leaf N allocation and mobilization	74
Potential implications of N dynamics on the respiratory metabolism	76
Conclusions.....	78
Chapter 5 - Kernel weight contribution to genetic gain of maize: A global review and US case studies	82
Abstract.....	82
Introduction.....	83
Materials and methods	85
Systematic review	85
Case studies I – 2017 and 2018 field experiments.....	86
Case studies II – 2019 and 2020 field experiments	87
Phenotypic measurements and calculations.....	88
Statistical analysis	89
Results.....	92

Descriptive summary of historical changes in kernel weight	92
Effect of crop growth conditions on maize genetic gain	94
Physiological traits underpinning kernel weight genetic progress of USA – Pioneer ERA hybrids.....	95
Discussion.....	98
Chapter 6 - Final remarks	108
References.....	111
Appendix A - Chapter 2 - Figures and tables	137
Appendix B - Chapter 3 - Figures and tables.....	140
Appendix C - Chapter 4 - Figures and tables.....	142
Appendix D - Chapter 5 - Figures and tables	144
Appendix E - Chapter 5 - References for the literature review	146

List of Figures

Figure 2.1. Description of fertilizer nitrogen (N) management variables across the dataset. Upper section: A, B, and C) Relative frequency (%) of the number of N applications, method of N application, and N fertilizer source, respectively. Abbreviations: Zero N, no N applied; AA, anhydrous ammonia; AN, ammonium nitrate; AS, ammonium sulfate; CAN, calcium ammonium nitrate; UAN, urea ammonium nitrate. Lower section: D) Fertilizer N rates density distribution plot (kg ha^{-1}), and E) accumulated frequency for the two N-timing groups considered (E_N : Early N; L_N : Late N). Dashed vertical lines and values represent the mean N rates. Abbreviations: P, planting; Vn, vegetative (nth) stage; Rn, reproductive (nth) stage. 25

Figure 2.2. Forest plot summarizing a yield effect comparison between late-season and early-season N for each experiment. Effect sizes and 95% confidence intervals (CI) are expressed as a late-N effect ratio (percentage of grain yield variation in L_N / E_N) calculated as (6). Square symbols represent point estimates and whiskers depict their respective 95% CI. The weight of each study is expressed in percentage of the overall model and illustrated by the thickness of box and whiskers. RE = random effects model, Q = Cochran's Q test statistic; I^2 = I-square statistic. 26

Figure 2.3. Forest plot with aggregate summary effect sizes of the late-N effect ratio (%) for partial factor productivity (PFPN), fertilizer N recovery efficiency (REN), and agronomic efficiency of N (AEN), calculated as the percentage of variation in L_N to E_N ratio. Square symbols represent point estimates and whiskers depict their respective 95% CI. Means for each N-timing group (early and late N) and mean effect ratios are presented..... 26

Figure 2.4. (A) Relationship between Nitrogen Nutrition Index at silking (NNI_{SILKING}) and relative grain yield. Solid line represents a bilinear regression for the data. Model parameters (standard errors listed in parenthesis) are: $Y_1 = -0.11(0.09) + 1.15(0.12)X$ if $X < X_0 = 0.88(0.03)$, and $Y_2 = 0.89(0.01)$ if $X > 0.88(0.03)$; $R^2 = 0.73$. (B) Relationship between NNI_{SILKING} and $NU_{\text{Post-Silking}}$ (%). Solid line represents a quadratic function fitted for the data. Model parameters (standard errors in parenthesis) are: $Y = 166(18.63) - 341(43.79)X + 190(25.01)X^2$; $R^2 = 0.49$. Dashed line indicates X_0 of 4A fitted regression to differentiate N nutrition conditions. $NNI_{\text{SILKING}} > 1$ was differently shaded to illustrate a situation of no

N deficiency. N_A = N concentration of shoot biomass; N_C = critical N concentration (Plénet and Lemaire, 2000). 27

Figure 2.5. A) Density distribution plot for $NU_{\text{Post-Silking}}$ on a subset of the general database reporting N uptake information on N-fertilized cases (n=84). Dashed lines and colors are separating the data in lower, median, and upper 33.3th percentiles. Reported values are for lower and upper sections: \bar{X} = mean $NU_{\text{Post-Silking}}$ (%); n = number of observations; s = number of locations by years. At the bottom, mean grain yield values in kg ha^{-1} for E_N and L_N for the B) lower, and C) upper thirds on the post-silking N dataset (Supplementary Material, Table A.2). \bar{X} = means; N rate = fertilizer rates in kg ha^{-1} ; $NU_{\text{Post-silking}}$ = post-silking N uptake proportion in %. Different letters indicate significant differences at $P \leq 0.05$ 28

Figure 2.6. Bars representing fertilizer N recovery efficiency (REN) for each N group (E_N , n = 56; L_N , n = 44) (A). Whiskers represent standard errors (S.E.) for the mean. At the right, bars for pre-silking REN (Δkg pre-silking N uptake relative to $Z_N / \text{kg N}$ applied) (B), and post-silking REN (Δkg post-silking N uptake relative to $Z_N / \text{kg N}$ applied) (C) for E_N and L_N groups. Different letters indicate significant differences at $P \leq 0.05$ 29

Figure 3.1. Framework for explaining yield changes through the underlying N and carbohydrate mechanisms. Processes shaded in grey and dashed lines represent dynamics not evaluated in this study but incorporated in the interpretation of results. Δ : change between hybrids, WSC: water-soluble carbohydrates, SLN: specific leaf N, [N]: N concentration. 52

Figure 3.2. Relationships between yield (A), grain number (B), grain weight (C), and harvest index (D) with total N uptake for 3394 (closed symbols, solid lines) and P1197 (open symbols, dashed lines) under zero (squares) and full N (circles) treatments during 2017 and 2018 seasons. Symbols represent individual observations. Statistical significance for hybrid factor was tested and plotted accordingly at a level of $\alpha = 0.05$. Best Linear Unbiased Estimates and standard errors are reported in Supplementary Table S1. The best regression model was based on lower AIC values (Table S2). 53

Figure 3.3. Relationships between yield and post-flowering N uptake (A), post-flowering N uptake as a linear function of the grain number set at flowering (B) for both hybrids across two years \times two N conditions. Symbols represent observed values for 3394 (closed symbols) and P1197 (open symbols) under zero (squares) and full N (circles) treatments.

(C) Relationship between grain N content and grain weight, slope represents the grain [N] for each hybrid, throughout the grain filling period for the full N treatment. (D) Estimated grain yield and grain [N] for the two hybrids under two N levels in 2017 and 2018 seasons. Isolines represent levels of grain N yield from 50 to 250 kg ha⁻¹. For panel D, whiskers represent the standard errors of the means. 54

Figure 3.4. Evolution of N content in stem (A and B) and leaf (C and D) fractions, and of water-soluble carbohydrates (WSC) in stem (E-F) for 3394 (closed symbols) and P1197 (open symbols) maize hybrids, under zero (squares) and full N (circles) during 2017 and 2018 seasons. Arrows in (E) and (F) portray flowering (R1) stage. Vertical bars denote standard error of the mean. 55

Figure 3.5. Progression of leaf and stem N remobilized related to the grain N content during grain filling (A and C), for two hybrids under full N conditions in 2017 and 2018. Symbols represent the estimated mean values at each sampling time for 3394 (closed symbols and solid lines) and P1197 (open symbols and dashed lines) maize hybrids. Vertical bars represent standard error of the mean. Bivariate outliers (stars) were identified based on studentized residuals (values > 3). Overlapping symbols were offset horizontally for clarity (at a 0.1 value of x). Nitrogen remobilized was calculated by subtracting the N content at each sampling time from the estimated maximum N content around flowering for each hybrid × year. Temporal dynamics of SLN on a thermal time basis from flowering, for hybrids under full N treatment (B). Quantile regression (tau = 0.05) on the stem [N] during the post-flowering period to estimate the minimum stem [N] on each hybrid under full N (D). Model parameters for the quantile regression lines are: [3394: $y = 4.19 + (5.45 - 4.19) * \exp(-\exp(-4.37) * x)$], [P1197: $y = 3.30 + (5.19 - 3.30) * \exp(-\exp(-4.45) * x)$]. 55

Figure 3.6. General description for the simultaneous rates of grain growth (A), leaf and stem net N accumulation (B and C), stem net WSC accumulation (D), and plant N uptake (E) during post-flowering under full N conditions. Hybrids 3394 (closed symbols and solid lines) and P1197 (open symbols and dashed lines). Symbols represent the derivatives of the estimated models for grain dry matter, leaf N, stem N, stem WSC, and plant N accumulation in g m⁻² (respectively for A to E) at each sampling time. Positive values in B, C, and D show an accumulation of N or WSC in the tissue while negative magnitudes represent remobilization. 56

Figure 4.1. Framework to investigate post-silking N dynamics and grain N sources in maize. At a given time, N is absorbed and distributed across all stover and grain fractions (exogenous-N). Simultaneously, a fraction of N stored in these organs is remobilized and transported to the developing tissues (endogenous-N). This two-way flux model considers that grains are then sinks of (1) exogenous-N absorbed and directly allocated to grains and (2) endogenous-N translocated from stover, which derives from pre- and post-silking N initially allocated to stems, leaves, and cob-husks. 79

Figure 4.2. Relative allocation of ^{15}N (RA^{15}N) across plant organs throughout the post-silking period, across two maize hybrids (3394 and P1197) and two N fertilization levels (zero and full N). Solid lines represent medians from samples of the posterior predictive distribution, their corresponding shaded areas represent the 2.5% quantile (i.e. representing half of the 95% credible interval), and symbols show the mean of three replications for each plant fraction \times sampling \times site. 79

Figure 4.3. Summary of posterior predictive distributions for post-silking N fluxes in leaves, stem, cob-husks, and grain fractions for two maize hybrids (3394, orange symbols; and P1197, blue symbols) under two N fertilization levels (zero and full N). Points represent the median of the posterior distributions and whiskers their 95% credible intervals. Values on the left side of the zero-line (dashed line) indicates an export of N from the organ, while to the right, an import of N. Exogenous-N (A, B, C, and D) represents the amount of N absorbed from soil and directly allocated to each organ. Endogenous-N (E, F, G, and H) represents the N translocated from/to other tissues. Net N accumulation (I, J, K and L) represents the difference between N content at R1 and R6. All values represent the cumulative balance over the R1-R6 period. Seasonal posterior predictive estimates expressed in thermal time after silking are depicted in Supplementary Figure S4..... 80

Figure 4.4. Summary of the posterior distributions for post-silking plant C accumulation (*y-axis*) and the proportion of exogenous-N (*x-axis*) allocated to (A) stem, (B) leaves, (C) cob-husks, and (D) grains during the post-silking period. Means and credible intervals are depicted for two maize hybrids (3394 and P1197) under two N fertilization levels (zero and full N – open and closed symbols, respectively)..... 80

Figure 4.5. (A) Sources of grain N at maturity for two maize hybrids (3394 and P1197) under two N fertilization levels (zero and full N - ZN and FN, respectively). The four sources

considered are: 1) exogenous-N to grains, which denotes N absorbed and directly allocated to grains during post-silking, and 2-4) Endogenous-N from leaves, stem, and cob-husks, which represents the N translocated respectively from each organ to grains (originated from pre-silking N or post-silking N allocated to the stover). Bars and solid points represent the median from samples of the posterior predictive distribution, and horizontal lines to the right of each bar denotes their corresponding 95% credible interval. (B) Relationship between grain N content and grain weight, throughout the grain filling period, for 3394 and P1197 under zero and full N treatments. Solid line represents the total grain N content [adapted from Chapter 3, Fernandez et al. (2021)], for which the slope represents the grain N concentration for each hybrid by N condition. Dashed lines denotes the expected exogenous grain N content calculated in the present study. 81

Figure 5.1. General information of the sites (n = 134) included in the review analysis. (A) Number of studies, management factors, and years of release of hybrids evaluated across locations. Comparison of rates of genetic progress across regions (and breeding programs for the USA) for (B), grain yield and (C), kernel weight. Size of symbols represents their weight in the global meta-regression estimate across all regions, influenced by both number of observations (n) and sites within the individual region. 103

Figure 5.2. Contribution of kernel weight to the genetic gain in maize. (A) Genetic gain in kernel number and kernel weight across sites (n = 134) included in the review analysis. Isolines represent levels of yield genetic gain from 0 to 30 g m⁻² year⁻¹. Size of symbols represents the number of observations within each study. Dark and white symbols represent hybrids from USA – Pioneer ERA and other global breeding programs, respectively. (B) Proportion of the variation in yield genetic gain explained by improvements in kernel number and kernel weight, calculated as the coefficient of determination (*r*²) of the association between variables. Whiskers represent their 95% CI. 104

Figure 5.3. Genetic gain of USA – Pioneer ERA hybrids in multiple case studies from 2017 to 2020 growing seasons. Relationships between years of hybrid introduction and (A) grain yield, (B) kernel number, and (C) kernel weight. Symbols represent Best Linear Unbiased Estimates (BLUEs) of hybrids at the group or marginal levels of inference based on 2-way interactions significance. Grey markers show observations from other studies that were included in the review analysis. 104

Figure 5.4. Description of analyses on kernel-filling parameters of USA – Pioneer ERA hybrids in multiple case studies from 2017 to 2020 growing seasons. Schematic diagrams of kernel-filling traits of interest and non-linear models used for (A) kernel dry matter, and (B) kernel water content dynamics. Relationships between years of hybrid introduction and (C) linear kernel-filling rate, (D) kernel-filling duration, (E) lag phase duration, (F) kernel growth during lag phase, (G) days from flowering to MKWC, and (H) kernel weight plasticity calculated as: [(Max.KW at high source-sink ratio – Min.KW at low source-sink ratio)/(Max.KW at high source-sink ratio)](Valladares et al., 2006). Circles represent BLUEs of hybrids, and crosses identify outliers based on studentized residuals (values > 3).
 105

Figure 5.5. Importance of variables describing kernel weight genetic progress of USA – Pioneer ERA hybrids in multiple case studies from 2017 to 2020 growing seasons. (A) Partial least squares (PLS) regression biplot presented with two main components explaining kernel weight variance (y) based on six kernel-filling parameters as predictors (x). Arrows represent correlation loading among variables. (B) Variable importance scores for predictor variables of the PLS model. 106

Figure A.1. Forest plot for subgroup analysis on late season N effect on yield across different proportion of late N applied (late N less than 35%, between 35 and 60%, and more than 60% of final N rate) and water regimes (irrigated and non-irrigated). Effect sizes and 95 % confidence intervals (CI) are expressed as a late-N effect ratio (percentage of grain yield variation in L_N / E_N) calculated as (6). Square symbols represent point estimates and whiskers depict their respective 95% CI. Heterogeneity of the results is described through I^2 (I-square statistic). n = number of studies within subgroup. Different letters indicate significant differences between pooled effect sizes at $P \leq 0.05$ 137

Figure C.1. Posterior predictive check for Bayesian model on the relative allocation of ^{15}N absorbed across plant organs. 142

Figure C.2. Posterior predictive check for Bayesian models on stem, leaves, cob-husks, and grain N accumulation. 142

Figure C.3. Posterior predictive check for Bayesian model on plant C accumulation. 142

Figure C.4. Cumulative endogenous-N mobilized (solid lines) or exogenous-N absorbed (dashed lines) in stem, leaves, cob-husks, and grain fractions for 3394 (orange symbols) and P1197

(blue symbols) hybrids under zero and full N fertilization. Sections with black lines represent non-significant differences between hybrids, while colored lines and asterisks indicate significant differences ($\alpha=0.05$). 143

Figure D.1. Sankey diagram summarizing the literature review screening procedure. The width of each node represents the quantity of studies in the flow. 144

List of Tables

Table 2.1. Number of study, references, site - country, years of experiments, experimental design, tillage, main factors tested, and type of study (published or unpublished) for each maize experiment in the dataset.	30
Table 2.2. Summary statistics of the extracted dataset across Zero N, Early N, and Late N fertilization timing groups: n, number of observations; mean; SD, standard deviation; Min-Max, minimum and maximum. Grain yield per unit area and adjusted to a standard moisture basis of 155 g H ₂ O kg grain ⁻¹ . Abbreviations: PP = growing season precipitation, PNU _{PM} = plant N uptake at physiological maturity per unit area, PNU _{SILK} = plant N uptake at silking per unit area, Grain N = N in the grain fraction per unit area, GNC = grain N content, NU _{Post-Silking} = percentage of total PNU that occurs from the period that goes from silking until physiological maturity, REN = fertilizer N recovery efficiency; AEN = agronomic efficiency of N, PFPN = partial factor productivity of N.	31
Table 3.1. Monthly values for daily solar radiation, temperature, and total precipitation for the 2017 and 2018 growing seasons. Source: Kansas Mesonet (2019).	57
Table 4.1. Environmental and agronomic description of three experimental sites used in the study.*	81
Table 5.1. Subgroup meta-regression for the effect of crop growth conditions on the rate of genetic gain in grain yield, kernel number, and kernel weight of maize hybrids from USA – Pioneer ERA and other global breeding programs.	107
Table A.1. Sensitivity analysis for determination of late N proportion for subgrouping meta-analysis. Values (<i>i, j, k</i>) within each combination of thresholds represent number of studies allocated in the upper, middle, and lower late N subgroups, respectively. In bold, the selected combination based on the balance of studies and the range within intervals (difference between maximum and minimum limits).....	138
Table A.2. Subset of the overall dataset with reported values on plant N content at silking and at maturity (n ₁ =98). Mean ± standard deviation (SD) for each N-timing group of plant N uptake at physiological maturity per unit area (PNU _{PM}), plant N uptake at silking per unit area (PNU _{SILK}), and percentage of total PNU that occurs from the period that goes from	

silking until physiological maturity ($NU_{\text{Post-Silking}}$). When biomass at silking was reported, the N Nutrition Index at silking (NNI_{SILKING}) was calculated ($n_2=66$). 139

Table B.1. Grain yield (15.5% moisture), grain number, grain weight, harvest index, total plant N uptake at maturity, post-flowering N uptake, and LAI at maturity for 3394 and P1197 hybrids under Zero and Full N conditions during 2017 and 2018. Pairwise comparisons were performed only when the global test was significant for each factor evaluated. 140

Table B.2. Number of parameters (k) and AIC (Akaike's Information Criteria) values for linear and linear plateau models between grain yield, grain number, grain weight, and harvest index with total N uptake (Figures 2A to 2D). A lower score of AIC indicates a better fit (bold). Respectively for each variable and type of regression, model 1 and model 2 represent the best fit to the data based on a backward selection procedure for the number of coefficients. 141

Table D.1. Publication number and reference, country, years of experiments, experimental design, range of years of hybrid release (YOR), management practices, and number of means obtained for the historical maize experiments used for the meta-regression analyses. 145

Acknowledgements

First, I would like to express my sincere gratitude to my advisor, Dr. Ignacio Ciampitti for his guidance and mentorship during my studies. I truly appreciate his support, sound advice, and motivation on a personal and academic level, which were invaluable in helping me to succeed as a graduate student. I would also like to thank Drs. Charlie Messina, Jesse Nippert, and P.V. Vara Prasad for their feedback and insightful contributions to this project. Their passion for crop physiology was inspiring for me, and their guidance has been instrumental in my professional growth.

I am indebted to the past and current members of KSUCrops and Ciampitti Lab Team for their assistance during my project. Special thanks to the colleagues and friends I got to know here in Manhattan. In addition, the financial support from the Fulbright Program and the Ministry of Education - Argentina is highly acknowledged.

Finally, I would like to thank my family and close friends who have always believed in all my goals and aspirations throughout this time. To my parents, Maria Cecilia and Jose Antonio, my siblings, Diego and Maria Mercedes, and my life partner, Paula, for their endless love and support in every step of my life. - Thank you all!

Dedication

To my mother and father who have dedicated their lives to their children.

To my grandparents, Nely and Pochocho who are with us in spirit.

Chapter 1 - Introduction

Improvement of major staples crop yields is desirable to sustain food security for future decades. Agriculture faces today the unprecedented challenge of providing enough safe and nutritious food to nourish an ever-increasing human population in a world threatened by climate change risks (Nelson et al., 2010; Vermeulen et al., 2012; Jägermeyr et al., 2021). In the last few years, however, the rate of improvement in crop performance has been slowing in a number of important crops (Fischer and Edmeades, 2010; Brisson et al., 2010; Grassini et al., 2013) and currently lags behind the increasing food demand of the growing population (Hall and Richards, 2013; Ray et al., 2013). In such a complex scenario, the optimization of the nutrient resources in crop plants emerges as a prerequisite for obtaining high crop productivity while minimizing the environmental footprint of agriculture (Stewart and Roberts, 2012).

Nitrogen (N) is the major driver of yield improvement in many field crops. In maize (*Zea mays* L.), the largest staple crop in the world (FAO, 1997), production is largely dependent on N fertilization due to its key role in both plant growth and development. In the US, more than 6 Mt of N fertilizer is used annually in maize production and this number is expected to increase even more with the growing demand for food production (USDA, 2020; Li et al., 2017). However, current estimations show that only about half (in the best case scenarios) of N applied is typically taken up by the crop (Fageria and Baligar, 2005; Ladha et al., 2005; Fixen et al., 2015), causing a massive N loss and environmental pollution. This underscores not only the urgent need but also the high potential for improvements in N use efficiency (NUE) of maize production (Lynch, 2019). Genetic and agronomic improvements are both paramount components in this process by identifying genotypes and management practices adapted to the right environments and the projected (changing) climate regimes.

Historically, the complex system of variables surrounding crop N utilization has been studied using the concept of Genetic \times Environment \times Management ($G \times E \times M$) interactions. This separation allows determining the effects of the surrounding environment, management factors that a farmer can modify through practices, and the genetic component of the species. Using this concept, this research advances in the understanding of genotypic adaptations of hybrids to specific environments and N management factors affecting US maize production.

Over the past century, US maize productivity has seen remarkable progress owing to the combination of breeding and agronomic management improvements (Duvick et al., 2004). While all of these advances are reflected through significant NUE increases (Ciampitti and Vyn, 2012), they also underpin significant improvements in several other physiological traits. To rationalize progress in such an extremely complex trait, it is useful to separate NUE into two physiological phases: the uptake and utilization efficiencies of N (Moll et al., 1982). A comprehensive understanding of the mechanisms underlying both N uptake and utilization in crops (including N uptake, allocation, and translocation processes) is critical to design and breed future crop genotypes. Moreover, the description of these processes from a supply-demand perspective will enable us to identify candidate traits for future improvement. In this sense, this dissertation has been structured to dissect N use in US maize hybrids as affected by both $G \times M$ interactions, with a historical perspective on (i) synchronizing N fertilization supply and demand, (ii) integrating N dynamics with carbon resource capture and utilization, (iii) describing N uptake, allocation, and translocation among plant tissues, and (iv) analyzing the sink demand by genotypic modifications in grain development.

In the context of climate change, a key scientific pursuit has been the identification of morphological and physiological traits associated with a better N utilization in crops.

Investigations, such as the one presented in this dissertation, parameterizing $G \times E \times M$ pathways to enhance NUE in field-grown maize, help point the way forward to more concrete strategies for identifying future targets of breeding and sustainable management in agricultural production.

Chapter 2 - Late-season nitrogen fertilization on maize yield: A meta-analysis

Published in Field Crops Research

Fernandez, J. A., DeBruin, J., Messina, C. D., & Ciampitti, I. A. (2020). Late-season nitrogen fertilization on maize yield: A meta-analysis. *Field Crops Research*, 247, 107586.

Abstract

Late-season fertilizer N applications in maize (*Zea mays* L.) is a tactical agronomic practice that seeks to improve the synchrony between plant N demand and soil N supply. While this management practice can increase yield and limit unintended environmental impacts, a quantitative synthesis of the effects of late N applications on grain yield and resource use efficiency is lacking. A meta-analysis was conducted to identify patterns of yield response to late-N fertilization (post tenth-leaf, V10) across site-years studies. The goals of this study were to: 1) quantify the effect of late-season N fertilization on maize yield; and 2) identify an indicator for decision support of late-N fertilization. Published and unpublished sources from 1983 until 2018 were included in the meta-analysis (14 studies; n = 625 treatment means). Early-season (E_N , $\approx 100\%$ of fertilizer applied prior to the sixth-leaf, V6) and late-season (L_N , $< 50\%$ N applied before V10) N fertilization were compared to determine the effect of application timing on yield, N uptake, and N recovery efficiency (REN, N uptake increase per unit of N applied). Across studies, the timing of application of N was not associated with a quantifiable change in maize yield. Due to significant heterogeneity across experiments ($I^2 = 48\%$), there is an opportunity to explore plausible effects of the practice when N is limiting (L_N improved yield) on yield and effective use of N. Increased post-silking N uptake ($>28\%$ of N uptake at maturity occurring after silking) was positively related with yield increases for L_N (+577 kg ha⁻¹), and the

contrast in REN between L_N and E_N was 0.04 kg kg^{-1} . Environments prone to a greater N uptake during reproductive stages are proposed to be more suitable for late N applications. Prediction algorithms to inform tactical N management that can both increase productivity and sustainability could be developed provided adequate links between late-season N uptake and growing-season indicators could be established.

Introduction

Nitrogen fertilization strategies vary among maize production systems but greater than 50% is applied before planting (Cao et al., 2018), which is implicated in the low N fertilizer recovery efficiency (REN). Nitrogen losses from denitrification, leaching, volatilization, and surface run-off increase with increasing N availability at planting or pre-planting. A greater synchrony between plant N demand and fertilizer N supply (Cassman et al., 2002; Chen et al., 2006; Raun and Johnson, 1999; Tilman et al., 2002; Ciampitti and Vyn, 2012) can reduce N losses and improve both N recovery (e.g., N uptake to N fertilizer) and N internal efficiencies (e.g., yield to N uptake) at a crop level. Whereas, late-N applications could be a potential alternative practice to current N fertilization programs, its adoption will depend on the agronomic practice effect on yield, economic factors and logistics.

Grain yield response to delayed N applications in maize is variable. Adriaanse and Human (1993) reported that under dry conditions splitting and delaying N in two or three applications resulted in lower yields compared to a single application. Other studies document no yield reductions when N applications were delayed until V10 (Walsh et al., 2012) or V11 (Scharf et al., 2002), but moderate yield losses were reported when N was applied as late as VT (Walsh et al., 2012) or silking (Scharf et al., 2002; Silva et al., 2005). In contrast, Lü et al. (2012)

documented yield increases in a two-year field trial when late-N was applied at V6, V10 and 10 days after anthesis. Recent studies evaluating older and modern hybrids reflected inconsistent responses on the effect of late-season N application on maize grain yields across a three-year experiment (Mueller et al., 2017). Considering experimental evidence in its current form, it is not possible to generalize and model late-N fertilization impacts on yield and N use efficiency within genotype × environment × management systems.

Crop N accumulation could be thought as the outcome of a dynamic function of crop growth, root uptake capacity and soil N availability (Soufizadeh et al., 2018). Such a framework can help interpret the effects of late N fertilization on maize yield. For example, when growth is not restricted by water and nutrients, N uptake rate is typically less than 3 mg plant⁻¹ GDD⁻¹ for early vegetative stages until V6 (Russelle et al., 1983). After that, root absorption rate increases rapidly concomitant with root biomass, placing its peak at around silking (Gao et al., 2017; Russelle et al., 1983). Under field conditions, maize root growth and activity are well documented as affected by N supply, among other agronomic practices. Although a general trend cannot be established due to the interaction effect with soil factors and fertility conditions (Feng et al., 2016), a number of studies have shown that moderate N supply stimulates root growth and function yet excessive N rates restrict them (Chen et al., 2015; Liu et al., 2017; Oikeh et al., 1999). Splitting early N rates and delaying N fertilization could therefore signify a strategy to maximize root development during vegetative stages. Consistent with this, compelling results on root system effects have been reported with the use of late N. For instance, root dry biomass at maturity was improved when N was top-dressed with irrigation at a pot experiment (Liang et al., 2013). Wang et al. (2003) reported that delaying N supply increased reproductive root activity at the surface and subsurface soil layers when N was applied at silking. However, disruptions on

root N uptake in field studies are expected due to the complex interactions involving environmental and management factors (Pan et al., 1985; Ren et al., 2017; Russelle et al., 1983; Veen et al., 1992). Based on this understanding, it is important to evaluate late N strategies under a wide spectrum of conditions, aiming to associate plant N uptake dynamics affecting maize grain yields with growing-season indicators.

Meta-analyses methods can help identify patterns only when the experimental data are combined and analyzed within an environmental and agronomic context (Philibert et al., 2012). A comprehensive meta-analysis was conducted using a dataset comprised of published and unpublished studies executed between 1983 and 2018. The data include a broad set of agronomic conditions and maize farming systems. This study is an integrative and quantitative synthesis emerging from the analyses of results on diverse and independent studies on yield responses to late-N fertilization. The goals of this study were: 1) to quantify the effect of late-N fertilization on maize grain yield, and 2) to identify an indicator of late-N fertilization responses that can potentially be used to recognize productive opportunities of this practice.

Materials and methods

Data

Research data was only included in the main database if specific criteria were fulfilled: 1) completeness of the information, 2) field studies with in-season N applications before and after (V10) tenth-leaf (early- and late-N), and 3) control (zero-N), N rates and fertilizer sources documented. Experiments with highly dissimilar fertilization rates (more than 40% difference between N treatments in a given experiment) were excluded to reduce noise of unfair comparisons due to distinct N rates. Within each selected study, agronomic management

practices were identical across N levels. When other agronomic factors were part of the treatment structure, data points were only included if factorial combinations were equally assigned and reported across N treatments. Grain yields from all studies were adjusted to a standard moisture basis of 155 g⁻¹ kg⁻¹.

A total of 14 research studies were selected that satisfied all requirements for data inclusion (Table 1). The final database includes data from published and unpublished sources: Nine studies were located in US, three in China, one in Germany, and one in Kenia. The database includes 625 data points along with metadata describing N management. Nitrogen rate vary between 0 and 315 kg N ha⁻¹, fertilizer applications range between 0 for controls and 3 applications for treatments, while sources of fertilizer include anhydrous ammonia (AA), ammonium nitrate (AN), ammonium sulfate (AS), calcium ammonium nitrate (CAN), urea ammonium nitrate (UAN), and urea.

Based on timing of application, treatments were classified as Zero-N (Z_N) for controls with no N application (n = 81), Early-N (E_N) when N fertilizer was applied prior to vegetative stage V10 (n = 295), and Late-N (L_N) for N applications after this development stage (n = 249).

Calculations and parameters evaluated

Nitrogen efficiency parameters were calculated within each N-timing group, based on the correspondent Z_N data points. Agronomic efficiency of N (AEN) represented by the ratio between ΔYield of fertilized plots (Yield_{fertilized} – Yield_{unfertilized}) to the fertilizer N rate applied (Ladha et al., 2005) was calculated as,

$$AEN = \frac{\text{Yield}_{\text{fertilized}} - \text{Yield}_{\text{unfertilized}}}{\text{fertilizer N rate}} \quad \text{Equation 2.1}$$

Fertilizer N recovery efficiency (REN), described as the proportion of fertilizer N applied that was recovered by the plant at physiological maturity (Ciampitti and Vyn, 2012), was calculated as follows,

$$\text{REN} = \frac{\text{N uptake}_{\text{fertilized}} - \text{N uptake}_{\text{unfertilized}}}{\text{fertilizer N rate}} \quad \text{Equation 2.2}$$

The ratio between yield and fertilizer N rate applied, referred as partial factor productivity of N (PFPN), was determined by,

$$\text{PFPN} = \frac{\text{Yield}}{\text{fertilizer N rate}} \quad \text{Equation 2.3}$$

Data analysis

Descriptive statistics were calculated for each group (Table 2) and complemented with plots to visualize the distributions of fertilizer N applications conditional to factors (source, method, rate, and timing; Figures 1A-D). A random effects meta-analysis was conducted following the methodology of Hedges et al. (1999) and performed using the *metafor* package (Viechtbauer, 2010) included in RStudio (RStudio Team, 2016). To estimate the response to a treatment in meta-analysis, outcomes of each study are typically summarized as an index that allow us to compare results across experiments (i.e. effect sizes, quantitative measure of the magnitude of the response) (Osenberg et al., 1999). The effect sizes (y_i) used to compare the response of late- (LN) relative to early- (EN) N fertilization was derived using the natural logarithm of the ratio between the mean yield for LN and EN,

$$y_i = \ln \frac{\text{Yield}_{\text{LN}}}{\text{Yield}_{\text{EN}}} \quad \text{Equation 2.4}$$

Effects sizes within the meta-analysis were weighted (w) using the inverse of the variance (v) of each individual study (i) computed as Hedges et al. (1999),

$$v_i = \frac{1}{w_i} = \frac{(SD_{LN})^2}{n_{LN} * (Yield_{LN})^2} + \frac{(SD_{EN})^2}{n_{EN} * (Yield_{EN})^2} \quad \text{Equation 2.5}$$

where *SD* is standard deviation, and *n* indicates the number of data points included in each of the groups E_N and L_N .

The 95% confidence interval was calculated for the mean effect size using bootstrapping methods (Adams et al., 1997). Bootstrapping procedures were executed with the *boot* package (Canty and Ripley, 2017; Davison and Hinkley, 1997) in R based on 10,000 iterations (Van Den Noortgate and Onghena, 2005). Including the N rate difference between treatments (N rate L_N – N rate E_N) as a factor in the random effects model was determined with the omnibus test. A significant effect was obtained for the yield response and thereby it was included as a moderator in the previous model. Heterogeneity between studies was calculated using the I^2 statistic to detect whether all of them are assessing the same effect. Based on Higgins et al. (2003), the I^2 value defines the percentage of total variation across studies that can be attributed to heterogeneity rather than experimental error. The same authors developing this factor categorized low, moderate, and high I^2 to values of 25%, 50%, and 75%, respectively. A forest plot (Lewis and Clarke, 2001) was used to summarize the effects on grain yield, expressing results as a late-N effect (%) calculated as,

$$\text{Late-N effect (\%)} = \left[\frac{\text{Yield}_{LN}}{\text{Yield}_{EN}} - 1 \right] * 100 \quad \text{Equation 2.6}$$

Subgroup analyses were conducted to assess the effect of water regimes (irrigated and non-irrigated) and of proportion of late season N fertilization applied on yield response. For the latter, a sensitivity analysis was carried out to establish intervals for a balanced subgrouping across studies, testing the number of studies available across different combinations

(Supplementary Material, Table A.1). Pooled estimates for three subgroups of L_N (less than 35%, 35 to 60%, and more than 60% of final N rate applied as late season N) were calculated in a multilevel model with study and late N proportion group as random effects. Differences among subgroups were tested with a Wald-type test. Equivalent procedure and equations (4) and (5) were used to estimate weighted effect sizes for AEN (1), REN (2), and PFPN (3) for N treatments (E_N and L_N). Likewise, these were expressed as in (6), representing the percentage of variation in L_N / E_N indices (relative late-N effect ratio).

A first subset of the overall dataset (Supplementary Material, Table A.2) from five published and unpublished sources was utilized to calculate post-silking N uptake ($NU_{\text{Post-Silking}}$) as the difference between plant N content at silking and at physiological maturity ($n=98$ treatment means). Statistical comparisons were performed in R program with *nlme* package (Pinheiro and Bates, 2000) using a mixed effects model with N-timing and post-silking N defined groups as fixed effects, and location by year combinations as random effects. Rate of N was included as covariate in the model and an adjustment for different variances per N timing stratum was used to correct for heterogeneity of residuals. Residual plots were verified for constant error variance, and normality assumptions. Pairwise comparisons with a type I error rate set at 0.05 were performed using Tukey-Kramer method.

The second subset of the dataset (Supplementary Material, Table A.2) was utilized to calculate N Nutrition Index at silking (NNI_{SILKING}). It consisted of four published and unpublished sources that reported shoot biomass and N content at silking ($n=66$ treatment means). The NNI was calculated by dividing the N concentration of the shoot biomass ($\%N_A$) by the minimum N concentration required to achieve maximum shoot growth ($\%N_C = 3.4 W^{-0.37}$, with W as shoot dry biomass in Mg ha^{-1}) as proposed for maize by Plénet and Lemaire (2000).

Relative grain yield was determined as the ratio of each yield with the highest grain yield reported within each study.

Results

Descriptive statistics of crop variables: a comparison between E_N and L_N

Mean grain yield for both N-fertilized groups was 10.9 and 10.4 Mg ha⁻¹, for E_N and L_N respectively, while the Z_N control group averaged 7.5 Mg ha⁻¹ (Table 2). A limited number of studies presented Harvest Index but results followed a similar trend to grain yield with 0.54 (E_N), 0.51 (L_N), and 0.47 (Z_N). The large range between minimum and maximum yield (2.3 to 17.5 Mg ha⁻¹) can be attributed to the diversity of cropping systems (tillage, irrigation, planting date, plant density, crop rotation, genotypes), and environments (soil properties, topography, and climatic conditions) included for analyses in this study. Data distributions for grain yield (across fertilized N groups) were slightly skewed (skew = -0.74 and -0.50, for E_N and L_N respectively), and close to a mesokurtic distribution (kurtosis = 0.58 and -0.24, for E_N and L_N respectively). Correspondingly, grain yield distribution for Z_N was shortly skewed to greater values (skew = 0.18) and slightly flat (kurtosis = -0.63).

Data summaries for agronomic management and environmental variables reported are presented in Table 2. Growing season precipitation (mm), was described in 54% of the cases (n=337). The mean rainfall was 510 mm, whereas the majority of the experiments were not irrigated (64%, data not shown). Management practices such as seeding rate and row spacing were not consistently reported; in general, seeding rate values ranged between 5 to 15 pl.m⁻² with row spacing between 0.6 to 1 m. While summary values are the outcome of a different number of

observations (i.e. studies), it is important to recall that N-timing treatments within each study were conducted under the same agronomic and environmental conditions.

The database contained studies with 1, 2, and 3 N applications with approximately similar yield across the number of N-applications (10.6, 10.9, and 10.4 Mg.ha⁻¹ for 1, 2, and 3 applications respectively). Observations with one N application were the most frequent (47%, Fig. 1A). But two N applications was the most common strategy for the L_N group (56%). This application strategy was usually composed of a major rate at planting or early growth stages and a minor fertilizer N rate for post-V10 application. The latter appears as a logical approach since fertilizer N is being supplied as it is required by the crop (Keeney, 1982). Although broadcasting and soil-incorporating methods were the general trend (28% and 31% respectively; Fig. 1B), side-dressed N was more common among L_N data. Nitrogen sources, urea ammonium nitrate (UAN) and urea were the most frequent sources accounting for more than 52% of N fertilizations across the database (Fig. 1C).

In fertilized treatments, 69% of the N rates observations were between 50 to 250 kg N ha⁻¹, while the overall mean rate was 164 kg N ha⁻¹ (Fig. 1D). Decoding by groups, the distribution for E_N peaked at N rates from 50-200 kg N ha⁻¹, while the distribution for L_N was flatter and skewed towards greater N rates (>260 kg N ha⁻¹). In parallel, a slight increase in summary mean N rates for L_N over E_N was observed (174 versus 155 kg ha⁻¹ respectively; Fig. 1D).

Mean N rates changes, across N-timing groups (E_N and L_N), were evaluated using a mixed model with location by year combinations considered random factors. Homogeneity of variances was tested with a Fligner-Killeen test using the `fligner.test()` R function; this is a robust method for non-normal distributions. No evidence for differences on N rates means and

variances components were detected across fertilizer N timing categories, demonstrating a reasonable balance across N groups for posterior comparisons ($\alpha=0.05$).

Although the established cut-off point between groups was V10, it was observed that more than 96% of total N was applied before V6 in E_N . At the same growth stage, L_N group has a total N applied of 42% (Fig. 1E). Specifically, fertilizer N applications at planting were the most frequent for E_N (42%), differing from L_N in which the most frequent practice was to split applications between planting, V10 and VT (23, 14, and 16%, respectively). Less than 13% of the database included data that enables the study of effects of N supply after silking (R1) on maize yield.

Late season application of N neither increased maize yields nor N efficiency indexes

The results of the meta-analysis, expressed as a percentage of late N effect (relative L_N / E_N yield ratio), were displayed in a forest plot for individual studies (Fig. 2). Square symbols represent point estimates and whiskers depict their respective 95% confidence interval (CI). The weight of each study is expressed as a percentage of the model and illustrated by the thickness of box and whiskers. The summary effect size expressed an overall lack of maize yield benefit when comparing L_N vs E_N groups (L_N/E_N effect = -2.01%, 95% CI = -5.22- 1.36 %), represented by the polygon presented in Fig. 2. Significant heterogeneity was detected in the current model ($p = 0.05$). The I^2 statistic was 47.90%, which suggests a moderate value of inconsistency among experiments. From a between-experiments perspective, late-N effect ratio ranged from -15.35 to +6.79%. Interestingly, only three studies yielded significant variations on the analyzed ratio, observed by the CI beyond the vertical line indicating zero effect.

Two subgroup analyses were conducted for grain yield responses to late N: 1) between two water conditions (irrigated and non-irrigated), and 2) across three N groups (late season N representing less than 35%, between 35 and 60%, and more than 60% of final N rate applied) (Supplementary material, Figure A.1). For the effect of irrigation, no significant differences between pooled effect sizes were identified. However, greater variability in late N responses in non-irrigated studies was shown by I^2 statistic equal to 67.72%. With the application of irrigation, the I^2 decrease to 2.33%. Pairwise comparisons of pooled effect sizes for late N proportion showed significant differences between the lower N subgroup (from 0 to 35% of late N) and the middle (from 35 to 60%). The subgroup with more N applied pre-V10 had a smaller amount of heterogeneity among studies (I^2 of 21.98%). As greater proportion of N was applied later in the season, in middle and upper N subgroups, different response patterns seemed to diverge into a greater heterogeneity (I^2 of 42.95% and 54.11%, respectively). The overall trend of lower mean ratios and greater variability with late N proportion might reflect the negative impact due to an insufficient basal or early N supply. Although results should be interpreted with caution in these subgroup analyses, it is interesting to point out that both variables (irrigation and late N proportion) were identified as potential relevant sources of heterogeneity for yield responses.

Efficiency indices were also evaluated fitting a meta-analytic model investigating potential changes in AEN, REN, and PFPN. A forest plot with aggregate summary estimates was plotted in Figure 3 accompanied by the means per N group (%). According with grain yield results, all indices include 0 (zero) in their 95% CI implying no evidence for differences between E_N and L_N . Only positive pooled estimates were identified for REN, revealing a low

heterogeneity across studies ($I^2 = 18.24\%$, not shown). A subsequent sub-group analysis was performed aiming to distinguish conditions for REN increases with late season N.

Yield and N recovery efficiency are dependent on N nutrition index and post-silking N uptake

The N Nutrition Index at silking (NNI_{SILKING}) was calculated for each data point whenever shoot biomass and N content at silking were reported. The relationship between NNI_{SILKING} and relative grain yield is depicted in Figure 4A ($R^2 = 0.73$). With decreasing NNI_{SILKING} below 0.88 (X_0 ; 95% CI = 0.810 to 0.936), relative grain yield decreased. For NNI_{SILKING} above 0.88, relative grain yield reached its maximum, close to one. NNI_{SILKING} on non-fertilized points (Z_N) averaged, as expected, lower values, with a mean NNI_{SILKING} of 0.56. Additionally, E_N mean NNI_{SILKING} was 0.91 and was slightly inferior to L_N mean of 1.08.

Post-silking N uptake ($NU_{\text{Post-Silking}}$) changes were observed across levels of NNI_{SILKING} . A quadratic model was fit (Fig. 4B, $R^2=0.49$), and two N nutrition situations were defined by NNI_{SILKING} equal to 0.88 (X_0 , Fig. 4A). Increasing $NU_{\text{Post-Silking}}$ was estimated in points where NNI values were below 0.88 (N deficiency for yield) or above it (N sufficiency for yield plateau). Between NNI_{SILKING} values of 0.88 and 1.0 ($N_A=N_C$), lower values were mainly described. Still, residuals for the fitted model were observed to increase as values approach the N deficiency threshold for our database (not shown).

The distribution of treatment means for $NU_{\text{Post-Silking}}$ was produced for E_N and L_N groups ($n=108$, Fig. 5A) in an exploratory study seeking to identify an indicator for positive response to late N practice. A division in thirds (breaks at 33.3% and 66.7% of the total distribution) was used to determine a sub-group analysis, on which both the lower and the upper thirds were

examined for yield responses to N-timing. Sensitivity of the results was assessed by testing different cut-off points for sub-groups. The chosen criterion was determined by considering enough studies by years in each subgroup ($s = 5$ for both sub-groups) and comparable fertilizer N rates and $NU_{\text{Post-Silking}}$ for N-timing groups. When $NU_{\text{Post-Silking}}$ was low at an environment ($< 16.4\%$), yield was significantly greater for E_N points, with 10103 and 9065 kg ha^{-1} for E_N and L_N , respectively (Fig. 5B). On the other hand, a noticeable mean yield increase ($+577 \text{ kg ha}^{-1}$) was observed in favor of L_N treatment studies when $NU_{\text{Post-Silking}}$ was greater than 28.6% ($\alpha = 0.05$, Fig. 5C). Finally, for the center third (between 33.3th and 66.7th percentiles) no yield differences were observed among sub-groups representing a non-effect zone (data not showed).

Fertilizer REN, expressed as the increase in N uptake per unit of fertilizer N applied, significantly varied among N groups (0.56 kg kg^{-1} for E_N and 0.60 kg kg^{-1} for L_N ; Fig. 6A; $n=98$, $s=13$). These results show an apparent overall increase in fertilizer recovery when N was split and delayed. To isolate these differences, REN was evaluated for both the pre- and post-silking periods. Pre- and post-silking REN were calculated as the increase of pre- or post-silking N uptake relative to Z_N respectively for each N-timing group. Slightly greater pre-silking REN was estimated for early N (0.37 kg kg^{-1}) than for the late N group (0.33 kg kg^{-1}). At contrast, large differences in post-silking REN were observed between N-timing groups (0.12 kg kg^{-1} for E_N and 0.19 kg kg^{-1} for L_N , Fig. 6C), explaining the observed improved efficiency for late-season fertilization.

Discussion

Effect of late season fertilizer N applications on maize yields and REN

The influence of late season fertilizer N applications on maize yield was assessed using a large and diverse dataset assembled from published and unpublished sources representing several agricultural systems. The meta-analysis provided strong evidence for the lack of a main effect of late N application on yield, but a relation governed by complex interactions. This interpretation is supported by the large heterogeneity of results observed across studies (Jaynes and Colvin, 2006; Mueller et al., 2017; Roberts et al., 2016; Walsh et al., 2012; Yan et al., 2014) and by the many factors affecting the dynamics of plant N accumulation rate. These factors include weather (Russelle et al., 1983), soil conditions (Veen et al., 1992), and genotype (Pan et al., 1985) through effects of selection on the N allocation and remobilization from stems and leaves during grain filling (Mueller et al., 2019a). This review provides a quantitative synthesis for the response to late season (post-V10) N fertilization in maize and further confirms variable responses across wide-ranging conditions, previously referred by individual studies as site-specific (Crozier et al., 2014; Killorn and Zourarakis, 1992; Kovács et al., 2015). This meta-analysis enable us to generalize these conclusions.

A constraint for this review was the small number of studies exploring post-V10 N applications (n = 14), further investigation is still required to explore relevant agronomic and environmental factors affecting maize grain yield responses. Given the number of studies that fulfilled our criteria and reported yield data, the methodology employed for subgroup analyses limited our evaluation of explanatory variables and potential interactions among them that resulted in heterogeneity among studies. Moreover, although specific criteria (on variability of the data, N treatments, N rate differences, and type of publication) was followed for dataset

inclusion, the number of factors we could control for identical comparisons when pooling experiments (i.e. design structures, identical N rates and late N application timing) was restricted. However, these exploratory results still should be taken as an apparent signal revealing the irregularity in yield responses to late season N application. Future research should focus on linking late season N uptake variations with growing-season indicators, aiming to anticipate environments with a high likelihood of positive late season N fertilization effects on grain yield for maize crop.

This review explored the relationship between $NNI_{SILKING}$ and relative grain yield, and the fact that the N nutrition boundary for yield plateau was at 0.88 and not at 1 should also be highlighted. Similar values were obtained in studies by Ziadi et al. (2008a, 2008b) in single and early split N (V6/V8 - V10 stage), and by Mueller and Vyn (2018) for early (V4) and late (R1) N application studies. Mueller and Vyn (2018) suggested that crops are able to express relative high yields even under small N stresses. Furthermore, although not evaluated in this study due to the limitation of shoot biomass data, the threshold of N sufficiency for yield plateau in this review could be the result of underlying changes in harvest index. This raise a future research question on the responsiveness of potential harvest index with crop N status. Previous work in wheat have comparably determined a negative slope for harvest index when NNI was above the level of N sufficiency for yield (Hoogmoed et al., 2018). In maize, previous studies have provided suggestive evidence of smaller vegetative growth but enhanced grain-stover ratio when N was late side dressed (Bigeriego et al., 1979), but not consistent results were given to this question.

The $NU_{Post-Silking}$ evaluation across $NNI_{SILKING}$ conditions showed that high relative yields (≈ 1) could be attained within a considerable range of post-silking N uptake proportions. Greater

NNI values, even suggesting luxurious N uptake (Ciampitti et al., 2012), were related to high proportion of N absorbed after silking. This is based on $NNI_{SILKING}$ as an indicator of the N remobilization pool and the state of the photosynthetic complex (Coque et al., 2008). Hence, post-silking N accumulation was proposed as a driver for variable grain yield responses across N-timing strategies.

In Lemaire and Gastal (1997), NNI is proposed as a quantification index of N deficiency and luxury consumption of a crop. Due to the association between plant N status with leaf N and chlorophyll content, NNI at the onset of grain filling might allow for interpretation of the photosynthetic capacity of the plant during the reproductive period. Gallais and Coque (2005) reported a strong correlation between NNI at silking and delayed leaf senescence. In this study, non-N deficient plants at silking ($NNI \geq 1$) expressed an enhanced reproductive N uptake and presumably a reduction in leaf N remobilization. Delayed remobilization and prolonged photosynthetic activity seems to maintain C assimilate supply to the root system during grain filling to support N uptake and assimilation processes (Borrell et al., 2001; Gastal et al., 2014). Still, it is important to highlight the variability of observed N uptake with NNI near or above the N deficiency threshold in our dataset. This also depicts environments where late season N uptake could be restricted even at high NNI levels. Previous studies with low N availability or under N stress during grain development have shown that pre-anthesis stored N might support N demand through greater N remobilization (Nasielski et al., 2019; Plénet and Lemaire, 2000). Because of the nature of late N treatments considered in this review, we speculate that a significant portion of the studies explored high soil N availability at the end of the growing season, thus also favoring conditions for post-silking N uptake.

A comparative analysis on fertilizer REN (N uptake increase per unit of N applied) was conducted and showed promising results. Although there are reports in the literature showing enhanced fertilizer REN in response to early-season split applications (Randall and Vetsch, 2005; Sainz Rozas et al., 2004; Sitthaphanit et al., 2009), similar evaluations on post-V10 applications has not been thoroughly studied. Increasing REN, by identifying sites with high reproductive N demand, might result in an increase in economic net return to the farmer and a reduction of unintended negative environmental impacts due to N losses (Sainz Rozas et al., 2004). The distinction between pre- and post-silking REN was useful to identify the contribution of each factor for an efficient N uptake. Increasing fertilizer efficiency in late N group was driven by post-silking efficiency, confirming that high post-silking N accumulation is one of the traits that characterizes N-efficient maize germplasms (Chun et al., 2005). Identifying N rates that simultaneously improve yields and REN for a given genotype \times environment \times management system are required to maximize benefits when late N fertilization is implemented.

Due to the complexity of the dynamics of N within the plant and interactions with the agricultural system and the environment, post-V10 N fertilization can have negative impacts on yield as revealed in this review. Environmental conditions limiting N accessibility by the active root system, especially affecting N accumulation after silking, can result in ineffective responses to split and delayed N applications. Therefore, the effect of water supply on the observed variability for late N was studied in subgroups. Under water-limited conditions during the growing season, soil N mobility is limited. In these scenarios, preplant applications of N showed superior yield response than for splitting N (preplant + V5-V6, Randall and Schmitt, 2004). Similarly, no benefit of splitting N was observed when excessive irrigation altered post-silking N uptake (Sainz Rozas et al., 1999). The influence of water availability to the crop is perceived as a

significant source of variation for yield responses. The association of limiting water with N fertilization responses has been well documented in maize (Moser et al., 2006; Pandey et al., 2000; Tremblay et al., 2012). Kunrath (2018) postulated that this association can be explained by two main components; one related to the direct impact of water deficit on plant growth, and the other related to the reduction of N availability in the soil caused by drought. A similar concept could be adapted for post-silking N uptake when considering variations on water supply. Considering that water deficit in major maize production regions occurs during grain filling (Cooper et al., 2014a; Messina et al., 2009), development of late N fertilization strategies should be tactical and consider the timing and intensity of water deficit. Overall, these results illustrate the associated risks of late-season fertilizer N applications that should not be neglected and strengthens the necessity to characterize field level indicators for the success of this practice. Crop models that include mechanisms to simulate effects of water deficit in reproductive physiology (Messina et al., 2019) and simulate N balances (Soufizadeh et al., 2018) can enable the design of late fertilization management practices.

Although this review primarily focused effects of late N application on grain yield, future studies can extend these analyses to quantify the effects of late N fertilization on grain N and quality traits. Studies have shown that considerable increases in grain N concentration were caused by delaying fertilization as late as flowering (Jung et al., 1972; Silva et al., 2005). The contribution of genetic control could also be considered across distinctive hybrids to develop models that capture the N and water co-limitation in yield and grain quality (Messina et al., 2019; Soufizadeh et al., 2018). Ultimately, a potential benefit on grain protein may result from late N fertilization, yet still is an area which remains underexplored in the literature.

Relationship between post-silking N uptake and late season fertilizer N applications

The analysis on post-silking N uptake revealed that grain yield can be positively impacted by late season N fertilization mainly under environments that promote greater partitioning of N uptake during reproductive periods. Disruptions in N uptake proportion can be attributed to changes occurring first at the level of pre-silking N uptake and then on post-silking N. A recent review comparing high (>8 to 19 Mg ha⁻¹) and low (<8 to 1 Mg ha⁻¹) yield environments (Ciampitti and Vyn, 2013) observed smaller changes in post- than in pre-silking N uptake (45% and 71% improvements, respectively). Accordingly, one first type of late season N fertilization response in grain yield can be differentiated under reduced pre-silking N or source-limited conditions, where the tradeoff between post-silking and remobilized N is central (Ciampitti and Vyn, 2013). Adverse conditions during early growth stages followed by improved ones after silking may boost reproductive N uptake proportion and, in this way, potential benefits for late-N supply. Mueller et al. (2017) reported a greater proportion of post-silking N was accumulated when soil moisture was low during vegetative season but was followed by normal-levels of rainfall after V12 N fertilization. In contrast, a lack of N uptake increase was observed by Ning et al. (2017) with supplemental late-season N applications when high vegetative N supply was achieved (pre-silking N uptake > 157 kg ha⁻¹). Changes in N uptake proportion seems to be primary dependent on early growth conditions determining vegetative N, while post-silking N uptake is attached to the correspondent source-sink ratio and directed by late-season plant growth conditions.

In unconstrained environments, considerations on the role of source-sink ratio in late N uptake in maize are critical due to the negative association between N remobilization with increasing source-sink levels (Uhart and Andrade, 1995). In particular, the source-sink regulation

supports the idea that post-silking N uptake is driven by dry matter accumulation (Yang et al., 2016). Under normal growth conditions, N uptake is related with the level of carbohydrates supply to the roots (Pan et al., 1995). In the same way, N uptake is known to be C regulated and stimulated by the photosynthetic flow (Lillo, 2008; Masclaux-Daubresse et al., 2010). Therefore, assimilate availability during the grain filling period, by consequence, affects the proportion of post-silking N uptake. Lower post-silking N uptake (< 17% relative to the total N at maturity) was documented under artificially source-limited conditions (Rajcan and Tollenaar, 1999a; Yang et al., 2016). On the other hand, with increasing source-sink environments, greater proportion of post-silking N uptake was observed, demonstrating the role of sink strength in promoting N uptake (Rajcan and Tollenaar, 1999a; Yang et al., 2016). Thus, under non-limiting yield environments, late-season N applications may be beneficial in a window of source-sink balance where the assimilate availability is sufficient for maintaining N uptake for supplying the grain N demand.

Conclusions

A repeatable grain yield response to late N fertilization was not identified in maize, but heterogeneous effects in a meta-analysis did quantify scenarios where L_N did improve yield. Post-silking N uptake was proposed as a potential indicator of grain yield and REN responses to late N fertilization. The use of NNI can bring opportunity to develop an index to inform tactical decisions. This review suggests the existence of crop growth conditions prone to a greater N uptake during reproductive stages, where this type of applications might be more suitable. Due to the complex plant C and N economy, future research should attempt to integrate carbohydrates levels with N dynamics in the plant upon which to elucidate critical thresholds for potentially

assisting in the identification of productive opportunities to realize late-N fertilization in maize.

Advanced crop modeling frameworks can provide such integrative prediction frameworks.

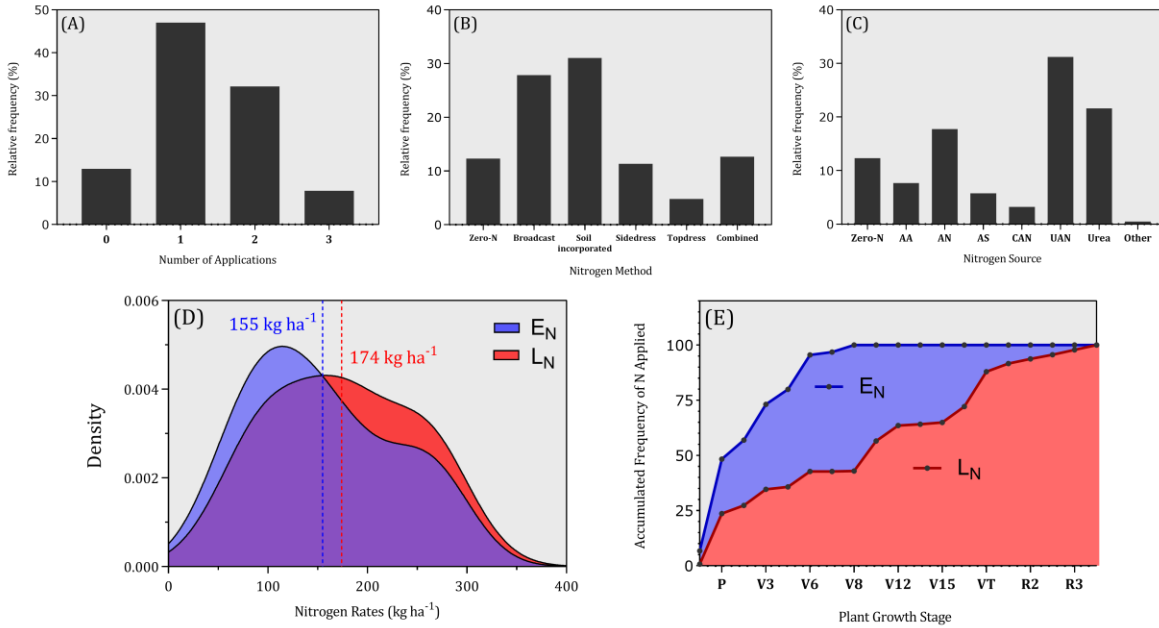


Figure 2.1. Description of fertilizer nitrogen (N) management variables across the dataset. Upper section: A, B, and C) Relative frequency (%) of the number of N applications, method of N application, and N fertilizer source, respectively. Abbreviations: Zero N, no N applied; AA, anhydrous ammonia; AN, ammonium nitrate; AS, ammonium sulfate; CAN, calcium ammonium nitrate; UAN, urea ammonium nitrate. Lower section: D) Fertilizer N rates density distribution plot (kg ha⁻¹), and E) accumulated frequency for the two N-timing groups considered (E_N: Early N; L_N: Late N). Dashed vertical lines and values represent the mean N rates. Abbreviations: P, planting; V_n, vegetative (nth) stage; R_n, reproductive (nth) stage.

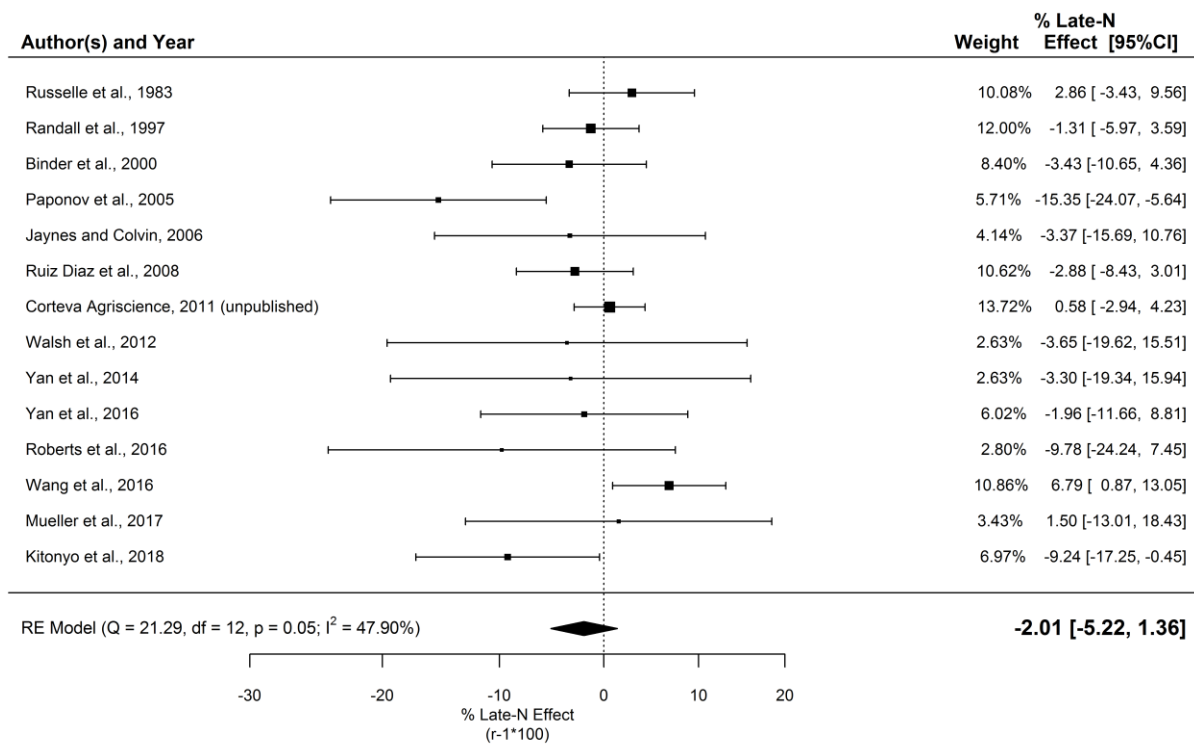


Figure 2.2. Forest plot summarizing a yield effect comparison between late-season and early-season N for each experiment. Effect sizes and 95% confidence intervals (CI) are expressed as a late-N effect ratio (percentage of grain yield variation in L_N / E_N) calculated as (6). Square symbols represent point estimates and whiskers depict their respective 95% CI. The weight of each study is expressed in percentage of the overall model and illustrated by the thickness of box and whiskers. RE = random effects model, Q = Cochran’s Q test statistic; I^2 = I-square statistic.

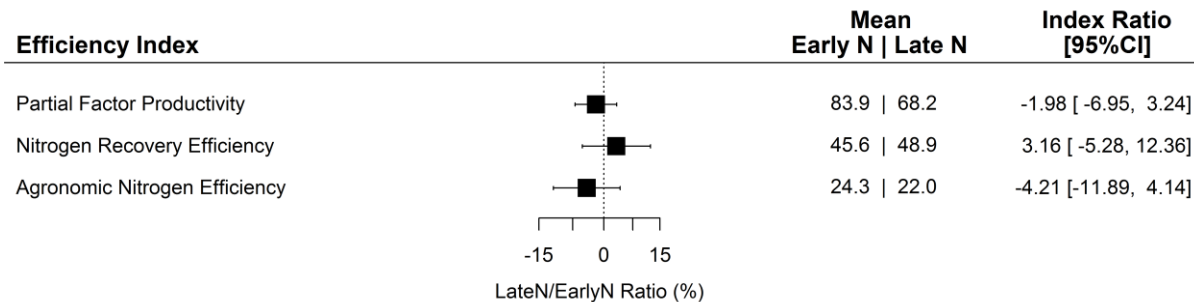


Figure 2.3. Forest plot with aggregate summary effect sizes of the late-N effect ratio (%) for partial factor productivity (PFPN), fertilizer N recovery efficiency (REN), and agronomic efficiency of N (AEN), calculated as the percentage of variation in L_N to E_N ratio. Square

symbols represent point estimates and whiskers depict their respective 95% CI. Means for each N-timing group (early and late N) and mean effect ratios are presented.

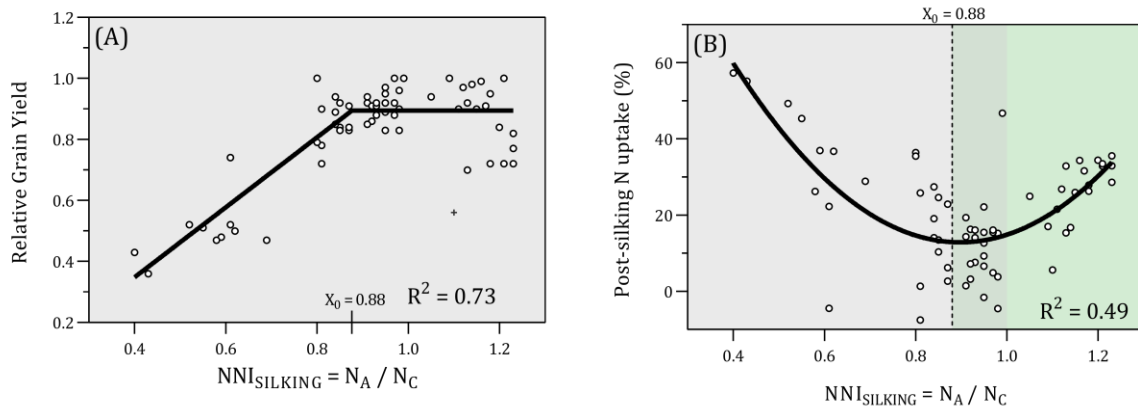


Figure 2.4. (A) Relationship between Nitrogen Nutrition Index at silking ($NNI_{SILKING}$) and relative grain yield. Solid line represents a bilinear regression for the data. Model parameters (standard errors listed in parenthesis) are: $Y_1 = -0.11(0.09) + 1.15(0.12)X$ if $X < X_0 = 0.88(0.03)$, and $Y_2 = 0.89(0.01)$ if $X > 0.88(0.03)$; $R^2 = 0.73$. (B) Relationship between $NNI_{SILKING}$ and $NU_{Post-Silking}$ (%). Solid line represents a quadratic function fitted for the data. Model parameters (standard errors in parenthesis) are: $Y = 166(18.63) - 341(43.79)X + 190(25.01)X^2$; $R^2 = 0.49$. Dashed line indicates X_0 of 4A fitted regression to differentiate N nutrition conditions. $NNI_{SILKING} > 1$ was differently shaded to illustrate a situation of no N deficiency. N_A = N concentration of shoot biomass; N_C = critical N concentration (Plénet and Lemaire, 2000).

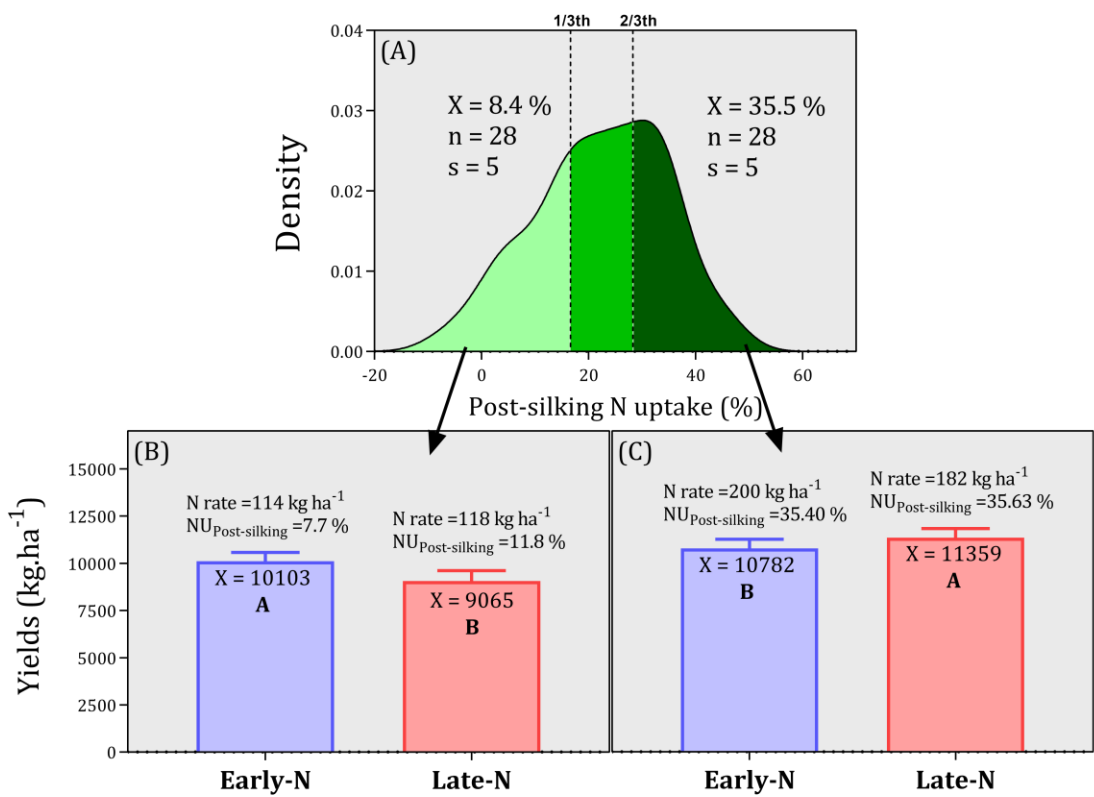


Figure 2.5. A) Density distribution plot for $NU_{\text{Post-Silking}}$ on a subset of the general database reporting N uptake information on N-fertilized cases ($n=84$). Dashed lines and colors are separating the data in lower, median, and upper 33.3th percentiles. Reported values are for lower and upper sections: X = mean $NU_{\text{Post-Silking}}$ (%); n = number of observations; s = number of locations by years. At the bottom, mean grain yield values in kg ha^{-1} for E_N and L_N for the B) lower, and C) upper thirds on the post-silking N dataset (Supplementary Material, Table A.2). X = means; N rate = fertilizer rates in kg ha^{-1} ; $NU_{\text{Post-silking}}$ = post-silking N uptake proportion in %. Different letters indicate significant differences at $P \leq 0.05$.

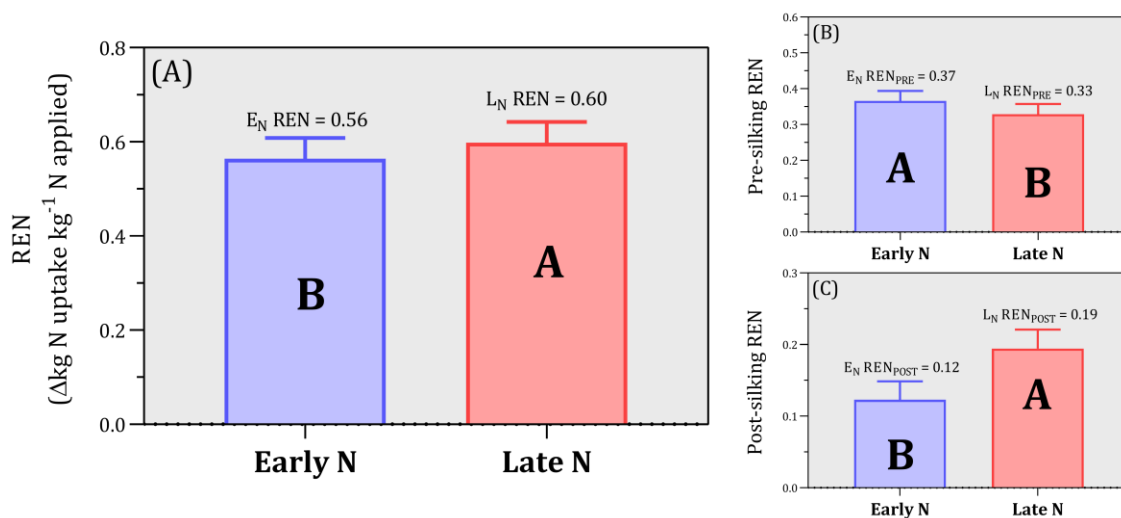


Figure 2.6. Bars representing fertilizer N recovery efficiency (REN) for each N group (E_N , $n = 56$; L_N , $n = 44$) (A). Whiskers represent standard errors (S.E.) for the mean. At the right, bars for pre-silking REN (Δkg pre-silking N uptake relative to Z_N / kg N applied) (B), and post-silking REN (Δkg post-silking N uptake relative to Z_N / kg N applied) (C) for E_N and L_N groups. Different letters indicate significant differences at $P \leq 0.05$.

Table 2.1. Number of study, references, site - country, years of experiments, experimental design, tillage, main factors tested, and type of study (published or unpublished) for each maize experiment in the dataset.

No	Reference	Site – Country	Year	Design	Tillage	Factors ¹	Study
1	Binder et al., 2000	Nebraska, USA	1993, 1994	RCB ² Split-plot	Conventional	NR, NT	Published
2	Jaynes and Colvin, 2006	Iowa, USA	2002, 2004	RCB	Reduced	NR	Published
3	Kitonyo et al., 2018	Embu, Kenia	2015 - 2016	Split-plot	Conventional / no-till	TS, NR, NT	Published
4	Mueller et al., 2017	Indiana, USA	2014, 2015, 2016	Split-plot	Reduced	NR, NT, G	Published
5	Paponov et al., 2005	Heidfeldhof / Muttergarten, Germany	1997	RCB	Not reported	NR, D, G	Published
6	Randall et al., 1997	Minnesota, USA	1986, 1987, 1989	RCB	Conventional	NT, NM, NR, NS	Published
7	Roberts et al., 2016	Arkansas, USA	2011, 2012	RCB	Not reported	NR, NT	Published
8	Ruiz Diaz et al., 2008	Iowa, USA	2004, 2005, 2006	RCB	Conventional / strip-till / no till	NR	Published
9	Russelle et al., 1983	Nebraska, USA	1979, 1980	Not reported	Not reported	PD, NR, NT	Published
10	Walsh et al., 2012	Oklahoma, USA	2005, 2006, 2007	RCB	Not reported	NR, NT	Published
11	Wang et al., 2016	Changwu, China	2013, 2014	RCB	Not reported	NT	Published
12	Yan et al., 2014	Hebei, China	2010, 2011	Split-plot	No till	NR, G	Published
13	Yan et al., 2016	Hebei, China	2013, 2014	Split-plot	Not reported	NR, D	Published
14	Corteva Agriscience, 2011	Illinois, USA	2011	Split-plot	Conventional	G, NR	Unpublished

¹ NR = Nitrogen rates, NT = nitrogen timing, NM = nitrogen method, NS = nitrogen source, G = genotypes, PD = planting dates, D = planting density, TS = tillage system.

² RCB = Randomized complete block

Table 2.2. Summary statistics of the extracted dataset across Zero N, Early N, and Late N fertilization timing groups: n, number of observations; mean; SD, standard deviation; Min-Max, minimum and maximum. Grain yield per unit area and adjusted to a standard moisture basis of 155 g H₂O kg grain⁻¹. Abbreviations: PP = growing season precipitation, PNU_{PM}= plant N uptake at physiological maturity per unit area, PNU_{SILK}= plant N uptake at silking per unit area, Grain N = N in the grain fraction per unit area, GNC = grain N content, NU_{Post-Silking} = percentage of total PNU that occurs from the period that goes from silking until physiological maturity, REN = fertilizer N recovery efficiency; AEN = agronomic efficiency of N, PFPN = partial factor productivity of N.

Variable	Unit	Zero-N (Z _N)				Early-N (E _N)				Late-N (L _N)			
		n	Mean	SD	Min-Max	n	Mean	SD	Min-Max	n	Mean	SD	Min-Max
Grain yield	Mg ha ⁻¹	81	7.5	2.7	2.3-13.0	295	10.9	2.9	2.3-16.9	249	10.4	3.3	2.7-17.5
Harvest Index	Dimensionless	16	0.47	0.05	0.36-0.54	12	0.54	0.03	0.51-0.60	42	0.51	0.05	0.38-0.61
Season PP	mm	32	473	206	274-1139	131	532	204	274-1139	174	499	204	274-1139
Seeding Rate	pl m ⁻²	50	7.62	2.09	5.0-15	183	7.02	1.13	5.3-10	212	7.19	1.75	5.0-15
Row Space	m	81	0.76	0.08	0.6-1	295	0.76	0.05	0.6-1	249	0.76	0.07	0.6-1
N Rate	kg ha ⁻¹	-	-	-	-	295	155	69.5	60-270	249	174	68.6	45-315
PNU_{PM}	kg ha ⁻¹	23	105.3	33.7	52-175	81	170	52	49-306	59	200	51	103-291
PNU_{SILK}	kg ha ⁻¹	14	61.4	16.3	40-84	45	133.8	22.3	103-190	39	143.3	21.8	108-190
Grain N	kg ha ⁻¹	21	62.0	19.9	19-106	92	117.3	47.8	26-263	146	118.9	43.2	35-254
GNC	mg g ⁻¹	19	11.2	1.9	6.9-15.0	84	12.7	2.8	9.6-26.6	141	12.3	2.7	8.9-29.1
NU_{Post-silking}	%	14	32.2	16.2	-4.4-57.3	45	18.1	12.9	-7.5-44.1	39	27.2	9.4	5.6-46.8
REN	kg N kg ⁻¹ N applied	-	-	-	-	111	45.6	22.1	0-106	108	48.9	28.8	0-111
AEN	kg GY increase kg ⁻¹ N applied	-	-	-	-	271	24.3	17.1	-9.9-79.1	193	22	15.1	-9.5-85.2
PFPN	kg GY kg ⁻¹ N applied	-	-	-	-	295	83.9	41.9	14-218	249	68.2	32.9	15-216

Chapter 3 - Integrating nitrogen and water-soluble carbohydrates dynamics in maize: A comparison of hybrids from different decades

Published in Crop Science

Fernandez, J. A., Messina, C. D., Rotundo, J. L., & Ciampitti, I. A. (2021). Integrating nitrogen and water-soluble carbohydrates dynamics in maize: A comparison of hybrids from different decades. *Crop Science*, 61(2), 1360-1373.

Abstract

During a century of maize (*Zea mays* L.) breeding, yield genetic gain was largely determined by increased reproductive resilience under stress and establishment of sink size (number of grains per unit area). Considering grains as competing sinks for C and N assimilates, understanding changes in the C and N economy can provide insights to define selection criteria towards a sustained yield improvement. A cognitive framework to define such criteria may consist in connecting the water-soluble carbohydrates (WSC) and N dynamics in stem and leaves with the reproductive sink strength during post-flowering. The objectives of this study were to advance such framework by (a) quantifying grain N demand and remobilization capacity in two hybrids as affected by N availability, and (b) formalizing how the interplay between N and WSC remobilization influence grain growth. Single cross hybrids 3394 and P1197 (released in 1991 and 2014) were evaluated to represent keystone phases of germplasm development (conventional and molecular breeding eras). P1197 outyielded 3394 consistently under high N supply, and its better N utilization efficiency was reflected through a lower grain N concentration. Under high N, the ability to maintain a greater leaf area during late grain-filling for P1197 resulted in a reduced leaf N remobilization. Although yield was not limited by C supply, 3394 exposed greater remobilization of WSC during late grain-filling. This study contributes to advance the

development of a relevant C to N framework to further analyze drivers of genetic yield gain and assist in selection strategies in maize.

Introduction

In maize (*Zea mays* L.), grain yield can be conceived as a function of two interdependent components: the amount of photoassimilates produced by “source” organs via plant growth, and the capacity to transform them into harvestable yield in the reproductive sink. Over a century of maize breeding and selection, both source and sink were implicated in grain yield increments (Duvick, 2005a; Cooper et al., 2014b). From a sink strength standpoint, several authors emphasized on the greater grain number per unit area as the major contribution in historical hybrids studies, while grain weight contribution was less significant (Duvick, 2005a; Hammer et al., 2009; Haegele et al., 2013; Egli, 2015; Reyes et al., 2015). In addition, changes in leaf angle and standability were implicated in improvement in light use efficiency further increasing source capacity (Duvick et al., 2004). While plant growth and photosynthesis have been linked to kernel set improvement (Echarte et al., 2004, 2008; Messina et al., 2019), leaf nitrogen (N) dynamics were affected and retention of N in the leaves led to the phenotype known as “stay green” (Duvick and Cassman, 1999; Chen et al., 2015; DeBruin et al., 2017). The current hypothesis proposes that reproductive efficiency increased over time (sink size) underpinning a concomitant increase in leaf area, light interception, and retention of leaf N, thus increasing canopy photosynthesis (source capacity). Because of the underlying carbon (C) and N interplay, it is intuitive to study how both source and sink capacities may affect grain number and weight determination in hybrids from different Eras.

The accumulation and partitioning of carbohydrates among plant structures are dependent on the relative sink strength of each organ. During vegetative stages when the demand of C for

reproductive growth is low, plants accumulate non-structural sugars in stems revealed mainly by high concentrations of sucrose (Bihmidine et al., 2013). This phenomenon is well documented in maize where stem parenchyma plays an important role as storage organ (Fairey and Daynard, 1978) that supplies additional carbohydrates to maintain grain growth during grain filling (Daynard et al., 1969; Setter and Meller, 1984; Ouattar et al., 1987a). During the critical window for grain set around flowering and lag phase, cob and husks play a transient role as reservoir for later translocation to the grains (Palmer et al., 1973; Cliquet et al., 1990; Paponov and Engels, 2005). During reproductive stages, fixed C is primarily destined for the growth of the developing grains (Cliquet et al., 1990) and changes in stem water-soluble carbohydrates (WSC) concentration ([WSC]) may occur reflecting the net balance of sugars (Ouattar et al., 1987a). This balance varies across hybrids and growing conditions, with carbohydrates remobilization during grain filling ranging from -7 to 19 % under non-stressed (Simmons and Jones, 1985; Uhart and Andrade, 1995; Sekhon et al., 2016) and from 26 to 74 % in stressed maize crops (Ouattar et al., 1987a; Uhart and Andrade, 1995). Assimilates for grain filling are thus supplied by carbohydrates from current photosynthesis and from remobilization of reserves stored in vegetative organs (Gastal et al., 2014) in a ratio that depends on the genotype-environment combination. Characterization of the dynamics of C reserves in contrasting hybrids can advance our understanding of the changes in C assimilation and utilization between different phases of germplasm development. While increased C fixation at the canopy level due to increased plant density may lead to the utilization of pre-grain fill stored C and the associated reduction in [WSC], extended photosynthetic capacity due to N retention in leaves (Mueller et al., 2019a) may be conducive to the maintenance of [WSC].

The close relationship existing between C and N metabolisms (Below et al., 1981) implies that the supply on one of them may trigger disruptions on the other (Valluru et al., 2011). Nitrogen uptake and assimilation processes occur upon C consumption (Banziger et al., 1994) as C skeletons are essential for amino acids biosynthesis (Foyer et al., 1998). At plant-level, N deficiency reduces leaf N and photosynthetic rate (Sinclair and Horie, 1989). During grain development, a feedback control on the sink capacity regulates not only C demand but also amino acids biosynthesis (Ning et al., 2018). Understanding the dynamics of C and N assimilates can help develop an integrated C-N framework to inform selection strategies to sustain yield gain.

The concept of yield genetic gain over time conceal intrinsic changes in source and sink components for both N and C dynamics. An adequate framework should recognize the relevance of grain demand for N and carbohydrates (i.e. sink), and shoot remobilization capacity (i.e. source), while considering their interactions with current N and C assimilation (Lawlor, 2002; Jones et al., 2003; Messina et al., 2009; van Oosterom et al., 2010). To advance on this concept, this study proposes to analyze yield changes in genotypes through the underlying N and WSC fluxes following the framework presented in Figure 1. Firstly, the demand for N from the developing grains can be described through the product between grain [N] and the grain growth rate during post-flowering (van Oosterom et al., 2010). Variations in sink strength between hybrids have to be weighted against rates of stem and leaf N translocation to capture differences in N supply from remobilization of vegetative tissues. As stem N remobilization can be assumed to occur when the [N] is above a structural N value (Jamieson et al., 2008), it is also required to describe underlying changes in the minimum [N]. The effect of leaf N remobilization on photosynthesis can be captured through the N content per unit of leaf area (SLN, specific leaf N)

(Sinclair and Horie, 1989; Muchow and Sinclair, 1994). The isolation of grain, stem, and leaf N utilization mechanisms in this model may allow us to determine their contribution to the enhanced N internal efficiency in modern hybrids (grain yield per unit of N uptake at maturity) (Ciampitti and Vyn, 2012). As an alternative, enhanced reproductive efficiency can be analyzed as the result of increased carbohydrate assimilation and allocation to the grains (Reyes et al., 2015). Soluble carbohydrates (reflected as WSC) stored in the stems can be used as an indicator of C assimilate availability (Rajcan and Tollenaar, 1999a). Therefore, genotypic changes in WSC content at flowering and WSC remobilization rates during post-flowering are considered within the proposed framework. While such model can be used to relate yield variations between hybrids with trajectories of N and WSC remobilization, it is essentially structured to provide a quantitative description of both C and N dynamics but contemplating regulations on source-sink dynamics.

This research can contribute to advance on a C and N framework to enhance future selection by considering a co-regulation on the reproductive resilience of maize hybrids. The specific objectives of this study were to i) implement the proposed N and WSC framework to explain yield determination in two hybrids as affected by contrasting levels of N availability, and to ii) describe how the interplay between N and WSC remobilization influence grain growth through changes in stem and leaf N and C economy.

Materials and methods

Field experiments

Field experiments were conducted at the Kansas State University Ashland Bottoms Research Farm, Manhattan, KS (39°08' N, 96°37' W) during 2017 and 2018 growing seasons.

Soil analyses were conducted pre-planting to characterize initial conditions. Overall, soil properties for the area in 2017 and 2018 respectively were: i) at a 15 cm layer: pH, of 6.08 and 6.13; organic matter (OM-LOI), 15 and 16 g kg⁻¹; phosphorus (Mehlich), 45 and 48 mg kg⁻¹; and ii) at a 60 cm depth: available N was 79 and 61 kg ha⁻¹ (inorganic N pool). Table 1 presents climatic data for the 2017 and 2018 growing seasons.

Two maize Pioneer (Corteva Agriscience, Johnston, IA, US) hybrids (year of release in parenthesis) 3394 (1991) and P1197 (2014) were evaluated under two contrasting N scenarios, in two sites during 2017 (one under furrow irrigation using gated pipes, and one rainfed conditions) and one (furrow irrigated) during 2018. The 3394 and P1197 hybrids were evaluated to represent a sample of the 1990's and 2010's phases of germplasm development, respectively. The 3394 is a pre-GMO maize hybrid while the P1197 is from the post-GMO era (www.corteva.com). These were among the most stable and successful hybrids in 100 years of breeding, with 3394 more tolerant to stress than P1197 (Cooper et al., 2020). Physiological differences due to breeding and tolerance to stress can help unravel or expose novel mechanisms in the economy of C and N.

Experiments were planted on May 5th in 2017 and April 24th in 2018, with a plant density of 76,000 (2017 and 2018) and 61,000 (2017) plants ha⁻¹ for irrigated and rainfed sites, respectively. The previous crop was soybean [*Glycine mar (L.) Merr.*] in 2017 and maize in 2018. Soil available-water content at planting was 93 mm (2017) and 80 mm (2018) to a depth of 0.6 m. Irrigation started at five-leaf growth stage (V5, Ritchie et al., 1997) and ended at R6, and was performed to maintain soil moisture above 60% of the soil saturation percentage (two and five times, respectively for 2017 and 2018). The experimental layout was arranged in plots of 4 rows, 76 cm apart, and size of 3 m wide × 21 m long. The experimental area was kept free of weeds, pests, and diseases during the growing season.

Each site in 2017 was performed in a split-plot design (with three replications) with hybrid at the whole-plot level and N at the sub-plot. Two N scenarios were analyzed: i) zero N, with no N applied as fertilizer; and ii) full N, nesting two sub-treatments within (ii_a and ii_b), differing only in the timing of the last N fertilization. Nitrogen fertilization rates differed between water environments as it was adjusted for N demand based on yield target for each condition. Total N applied was 137 kg N ha⁻¹ and 218 kg N ha⁻¹, respectively for rainfed and irrigated conditions, as urea-ammonium nitrate (UAN 28%). Fertilization program consisted of: an initial 56 kg ha⁻¹ application at planting; a second at V6 growth stage (56 kg ha⁻¹ and 112 kg ha⁻¹ for rainfed and irrigated, respectively), and a last N application (25 kg ha⁻¹ and 50 kg ha⁻¹ for rainfed and irrigated, respectively) performed at ii_a) flowering (R1, Ritchie et al., 1997) or ii_b) two weeks after R1 growth stage. While N timing sub-treatments were included as factors for statistical modeling, they were not of interest for interpretations, and treatment effects were analyzed at the level of fertilized versus non-fertilized treatment factor. In 2018, the study was carried out in two adjacent RCBD structures (with six replications), one per N level: i) zero N; and ii) full N, maintaining the final N rate as the preceding year for irrigated conditions; 56 kg ha⁻¹ at planting, and 162 kg ha⁻¹ at V6.

Measurements and laboratory analyses

Plant biomass samples were taken on three occasions in 2017 (R1, R1 + 14 days, and R6) and eleven in 2018 (V6, V12, V16, R1, and repeatedly from there, at one-week intervals until physiological maturity was reached). Harvest area was adjusted from 2.6 m² (20 plants) at V6, 1.3 m² (10 plants) at V12, to 0.66 m² (5 plants) during late vegetative and reproductive period, to compensate for lower plant tissue at early stages. Plants from the center rows were cut at the

ground level and fresh weight was determined. A representative subsample of three plants was separated in leaves (green leaf blades), stem (stems + leaf sheaths + attached dead leaves + tassels), ear (husks + cobs), and grain fractions (if present). Specifically, grain fractions were separated at all post-flowering samplings starting from R1 and including R6. Dry weight of samples was obtained after drying at 65°C until constant weight. For laboratory analyses, samples were ground through 0.25 mm sieve.

Green leaf area index (LAI) measurements were taken at the same date of the three biomass samplings in 2017 (R1, R1 + 14 days, and R6) and at five of the destructive sampling dates in 2018 (R1, R1+1, R1+2, R1+3, and R1+5 weeks). One above- and four below-canopy readings were obtained in each plot with the LAI-2200C plant canopy analyzer (LI-COR Biosciences Inc., Lincoln, NE). The LAI-2200C infers leaf area from measurements of the fraction of diffuse radiation passing through the canopy (LI-COR Biosciences Inc., Lincoln, NE). Below-canopy readings were taken on a 45° diagonal line between the two-center rows just below the first green leaf but above senesced leaves. Measurements were then analyzed to obtain LAI estimates using the FV2200 software (version 2.1.1, LI-COR Biosciences Inc.). Canopy SLN (g m^{-2}) was estimated as the leaf N content per unit area divided by the green LAI.

At physiological maturity, numerical yield components grain number and weight were determined. A subsample of 500 grains was counted and weighed separately to estimate grain weight. Grain number was quantified by the total amount of grains in the three subsampled plants at R6 sampling and adjusted by the wet weight in the total harvested area (0.66 m^2). Yield was determined with a plot combine from the two center rows; harvest area was corrected in rows where biomass samples were taken. Grain yield was adjusted and reported to a standard 155 g kg^{-1} moisture.

Ground samples for each fraction were analyzed in a laboratory for N concentration ([N]) by combustion (Matejovic, 1995). Total N uptake was calculated from the sum of N content in leaves, stem, ears, and grains (dry biomass multiplied by [N] of each tissue). The [WSC] was determined on stem fraction, by sequential extractions in water followed by colorimetric reaction using the anthrone reagent method (Galicia et al., 2009). The total content in the stem was calculated by multiplying the [WSC] with the respective dry biomass for that organ.

Statistical analysis and calculations

Data were subjected to an analysis of variance (ANOVA) for each trait in 2017 and 2018 experiments. Mixed effects models (with N and hybrid as fixed effects factors) were fitted in RStudio (RStudio Team, 2016) with *nlme* (Pinheiro et al., 2018) and *lme4* (Bates et al., 2015) packages. Due to the absence of a rainfed trial in 2018, and the relatively wet growing season in 2017 to explore variability between conditions, water environment was modelled as a random-effect factor. Fitted models for 2017 and 2018 experiments are described in equation (1) and (2) respectively (fixed effects are denoted using Greek alphabet characters and random effects using Latin characters),

$$y_{ijklm} = \mu + \alpha_i + \beta_j + \delta_{k(i)} + \alpha\beta_{ij} + \beta\delta_{jk(i)} + b_l + c_{m(l)j} + \varepsilon_{ijklm} \quad \text{Equation 3.1}$$

$$b_l \sim N(0, \sigma_b^2),$$

$$c_{m(l)j} \sim N(0, \sigma_c^2),$$

$$\varepsilon_{ijklm} \sim N(0, \sigma_\varepsilon^2),$$

where μ is an overall mean; α_i and β_j are differential effects of N and hybrid treatments; $\delta_{k(i)}$ the effect of N timing sub-treatments within N fertilization; $\alpha\beta_{ij}$ and $\beta\delta_{jk(i)}$ are the interaction terms among them; b_l is the random effect for each water environment; $c_{m(l)j}$ is the random

effect of the whole plot within site and by hybrid; and ε_{ijklm} is the random effect of the residual term;

$$y_{ijkl} = \mu + \alpha_i + \beta_j + \alpha\beta_{ij} + b_{k(i)} + c_{l(i)} + \varepsilon_{ijkl} \quad \text{Equation 3.2}$$

$$b_{k(i)} \sim N(0, \sigma_b^2),$$

$$c_{l(i)} \sim N(0, \sigma_c^2),$$

$$\varepsilon_{ijkl} \sim N(0, \sigma_\varepsilon^2),$$

where μ is an overall mean; α_i , β_j , and $\alpha\beta_{ij}$ are the differential effect of N, H, and interaction among them, respectively; $b_{k(i)}$ is the random effect of each N main-plot; $c_{l(i)}$ is the random effect of blocks within N main-plot; and ε_{ijkl} is the residual term. Significance for main effect of N (α_i) was not fit due to the lack of degrees of freedom considering that only one main-plot per N level was included in the experiment. Because dry biomass, N and WSC content, SLN, and LAI were sampled at multiple times during the growth cycle, a fixed factor γ_m representing the differential effect of sampling time, and the corresponding two- and three-way interactions with N and hybrid were included in models (1) and (2), as well as a random effect term to model the repeated measure structure within plots.

Residual graphs were verified for homogeneity of error variances, and heteroscedasticity corrections were made accordingly. Pairwise comparisons with a type I error rate set at 0.05 were performed using the Tukey-Kramer method. A relationship between grain N yield with grain [N] and yield was determined using the *loess()* function in R (Cleveland et al., 1992). Applying a prediction function on this relationship, grain N yield isolines were plotted in a contour plot to represent the effect of grain [N] on yield at a similar level of grain N accumulation.

Cubic-splines smoothers were fitted to the estimated means across fixed effect levels for plotting non-linear trajectories using *smooth.spline()* function. Statistical differences between smoothing spline estimates were tested based on 95% confidence intervals using bootstrapping procedures (5,000 iterations)(Efron and Tibshirani, 1993; Wang and Wahba, 1995). Grain growth rates, stem and leaf remobilization rates of N and WSC, and N uptake rates were calculated using the first derivative of the cubic-splines for grain dry biomass accumulation, stem and leaf N and WSC content, and total N uptake, respectively. Rates were estimated for each condition at a given time (t), where t represent the thermal time at each sampling date. Thermal time for each sampling date was calculated from the time of planting (provided that emergence date was not recorded) or flowering using a beta-function relationship between the rate of development and hourly temperature ($T_b = 8^\circ\text{C}$, $T_{opt} = 33^\circ\text{C}$, $T_u = 40^\circ\text{C}$)(Zhou and Wang, 2018). Since the crop ceases growth and deposition of assimilates at physiological maturity, evaluated grain growth rates were set to zero at the R6 boundary.

Results

Yield, yield components, and N uptake

On average across year \times N conditions, yield increased with increasing N uptake, but at a higher rate for P1197 (63 ± 4 and 59 ± 3 kg ha⁻¹ per kg of N for P1197 and 3394, respectively) (Fig. 2A). Yield increased with increasing N supply more in P1197 than 3394. On average, P1197 outperformed 3394 by 2.4 and 3.0 Mg ha⁻¹ under high N-input (in 2017 and 2018, respectively) (Table S1). However, yield differences under N stress were smaller in 2017 and negligible in 2018. This means that greater yield recorded for P1197 came not only from higher N uptake relative to the 3394, but also from an improved yield per unit of N ratio (Fig. 2A).

While yield increased up to $268 \pm 13 \text{ kg ha}^{-1}$ of N uptake for P1197, grain number reaches a plateau at 4417 grains per square meter with $223 \pm 17 \text{ kg ha}^{-1}$ of N uptake (Fig. 2B). Hybrid 3394 showed an inferior grain set per unit of N, achieving a similar grain number at a level of N uptake of 289 kg ha^{-1} . Since the response of grain weight to N uptake was constant and statistically same between hybrids ($\alpha=0.05$, Fig. 2C), the greater yield observed for P1197 relative to 3394 at a high N availability was due to the improved ability of P1197 to set grains per unit of N absorbed. Harvest index followed the same pattern of response to total N uptake as grain weight, reaching a plateau at $166 \pm 18 \text{ kg N ha}^{-1}$ with a value of 0.52 for P1197 and 0.50 for 3394 (Fig. 2D).

The use of contrasting N levels provided the opportunity to explore a broad range of post-flowering N uptake for the tested genotypes. In a similar manner for both hybrids, yield was improved with increasing N uptake during post-flowering period at an average rate of 0.12 Mg of grain per kg of N (Fig. 3A). The y-intercept of this function suggests that an approximate base yield of 3.67 Mg ha^{-1} could be attained with only N assimilated prior to grain fill and remobilized from vegetative mass. Above this baseline, the number of grains established around flowering defined the demand for post-flowering N uptake (Fig. 3B), averaging a demand of 2.7 mg N grain⁻¹, with a minimum grain set of 1268 grains m⁻².

When considering the full N treatment, one of the mechanisms associated with the improved grain set efficiency in P1197 was the reduction in the targeted grain [N] (Fig. 3C). The slope between dry weight and N content per grain during grain filling represents an average grain [N] of 13.8 mg g^{-1} for 3394 and of 12.6 mg g^{-1} for P1197. A similar analysis under zero N conditions resulted in non-significant differences in grain [N] between 3394 and P1197 (1.04 and 1.02 mg g^{-1} , respectively; data not shown). Essentially, observed differences in grain [N]

between genotypes were accentuated with high yield (Fig. 3D). However, isolines for grain N yield (kg ha^{-1}) revealed that the modern hybrid (P1197) presented a greater grain N accumulation. This outcome suggests that grain N dilution partially accounts for yield increases, thus underpinning adjustments in N uptake and remobilization dynamics between hybrids.

Dynamics of N and WSC in stems and leaves

Dynamics WSC content in stem and N content for stem and leaf fractions were plotted for each N level within hybrid for both study years (Fig. 4). During 2017, no differences between hybrids were observed for N and WSC content dynamics along the growing season. Variations perceived were mainly attributed to the tested N scenarios. In 2018, differences between N levels were consolidated due to a greater response to N fertilization in the full N treatment. Consistent with yield increases observed for this treatment \times year, dynamics of N and WSC were significantly different between hybrids. The P1197 showed less stem N content during post-flowering under full N (Fig. 4B). Meanwhile, differences in leaf N between hybrids were only noticeable during late grain fill ($p < 0.05$, Fig. 4D). The hybrid P1197 retained more N in the leaves than 3394 as approaching physiological maturity (at maturity, 1.5 vs. 2.9, g m^{-2} for 3394 and P1197, respectively). In line with this, and due to the close relationship between N and C remobilization, P1197 exhibited an increase in WSC relative to 3394 only during the last week before reaching maturity under full N (169 and 126 g m^{-2} at R6, respectively for each hybrid).

In a similar way for both genotypes, N deficiency did not affect the pre-flowering accumulation of WSC reserves. As a result, zero and full N treatments achieved comparable stem WSC contents around flowering. However, the effect of N supply on WSC remobilization was evident during post-flowering. Stem WSC was then consistently lower under zero N than full N

at the end of grain filling (at R6 in 2017: 63 and 98 g m⁻², zero and full N respectively and averaged between hybrids – and in 2018: 68 and 147 g m⁻², respectively; Fig. 4E and F).

Because yield differences between hybrids were mainly observed when the crops were fertilized, the analysis focused on describing genotypic differences in the remobilization processes under full N conditions. Under these conditions, N remobilization from leaves progressed linearly in response to grain N demand for both hybrids (Fig. 5A). However, differences in this relationship suggest that P1197 was able to remobilize less N from leaves per unit of N allocated to the grains ($p < 0.05$). It was estimated that 3394 remobilized 4.73 g N m⁻² from leaves at maturity, while P1197 a total of 4.52 g N m⁻². Interestingly, this was associated with a non-significant genotype effect on the SLN dynamics (Fig. 5B). These findings indicate that the reduced leaf N remobilization in P1197 was more associated with higher LAI rather than with changes in SLN. On average for both years, estimated LAI at maturity was 2.5 m² m⁻² for 3394 and 2.8 m² m⁻² for P1197 under high N-input (i.e. 11% increase for P1197; Table S1). At the same time, however, it is important to recognize that P1197 evidenced an 8% increase in green LAI at flowering under full N (4.8 and 5.2 m² m⁻², respectively for 3394 and P1197 and averaged for both years; data not shown). Hence, differences in LAI decline were only marginal and comparable to the small shift in leaf N remobilization between hybrids.

Differences in leaf N remobilization were in line with changes in N remobilization from stem tissues. The hybrid P1197 generally showed greater values of N remobilized during early stages of grain N accumulation (Fig. 5C). As such, the modern hybrid seems to hold N in the leaves longer at the expense of N remobilization from stem tissues. A lower minimum stem [N] in this hybrid may represent one of the mechanisms linked to this superior N supply from stem tissues (Fig. 5D). Under fertilized conditions, the asymptotic quantile regression indicates a

minimum stem [N] of 4.19 mg g⁻¹ in 3394 and of 3.30 mg g⁻¹ in P1197 under full N scenario (Fig. 5D).

Grain N demand related to N and WSC remobilization from stems and leaves

In this section, we aim to illustrate the close link between N and WSC remobilization. Figure 6 shows N translocation rates from stem and leaves along with grain growth rates during the post-flowering under full N (Fig. 6). The maximum grain growth rate per area was estimated at 538 °C d (3394) and 594 °C d (P1197) after flowering (Fig. 6A). During the first half of grain filling (i.e. before reaching maximum grain growth rate), N was primarily remobilized from stems but at a declining rate (Fig. 6C). In contrast, N translocation from leaves was intensified during early stages of grain filling following the increment in grain growth rates and, consequently, N demand (Fig. 6B). Regardless of minor deviations in stem net N accumulation and N uptake, comparable rates were obtained during this initial phase of grain filling for both hybrids.

After grain growth rate reached its maximum, the low N availability in stem tissues (Fig. 5D) appears to constrain N remobilization rates during advanced phases of grain-filling equally for both hybrids (average of -0.9 and 1.2 mg m⁻² °C d⁻¹, respectively for 3394 and P1197; Fig. 6C). Leaf N was the predominant N source for remobilization during the second half of grain filling. At this point, however, genotypic differences emerged in the outlined supply-demand balance. The hybrid P1197 showed greater dry matter accumulation in grains maintaining a relatively inferior leaf N remobilization rate (Fig. 6A and B). This hybrid was able to satisfy grain N demand through an increased N uptake rate (Fig. 6E). Due to the close relationship between N and C dynamics, the relative conservation of N in leaves was also reflected in an

accumulation of WSC in the stems (Fig. 6D). This was likely due to a greater C availability from current photosynthesis that could have supplied carbohydrates to satisfy the demand from the developing grains. In contrast, the hybrid 3394 exhibited a relatively rapid cease in grain growth and N uptake, at the cost of increasing N translocation rates from leaves. Additionally, mobilization of stem WSC reserves started for 3394 beyond 856 °C d (Fig. 6D). This initiation of WSC remobilization in 3394 was characterized by an SLN value of 1.19 g m⁻² under full N (Fig. 5B).

Discussion

Genetic improvement between P1197 and 3394 hybrids was predominantly evidenced under full N conditions. The lack of consistent differences under zero N in this study might be related to the intensity of N deficiency achieved. Suggested by grain yield values when N was restricted, N supply had a noticeably larger effect on crop growth during the 2018 season. This might be attributed to a greater N immobilization and lower mineralization rates derived from maize residues in 2018, compared to soybean residues in the first year of experiments (Li et al., 2013). It appears, therefore, that grain yield differences were smaller as N stress was more severe. These outcomes imply that genetic improvement between these two hybrids is the consequence of a better response on yield to N supply. This is consistent with studies reporting a greater long-term genetic gain under high N availability in maize hybrids (Ciampitti and Vyn, 2012; Haegele et al., 2013; DeBruin et al., 2017; Mueller et al., 2019a). The modern hybrid was able to set more grains per unit of area with a similar N content at flowering, resulting in a higher reproductive efficiency per unit of N absorbed. This can be attributed to the well-known reproductive adaptation of modern hybrids to higher plant densities, mediated by multiple traits

including the reduced anthesis-silking interval (ASI), barrenness, and tassel size, and increased leaf angle (Duvick and Cassman, 1999; Duvick, 2005a). The adopted framework was able to capture changes in post-flowering dynamics between this set of hybrids and realize the underpinning processes for yield improvement (Cooper et al., 2014b; Messina et al., 2019).

Post-flowering N uptake is determined by biomass accumulation during the reproductive period (Lemaire et al., 2007). As a consequence, increased post-flowering N uptake in P1197, as observed for other germplasm (Ma and Dwyer, 1998), can be interpreted as the result of greater reproductive crop growth rate in response to the greater sink demand (Borrell and Hammer, 2000; Triboi and Triboi-Blondel, 2002). Due to the negative relationship between grain yield and [N] (Triboi et al., 2006), the lack of differences in grain [N] under limiting N treatments can be understood in terms of the minor yield variations between hybrids. Although only two genotypes were tested, these results provide additional evidence of the decline in grain protein as an indirect consequence of long-term genetic selection for yield (Duvick and Cassman, 1999; Haegele et al., 2013; DeBruin et al., 2017). Thus, improvements in N utilization efficiency in P1197 (i.e. greater yield per unit of N) relative to 3394 can be partially attributed to the reduction in protein concentration (Muchow, 1998; Ciampitti and Vyn, 2012, 2013). Implementation of this framework across a wider set of historical hybrids may allow us to examine the impact of genetic selection on the co-evolution of yield and N utilization in maize.

Nitrogen remobilization from vegetative organs mapped the hierarchical seasonal ordering of stem in preference to leaf N translocation on both hybrids (van Oosterom et al., 2010; Ciampitti and Vyn, 2011; Soufizadeh et al., 2018). However, P1197 exposed a slightly lower contribution of N deriving from leaves at maturity. This is consistent with previous studies reporting a reduced senescence and leaf N remobilization over time in ERA hybrids (Duvick and

Cassman, 1999; DeBruin et al., 2017). In our study, this was related to an acceleration of stem N remobilization, particularly notorious during early stages of grain filling. These outcomes imply that the modern hybrid holds N longer in the leaves at the expense of remobilization from stem tissues (Mueller et al., 2019a).

The increased N remobilization from stem tissues in P1197 was attached to a shift in the minimum [N] boundary (i.e. realized minimum stem [N]). Although genetic variation in stem [N] has been previously reported for maize (Yan et al., 2014; Chen et al., 2015), the adopted framework allows us to recognize it as a descriptor of stem N remobilization efficiency. Upon this mechanism, this hybrid was able to preserve more green leaf area at maturity. Superior LAI during advanced phases of grain filling had likely enhanced canopy photosynthesis, C source capacity, and crop growth (Valentinuz and Tollenaar, 2004; Gallais and Coque, 2005). By contrast, the decrease in SLN was similar for both genotypes, so differences in crop growth at this stage were essentially in response to changes in the light interception capacity than in the radiation-use efficiency (Sinclair and Horie, 1989; Andrade et al., 2005). These findings support the concept of a greater use of stem N to increase leaf area duration as a strategy to enhance N utilization efficiency in modern hybrids (Foulkes et al., 2009).

Despite variations in grain set at flowering under high N availability, accumulation patterns of WSC until flowering were consistent between hybrids. These results acquire significant importance providing they represent keystone phases in germplasm development in maize, defined by the increasing assistance of molecular technology in genetic selection since the 1990s (Eathington et al., 2007; Jiang, 2013). Accumulation of C reserves persisted during grain filling but at a declining rate, due to increasing demand from the grains along with the initiation of leaf senescence. This implies that the current C supply from photosynthesis exceeded grain

sink demand and thus recognizes a C sufficient condition on both hybrids (Swank et al., 1982; Jones and Simmons, 1983; Uhart and Andrade, 1995; Peng et al., 2013; Ning et al., 2018). Nonetheless, hybrid 3394 showed utilization of WSC reserves during late stages of grain-filling, starting 856 °C after flowering. Greater leaf N remobilization in this hybrid may have likely impacted on the photosynthetic capacity and the amount of assimilated C (Wood et al., 1993) leading to remobilization of sugars from stems. Hence, differences in WSC utilization between hybrids were essentially in response to the deviations in N fluxes rather than in the C balance *per se*.

The functional framework used in this study provides a basis to analyze the N and WSC balance in maize within the interpretation of yield improvement on hybrids from different eras. Still, evaluation spanning a wider genotypic variability for grain and stem composition should be performed to advance on the applicability of such framework, which relates grain demand with N and C dynamics from “source” organs. Furthermore, and although in 2017 a rainfed site was included in the experiment, the relatively wet growing season did not allow to compare the physiological behavior of these hybrids under levels of substantial water limitation. Barker et al. (2005) reported reduced rates of maize genetic improvement when crop was exposed to drought stress at flowering and during grain filling. Considering that crop water status impacts on crop growth (Sadras and Lemaire, 2014), and thereby N and WSC dilution (Vos, 1981; Greenwood et al., 1990; Kunrath et al., 2020), including N by water interactions within the scope of this framework still deserves further research. Evidence for such physiological relationships can provide valuable guidance for screening and selection strategies for drought tolerant maize cultivars.

Conclusions

Higher yields observed for the modern hybrid were associated with a higher grain set efficiency per unit N, increased N demand, and sink induced N uptake. Greater post-flowering N accumulation, determined by grain set, was observed in P1197, likely preventing leaf senescence and leading to a higher LAI at maturity. The modern hybrid seems to hold N in the leaves longer at the expense of remobilization from stem tissues. Although yield was not limited by C supply under any of the conditions explored in this study, the interplay between an earlier N remobilization and C supply was revealed by the WSC remobilization during late grain filling for the hybrid 3394.

Despite noteworthy advances in recognizing C and N physiological associations, this knowledge has not been integrated yet into a framework accounting for C \times N interactions to understand genetic progress in maize. The differential physiological behavior of the two hybrids in response to high N availability allowed for a better representation of grains as competing sinks for C and N assimilates during the post-flowering period. The integration of this knowledge within crop growth models provides significant opportunities for future scientific research as well as assistance on future selection strategies for considering a holistic approach for the whole-plant C and N economy.

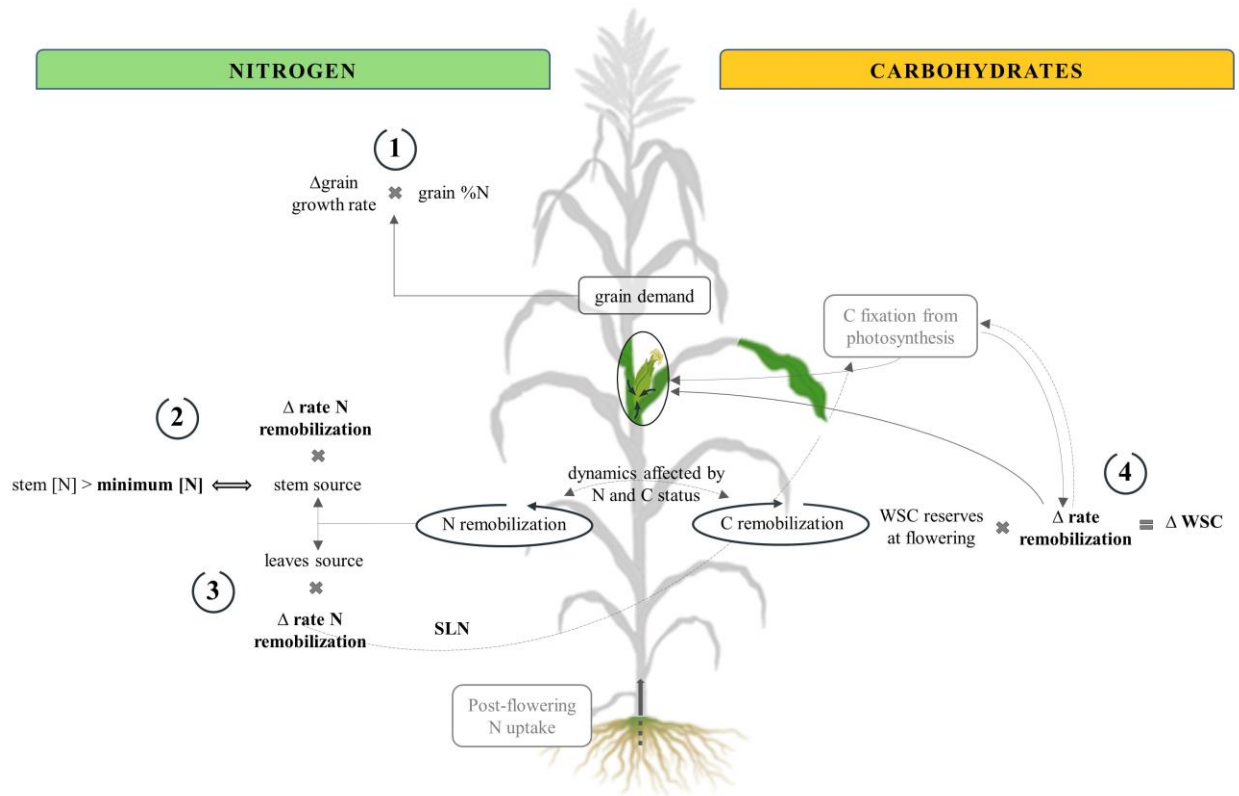


Figure 3.1. Framework for explaining yield changes through the underlying N and carbohydrate mechanisms. Processes shaded in grey and dashed lines represent dynamics not evaluated in this study but incorporated in the interpretation of results. Δ : change between hybrids, WSC: water-soluble carbohydrates, SLN: specific leaf N, [N]: N concentration.

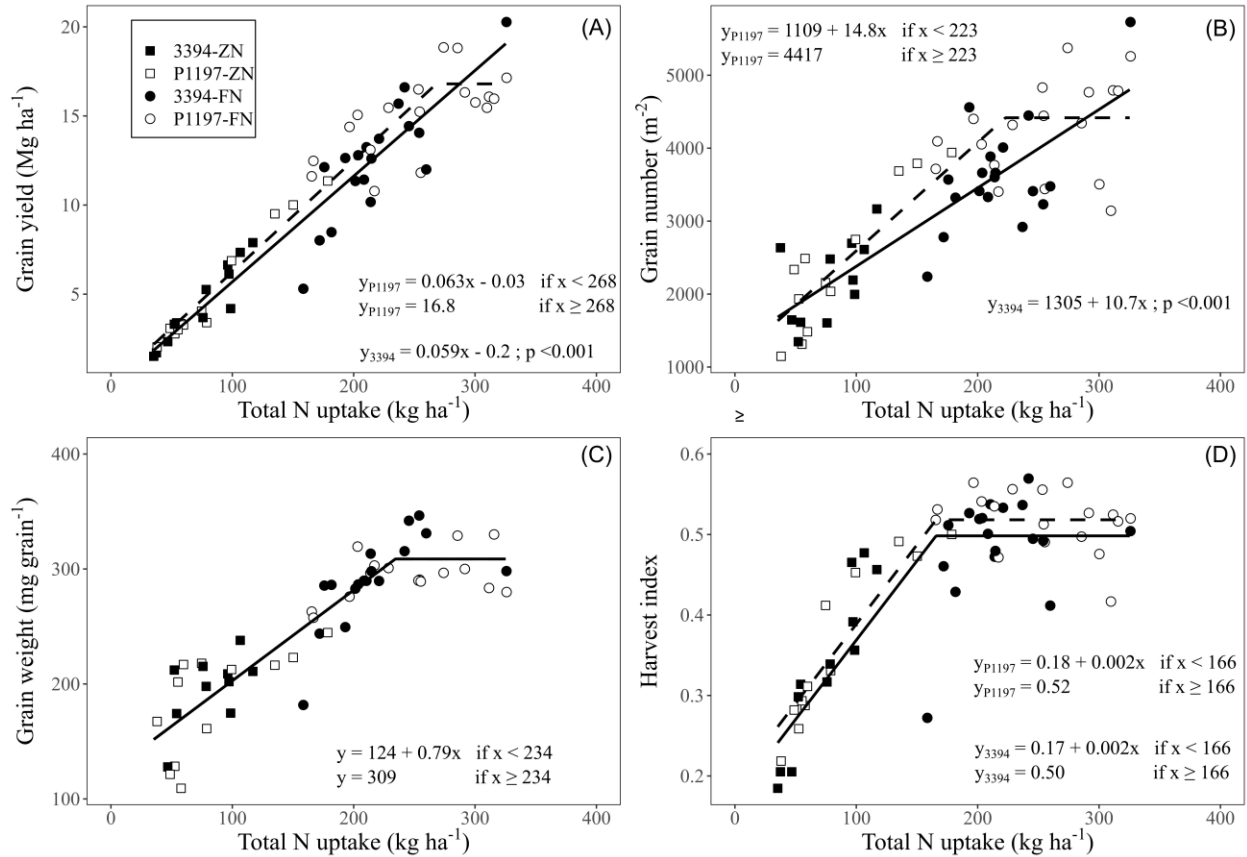


Figure 3.2. Relationships between yield (A), grain number (B), grain weight (C), and harvest index (D) with total N uptake for 3394 (closed symbols, solid lines) and P1197 (open symbols, dashed lines) under zero (squares) and full N (circles) treatments during 2017 and 2018 seasons. Symbols represent individual observations. Statistical significance for hybrid factor was tested and plotted accordingly at a level of $\alpha = 0.05$. Best Linear Unbiased Estimates and standard errors are reported in Supplementary Table S1. The best regression model was based on lower AIC values (Table S2).

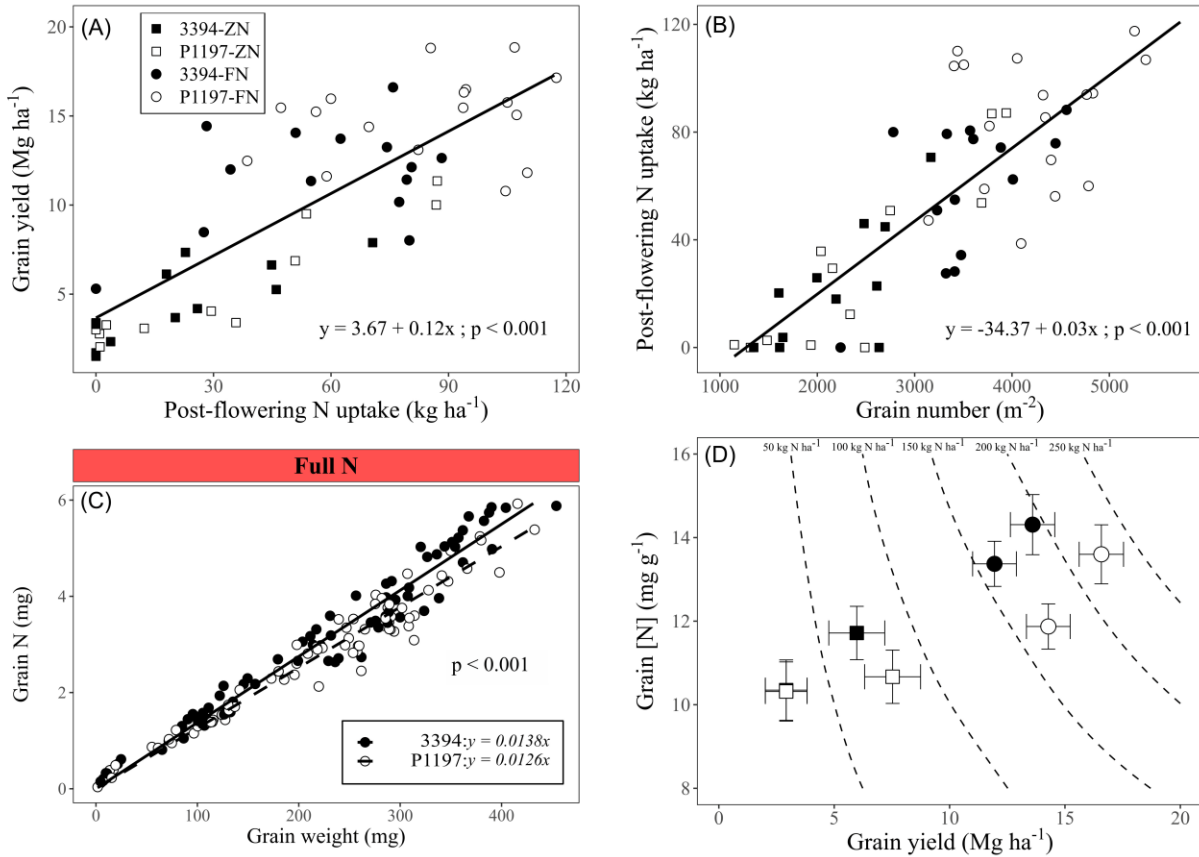


Figure 3.3. Relationships between yield and post-flowering N uptake (A), post-flowering N uptake as a linear function of the grain number set at flowering (B) for both hybrids across two years \times two N conditions. Symbols represent observed values for 3394 (closed symbols) and P1197 (open symbols) under zero (squares) and full N (circles) treatments. (C) Relationship between grain N content and grain weight, slope represents the grain [N] for each hybrid, throughout the grain filling period for the full N treatment. (D) Estimated grain yield and grain [N] for the two hybrids under two N levels in 2017 and 2018 seasons. Isolines represent levels of grain N yield from 50 to 250 kg ha⁻¹. For panel D, whiskers represent the standard errors of the means.

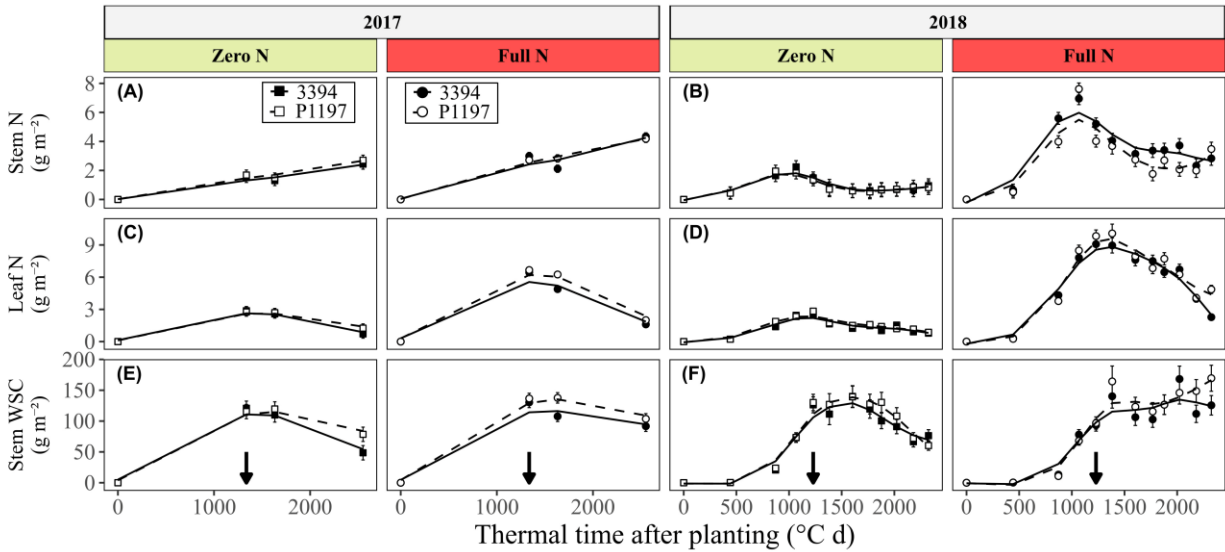


Figure 3.4. Evolution of N content in stem (A and B) and leaf (C and D) fractions, and of water-soluble carbohydrates (WSC) in stem (E-F) for 3394 (closed symbols) and P1197 (open symbols) maize hybrids, under zero (squares) and full N (circles) during 2017 and 2018 seasons. Arrows in (E) and (F) portray flowering (R1) stage. Vertical bars denote standard error of the mean.

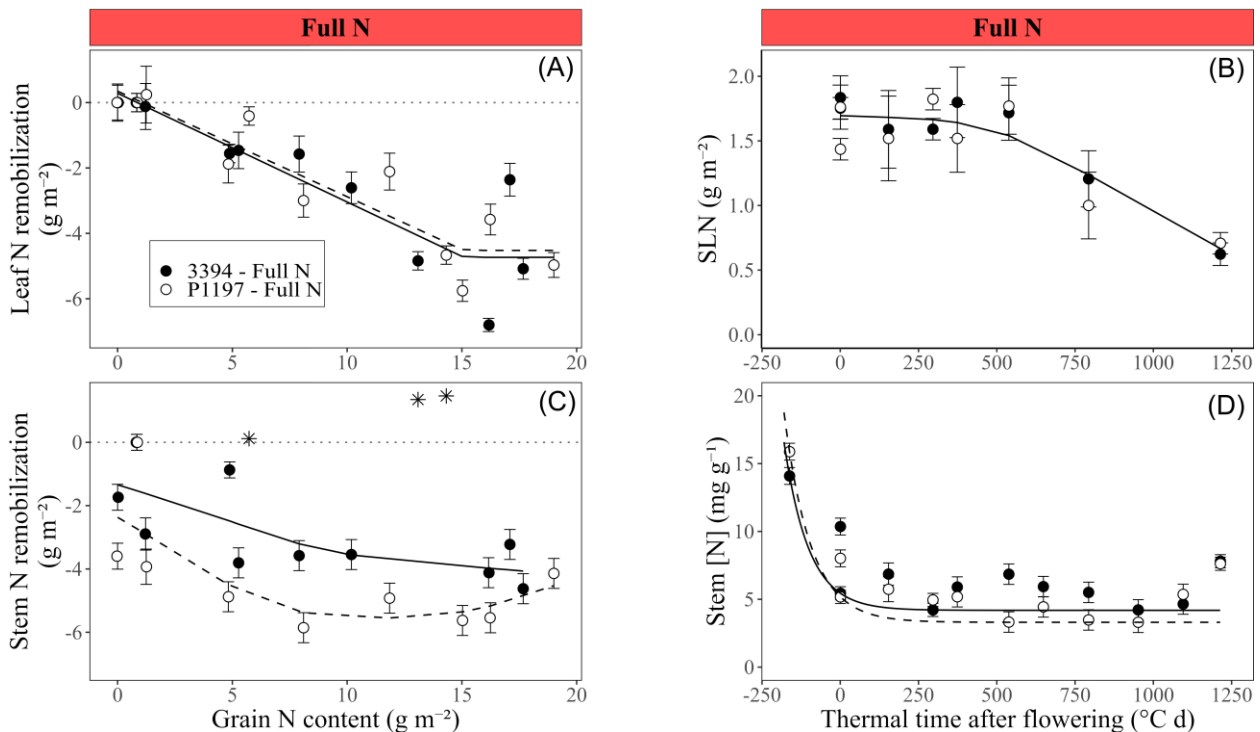


Figure 3.5. Progression of leaf and stem N remobilized related to the grain N content during grain filling (A and C), for two hybrids under full N conditions in 2017 and 2018. Symbols represent the estimated mean values at each sampling time for 3394 (closed symbols and solid lines) and P1197 (open symbols and dashed lines) maize hybrids. Vertical bars represent standard error of the mean.

standard error of the mean. Bivariate outliers (stars) were identified based on studentized residuals (values > 3). Overlapping symbols were offset horizontally for clarity (at a 0.1 value of x). Nitrogen remobilized was calculated by subtracting the N content at each sampling time from the estimated maximum N content around flowering for each hybrid \times year. Temporal dynamics of SLN on a thermal time basis from flowering, for hybrids under full N treatment (B). Quantile regression (tau = 0.05) on the stem [N] during the post-flowering period to estimate the minimum stem [N] on each hybrid under full N (D). Model parameters for the quantile regression lines are: [3394: $y = 4.19 + (5.45 - 4.19) * \exp(-\exp(-4.37) * x)$], [P1197: $y = 3.30 + (5.19 - 3.30) * \exp(-\exp(-4.45) * x)$].

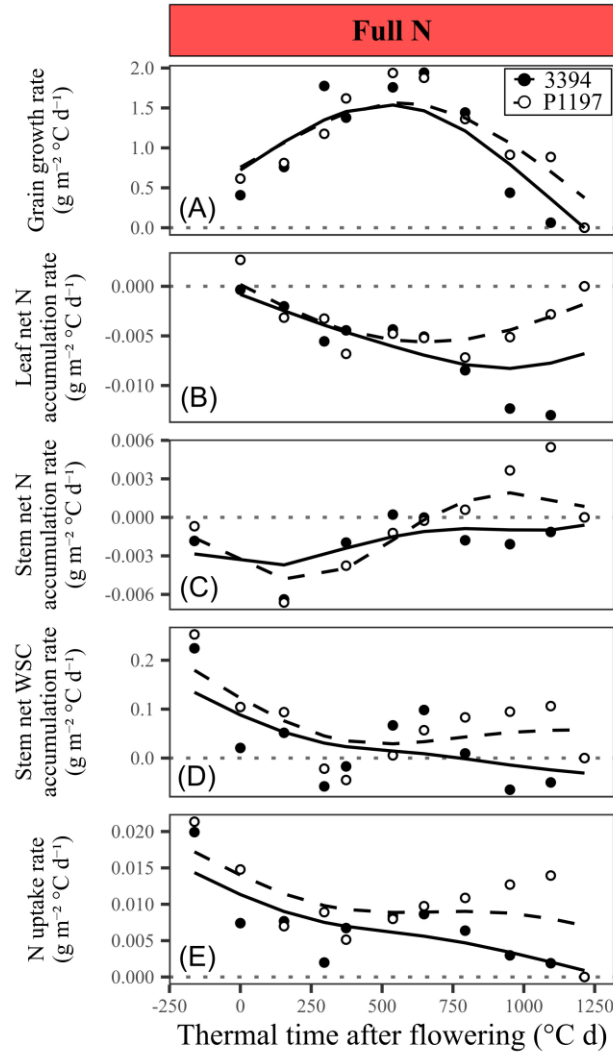


Figure 3.6. General description for the simultaneous rates of grain growth (A), leaf and stem net N accumulation (B and C), stem net WSC accumulation (D), and plant N uptake (E) during post-flowering under full N conditions. Hybrids 3394 (closed symbols and solid lines) and P1197 (open symbols and dashed lines). Symbols represent the derivatives of the estimated models for grain dry matter, leaf N, stem N, stem WSC, and plant N accumulation in g m^{-2} (respectively for A to E) at each sampling time. Positive values in B, C, and D show an accumulation of N or WSC in the tissue while negative magnitudes represent remobilization.

Table 3.1. Monthly values for daily solar radiation, temperature, and total precipitation for the 2017 and 2018 growing seasons. Source: Kansas Mesonet (2019).

	2017					2018				
	May	Jun	Jul	Aug	Sep	Apr	May	Jun	Jul	Aug
Solar radiation (MJ m ⁻² day ⁻¹)	25.2	27.3	26.5	23.0	19.7	22.8	23.7	26.4	24.5	21.9
Mean temperature (°C)	18.8	24.1	26.9	22.3	22.3	14.3	22.3	26.5	25.9	24.5
Precipitation (mm)	95.0	71.6	33.8	154.7	9.4	18.8	83.3	54.6	72.6	111.8

Chapter 4 - Post-silking ^{15}N labelling reveals an enhanced nitrogen allocation to leaves in modern maize (*Zea mays*) genotypes

Under review in Journal of Plant Physiology

Abstract

Nitrogen (N) metabolism is a major research target for increasing productivity in crop plants. In maize (*Zea mays* L.), yield gain over the last few decades has been associated with increased N absorption and utilization efficiency (i.e. grain biomass per unit of N absorbed). However, a dynamical framework is still needed to unravel the role of internal processes such as uptake, allocation, and translocation of N in these adaptations. This study aimed to 1) characterize how genetic enhancement in N efficiency conceals changes in allocation and translocation of N, and 2) quantify internal fluxes behind grain N sources in two historical genotypes under high and low N supply. The genotypes 3394 and P1197, landmark hybrids representing key eras of genetic improvement (1990s and 2010s), were grown under high and low N supply in a two-year field study. Using stable isotope ^{15}N labelling, post-silking nitrogen fluxes were modeled through Bayesian estimation by considering the external N (exogenous-N) and the pre-existing N (endogenous-N) supply across plant organs. Regardless of N availability, P1197 exhibited greater exogenous-N accumulated in leaves and cob-husks. This response was translated to a larger amount of N mobilized to grains (as endogenous-N) during grain-filling in this genotype. Furthermore, the enhanced N supply to leaves in P1197 was associated with increased post-silking carbon accumulation. The overall findings suggest that increased N utilization efficiency over time in maize genotypes was associated with an increased allocation of N to leaves and subsequent translocation to the grains.

Introduction

Nitrogen (N) is an essential nutrient required for plant growth and development. Nitrogen is absorbed by plants – as nitrate, ammonium, or other organic N forms – and incorporated into numerous metabolites such as amino acids and proteins (Tegeeder and Masclaux-Daubresse, 2018). In crop species, much effort has gone into identifying strategies for improving the efficiency on which plants absorb and utilize N for plant growth and development (Sinclair and Rufty, 2015). In cereals crops, grain production largely depends, along with carbon (C), on the supply of N to sink tissues throughout growth cycle (Ladha et al., 2016). The set of morpho-physiological mechanisms involved in the plant response to N availability during grain development in cereal crop species are of interest to plant breeders seeking to improve yields per unit of N fertilizer applied in crop production.

In maize (*Zea mays* L.), genetic yield improvement over the last few decades has been associated with increased N absorption, complemented by an enhanced crop N utilization efficiency (i.e. grain biomass produced per unit of N absorbed) (Ciampitti and Vyn, 2012; DeBruin et al., 2017; Haegele et al., 2013; Mueller et al., 2019a). To further understand the determinants of N changes in plant tissues, a dynamical N framework is needed to unravel the role of the interaction of processes such as N uptake, allocation among organs based on supply and demand signals, and translocation of N during crop growth. Particular interests have been addressed to study N utilization during reproductive stages of crop development where quality, size and yield of seeds is determined in annual crops (Dreccer et al., 2000; Kinugasa et al., 2012; Rossato et al., 2001; Salon et al., 2001; Weiland and Ta, 1992). In maize, the initiation of this reproductive period is manifested by the release of pollen by the anthers (anthesis) and the emergence of receptive stigmas (silking), indicating male and female floral maturity for

pollination. This is recognized as a central phase in N dynamics because uptake and assimilation starts to decline during the post-silking period (Fernandez et al., 2020a; Russelle et al., 1983). In addition, recycling of nutrients during senescence allows reutilization of N contained in vegetative organs (e.g. stems and mature leaves) and or translocation to reproductive organs (e.g. developing seeds) after hydrolysis of proteins to amino acids (Lambers et al., 2008). It is known that the plant N balance resulting from the interaction of these processes has been altered over time together with improvements in kernel set (i.e. number of grains per area) of modern genotypes (Ciampitti and Vyn, 2012; Duvick, 2005a). However, the complexity of the system has not been fully assessed by studying both the assimilation of external N supply and the remobilization of pre-existing N across organs. Such understanding will enable, for instance, quantifying the impact of breeding on the newly synthesized amino acids that are allocated to the stover before the onset of the leaf N remobilization process (Ta and Weiland, 1992).

Variations in the leaf N dynamics during grain-filling received recent attention as physiological adaptations to modern agriculture (Chen et al., 2015; Kosgey et al., 2013). Because photosynthetic rate is dependent, among other factors, on the leaf N content per unit leaf area (Sinclair and Horie, 1989), improvement in seasonal photosynthesis may arise as a consequence of a superior leaf N status per unit area (Borrell and Hammer, 2000; Vos et al., 2005). It is conceivable that plants with proportionally more N in the leaves at the expense of other organs can maintain photosynthesis rates during grain fill and, therefore, biomass production (Hirose and Werger, 1987; Hollinger, 1996). A recent comparison between historical hybrids led to the hypothesis that a longer retention of N in the leaves may underpin an accelerated N translocation from stems at early phases of grain-filling, thus enhancing N utilization efficiency (Fernandez et

al., 2021). However, the lack of field-level quantification of the underlying internal N fluxes remains to be determined to further test the above hypothesis.

Due to the relevancy of N economy for maize yield improvement, increased focus to develop models that identify N allocation and transport processes are of the highest priority. From the perspective of crop growth models, a necessary requirement to parametrize the mechanics behind N accumulation is to provide a realistic and efficient method to discriminate or differentiate the recently incorporated N from the pre-existing pool in a plant organ at a given time. The use of N stable isotopic ratios (^{15}N) has been largely demonstrated as an efficient tool to quantify current N absorption and allocation in plants (Knowles and Blackburn, 1993; Yoneyama et al., 2003). In particular for relative N allocation, short-term labelling has been widely employed in hydroponics (Arkoun et al., 2012; Friedrich and Schrader, 1979; Tanemura et al., 2008), or either under controlled environments in growth chambers (Lehmeier et al., 2013; Schiltz et al., 2005) or greenhouses (Avice et al., 1996; Cliquet et al., 1990; Yang et al., 2016). At a field-scale in maize, the use of this technique has been restricted to fewer studies (de Oliveira Silva et al., 2017; Ta and Weiland, 1992). In this study, measures of post-silking N allocation from multiple short-term ^{15}N labelling were assembled using dynamical models. Evidence of N distribution can be incorporated in a framework considering a two-way flux of N across all plant organs (Fig. 1) thus enabling the phenotyping of the internal N fluxes in the crop (Crawford et al., 1982; Gallais et al., 2006; Malagoli et al., 2005; Schiltz et al., 2005). Each day, absorbed N is allocated to leaves, stem, cob-husks, and grains (hereafter referred as exogenous-N). Simultaneously, a fraction of the pre-existing N stored in organs (hereafter referred as endogenous-N) is translocated to sink tissues. In this framework, the net N accumulation of an organ is captured as the resulting balance of inward and outward fluxes. With a functional

linkage with biomass and yield generation processes, a better understanding of such physiological aspects may help in the identification of promising targets for sustaining future genetic improvement. Furthermore, a biological N dynamics model structured upon such framework could provide the capacity to evaluate the potential value of breeding efforts in plant N utilization traits.

The present study provides an analysis of how the post-silking N allocation and translocation processes have been modified in two genotypes representing eras of genetic improvement (1990s and 2010s) under high and low N supply. By using a dynamical N model considering the external (exogenous-N) and the pre-existing (endogenous-N) N supply in the plant, this study aimed to 1) understand how patterns of allocation and translocation of N underpin genetic enhancement for N efficiency, and 2) quantify internal N fluxes as determinants of grain N.

Materials and methods

Field experiments and phenotypic determinations

A two-year field study was conducted during 2017 and 2018 growing seasons at the Ashland Bottoms Research Farm near Manhattan, KS, US (39°08' N, 96°37' W). The experimental sites during 2017 are described in-depth in Chapter 3 (Fernandez et al., 2021). The analysis in this study includes an additional experimental trial in 2018 with similar agronomic management and design of Chapter 3 (Fernandez et al., 2021). A detailed description of sites is shown in Table 1. Briefly, the experiments consisted of two irrigated (2017 and 2018) and one rainfed (2017) treatments modeled as a split plot design with two treatment factors and three replicates. Factors evaluated consisted of two maize Pioneer (Corteva Agriscience, Johnston, IA,

US) single cross hybrids with different year of release (3394 in 1991; and P1197 in 2014) as main plots, and two N scenarios (zero N, and full N, 137 kg ha⁻¹ for the non-irrigated and 218 kg ha⁻¹ for the irrigated sites) as subplots. Size of each plot was 64 m² (4 rows at 0.76 m between rows × 21 m length). Soil analyses were conducted at pre-planting to characterize initial conditions (Table 1). All trials were controlled and conducted free of weeds, pests, and diseases during the growing season.

Key developmental stages (Ritchie et al., 1997), anthesis (VT) and silking (R1) dates were recorded daily for 20 tagged plants per plot, and silking date for the plot was considered when 50% of the plants had exposed silks. For determination of physiological maturity (R6) dates, one ear of a previously tagged plant was collected every 3 to 4 days per plot, since kernel blister stage (R2) until harvest maturity. Ten kernels from the central portion of the ear were marked and sampled to track changes in kernel dry weight during the entire period. A bilinear model was fitted to the data of each experimental unit (N treatment × genotype × replicate × site) with the form:

$$\text{Grain weight (mg grain}^{-1}\text{)} = a + b \cdot d \quad \text{for } d < c, \quad \text{Equation 4.1}$$

$$\text{Grain weight (mg grain}^{-1}\text{)} = a + b \cdot c \quad \text{for } d \geq c, \quad \text{Equation 4.2}$$

where d is the thermal time after silking (°C d⁻¹), a is the y-intercept (mg grain⁻¹), b is the rate of grain-filling (mg grain⁻¹ °C d⁻¹), and c is the duration of the period until constant grain weight (°C d⁻¹). The R6 date of a plot was estimated, therefore, when 50% of the sampled plants reached constant grain weight. Thermal time for R6 and other samplings was calculated from the time of silking using a beta-function relationship between the rate of development and hourly temperature ($T_b = 8$ °C, $T_{opt} = 33$ °C, $T_u = 40$ °C) (Zhou and Wang, 2018).

Isotopic labelled fertilizer application and calculation of ¹⁵N plant traits

Stable isotope ¹⁵N abundance was utilized as a tracer to determine ¹⁵N allocation within plant organs during reproductive stages following the maize phenological scale of Ritchie et al. (1997). The ¹⁵N-labelling technique was used at silking (R1) and milk stage (R3) in 2017, and at R1, blister stage (R2), and dough stage (R4) in 2018. For each of these evaluations, microplots containing five consecutive plants in a row were established within each experimental unit. Labelled fertilizer Ca(NO₃)₂ (10.15% ¹⁵N) at 1 g per plant was applied with plastic syringes on both sides of the plants after diluting in 30 ml of water. Fertilizer was injected using the methodology employed in de Oliveira Silva et al. (2017), and the three center plants from each microplot were harvested five days after the ¹⁵N application. Additionally, non-enriched plants were sampled to determine the background ¹⁵N abundance in the fertilized and unfertilized soils, in order to account for possible variations in the standard values of natural ¹⁵N abundance (Cabrera and Kissel, 1989; Högberg, 1997; Fernandez et al., 2020b). Plants were separated into leaves (leaf blades), stem (stems + leaf sheaths + tassels), ear (husks + cobs), and grain fractions; after that, samples were dried at 65 °C until constant weight, and then ground through 0.10 mm sieve for laboratory analyses. Elemental abundance of N and C, and ¹⁵N abundance, were determined using an elemental analyzer (PyroCube – Elementar Americas) coupled to an isotope ratio mass spectrometer (visION, Elementar Americas, Ronkonkoma, NY, US) at the Stable Isotope Mass Spectrometry Laboratory at Kansas State University.

For each plant fraction, the atom percentage excess [At% (¹⁵N)Excess] was calculated using the following equation:

$$\text{At\% } (^{15}\text{N})\text{Excess} = \text{At\% } (^{15}\text{N})_{\text{sample}} - \text{At\% } (^{15}\text{N})_{\text{control}}, \quad \text{Equation 4.3}$$

where $At\% (^{15}\text{N})_{\text{sample}}$ represents the percentage of ^{15}N abundance in the ^{15}N labelled samples, and $At\% (^{15}\text{N})_{\text{control}}$ corresponds to the percentage of ^{15}N abundance in non-labelled control plants. Total ^{15}N uptake of each fraction and expressed in g m^{-2} was estimated by the following equation:

$$^{15}\text{N uptake}_{\text{fraction}} = \text{N uptake}_{\text{fraction}} \times \left(\frac{At\% (^{15}\text{N})_{\text{Excess}_{\text{fraction}}}}{100} \right), \quad \text{Equation 4.4}$$

where $\text{N uptake}_{\text{fraction}}$ is the dry biomass multiplied by N concentration and expressed in g m^{-2} .

The relative ^{15}N allocation proportion of each fraction was obtained as follows:

$$RA ^{15}\text{N} = \frac{^{15}\text{N uptake}_{\text{fraction}}}{^{15}\text{N uptake}_{\text{total}}}, \quad \text{Equation 4.5}$$

where $^{15}\text{N uptake}_{\text{total}} = \sum ^{15}\text{N uptake}_{\text{fraction} = \text{stem, leaves, cob-husks, grain}}$. Lastly, plant C accumulation was calculated as the dry biomass multiplied by C concentration and expressed in g m^{-2} .

Statistical analyses and calculations

Bayesian generalized additive mixed models (GAMMs) were fitted to the data using R program (version 3.6.1) in RStudio interface (RStudio Team, 2016) with programming language Stan via *brms* package (Bürkner, 2018, 2017). GAMMs are widely used in biological sciences to estimate functional relationships between the explanatory variables and the response using smooth curves (Pykälä et al., 2005; e.g. Yee and Mackenzie, 2002). In this study, we utilized a Bayesian approach via MCMC sampling for inference in a mixed model with varying coefficients for genotype and N treatment, random effects to recognize the experimental structure of the data, while including a generalized additive effect for the thermal time after silking. The implementation of a Bayesian modeling approach enabled the assessment of the

expected value of the predicted dynamics while determining a probabilistic component by means of their posterior distribution of samples (Ellison, 2004).

Relative ^{15}N allocations were modeled using a vector of y_c response variables following a Dirichlet distribution. The Dirichlet distribution is an extension of the beta distribution for C categories with y_c elements between 0 and 1, and for which the sum of all is equal to the unity (Douma and Weedon, 2019). The implemented model was then:

$$y_{ijkl,c} \sim \text{Dirichlet}(\mu_{ijkl,c}, \varphi), \quad \text{Equation 4.6}$$

for each i^{th} N treatment, j^{th} genotype, k^{th} site, l^{th} whole plot within site, and c^{th} plant fraction combination. The expected value for the relative ^{15}N allocation $\mu_{ijkl,c}$ is, therefore, between 0 and 1 and subject to the constraint $\sum_{c=1}^n \mu_{ijkl,c} = 1$ (Douma and Weedon, 2019). In addition, φ is a positive precision parameter, and the link between μ and n is a multinomial logit function

$$[\mu_{ijkl,c} = \frac{\exp(n_{ijkl,c})}{\sum_{d=1}^m \exp(n_{ijkl,d})}] \text{ (Bürkner, 2018). For other positive continuous quantities modeled,}$$

such as the plant-fraction N and C accumulation, distribution of the response variables was defined as:

$$y_{ijkl} \sim N(\mu_{ijkl}, \sigma^2), \quad \text{Equation 4.7}$$

with a log link function $[\mu_{ijkl} = \exp(n_{ijkl})]$. The linear predictor (n_{ijkl}) for all models was defined as:

$$n_{ijkl} = n + \alpha_i + \beta_j + \gamma_{ij} + \omega_{ij}(t) + b_k + c_{l(k)j}$$

$$b_k \sim N(0, \sigma_b^2) \quad \text{Equation 4.8}$$

$$c_{l(k)j} \sim N(0, \sigma_c^2),$$

where α_i and β_j are differential effects of the i^{th} N treatment and j^{th} genotype; γ_{ij} the interaction term between them; b_k is the site-level random effect for each k^{th} site; $c_{l(k)j}$ is the random effect

of the l^{th} whole plot within k^{th} site and by j^{th} genotype; and σ_b^2 and σ_c^2 their respective variances. To describe the nonlinear response patterns of variables expressed in thermal time progress basis, a cubic regression spline $\omega_{ij}(t)$ in the range of time after silking t was included in the model, which depends on the level of i^{th} N treatment and j^{th} genotype.

Due to the lack of previous information on the likely values of model parameters, non-informative priors were specified for all parameters. Sampling convergence was assessed by visual inspection of density and trace plots, and the use of Gelman-Rubin diagnostics (Gelman and Rubin, 1992). Posterior predictive checks are reported in Supplementary (Fig. S1-S2-S3). Inference was based on 4,000 iterations of Markov Chain Monte Carlo (MCMC) algorithm and 4 chains, with a warmup period of 2,000 draws for calibration of the MCMC. Pairwise comparisons between genotypes were assessed using two-sided 95% credible intervals of the difference between their respective posterior predictive samples.

Using the fitted Bayesian models, and based on the plant N traits introduced in previous section, the internal plant N distribution could be explained in the two-way flux framework from Fig. 1. Let $N_{\text{fraction}}(t)$ be the N content in a fraction at a time t in thermal time after silking, then the net N accumulation rate (i.e. the balance between inward and outward fluxes per unit of time) could be expressed as the first derivative of N_{fraction} with respect to time:

$$\frac{dN_{\text{fraction}}}{dt} = \lim_{h \rightarrow 0} \frac{N_{\text{fraction}}(t+h) - N_{\text{fraction}}(t)}{h}, \quad \text{Equation 4.9}$$

where,

$$N_{\text{fraction}}(t) = \%N_{\text{fraction}}(t) \times W_{\text{fraction}}(t), \quad \text{Equation 4.10}$$

$\%N_{\text{fraction}}$ is the N concentration in that fraction expressed in $\text{g } 100 \text{ g}^{-1}$, W_{fraction} is the dry weight in g m^{-2} , and $h = \Delta t$ value approaching zero.

Based on equation (9), plant N uptake rate at a given time could be estimated using the first derivative of the plant N accumulation,

$$\frac{dN_{\text{plant}}}{dt} = \lim_{h \rightarrow 0} \frac{N_{\text{plant}}(t+h) - N_{\text{plant}}(t)}{h}. \quad \text{Equation 4.11}$$

Considering the framework introduced in Fig. 1 for post-silking dynamics, N derived from uptake (exogenous-N) is allocated to every tissue of the plant at a ratio defined by its $RA^{15}N$ (equation 5). Therefore, the exogenous-N accumulation rate of a specific fraction at any given time t could be expressed as:

$$\frac{dN_{\text{fraction}}^{\text{exo}}}{dt} = \frac{dN_{\text{plant}}}{dt} \times RA^{15}N(t), \quad \text{Equation 4.12}$$

where,

$$RA^{15}N(t) = \left[{}^{15}N_{\text{fraction}}(t) / {}^{15}N_{\text{plant}}(t) \right]. \quad \text{Equation 4.13}$$

From there, the endogenous-N rate, which represents the N mobilized to/from each organ, was calculated as the difference between the net N accumulation and the inward flux of exogenous-N rates for that fraction:

$$\frac{dN_{\text{fraction}}^{\text{endo}}}{dt} = \frac{dN_{\text{fraction}}}{dt} - \frac{dN_{\text{fraction}}^{\text{exo}}}{dt}. \quad \text{Equation 4.14}$$

The integration of the abovementioned temporal dynamics over the post-silking period (i.e. from $t_{\text{silking}} = 0$ to $t_{\text{maturity}} = \text{thermal time at R6}$) represents the cumulative balance of net N accumulation (15), exogenous-N (16), and endogenous-N (17) on each fraction:

$$\int_{t_{\text{silking}}}^{t_{\text{maturity}}} \frac{dN_{\text{fraction}}}{dt} = N_{\text{fraction}}(t_{\text{maturity}}) - N_{\text{fraction}}(t_{\text{silking}}), \quad \text{Equation 4.15}$$

$$\int_{t_{\text{silking}}}^{t_{\text{maturity}}} \frac{dN_{\text{fraction}}^{\text{exo}}}{dt} = N_{\text{fraction}}^{\text{exo}}(t_{\text{maturity}}) - N_{\text{fraction}}^{\text{exo}}(t_{\text{silking}}), \quad \text{Equation 4.16}$$

where for post-silking dynamics $N_{\text{fraction}}^{\text{EXO}}(t_{\text{silking}})$ is the initial state set to zero, and,

$$\int_{t_{\text{silking}}}^{t_{\text{maturity}}} \frac{dN_{\text{fraction}}^{\text{endo}}}{dt} = \int_{t_{\text{silking}}}^{t_{\text{maturity}}} \frac{dN_{\text{fraction}}}{dt} - \int_{t_{\text{silking}}}^{t_{\text{maturity}}} \frac{dN_{\text{fraction}}^{\text{EXO}}}{dt}. \quad \text{Equation 4.17}$$

Results

The proportion of ^{15}N allocated to each organ during post-silking was modeled through Bayesian estimation, outlining the internal balance of N across sink tissues (posterior predictive distributions for all four treatment combinations in Fig. 2). Before the initiation of linear grain-filling ($0\text{-}200\text{ }^{\circ}\text{C d}^{-1}$), cob-husks tissues were the principal sinks for current N absorbed (on average, $0.34 [0.18, 0.51]\text{ g g}^{-1}$ in 3394 and $0.32 [0.16, 0.49]\text{ g g}^{-1}$ in P1197; values in brackets define the 95% credible interval, hereafter). Expected allocation to stem + leaves consistently accounted for more than 0.5 g g^{-1} of the N absorbed, but was particularly high under full N supply ($0.64 [0.53, 0.76]\text{ g g}^{-1}$ in 3394 and $0.62 [0.51, 0.75]\text{ g g}^{-1}$ in P1197). As linear-filling progressed, grains emerged as the main sink for N to the detriment of stover provision. Allocation of N absorbed close to physiological maturity ($600\text{ }^{\circ}\text{C d}^{-1}$ and beyond) was predominantly to the grains (on average, $0.58 [0.40, 0.74]\text{ g g}^{-1}$ in 3394 and $0.57 [0.36, 0.75]\text{ g g}^{-1}$ in P1197). At this point, P1197 exposed a marginally greater N distribution to leaves relative to 3394 (respectively for each genotype, 0.18 and 0.10 g g^{-1} for zero N, and 0.22 and 0.17 g g^{-1} for full N). Although the considerable variability observed in the posterior samples, P1197 exhibited greater N allocation to leaves during late grain-filling in 84% (zero-N) and 74% (full-N) of draws obtained, relative to 3394.

Post-silking N dynamics were assessed in terms of the underpinning exogenous- and endogenous-N balances across fractions (Fig 3). When no N was applied, P1197 exhibited greater exogenous-N accumulated in all organs relative to 3394 (Fig. 3 A-D). Under full N,

incremental exogenous-N was evident, particularly accumulated in leaves and cob-husks.

Exogenous-N to the photosynthetic tissues (i.e. green leaves) was 0.8 [0.6, 0.9] g m⁻² higher in P1197 compared with 3394 (Fig 3C); for cob-husks, the expected increment was of 0.5 [0.3, 0.7] g m⁻² (Fig 3D). The expected increase in exogenous-N to grains was only of 0.2 [0.1, 0.4] g m⁻² (Fig 3A).

Hybrid 3394 accumulated 2.8 [0.1, 5.6] and 5.7 [3.2, 8.1] g m⁻² of plant N during post-silking (under zero- and full-N, respectively), while P1197 accumulated 5.4 [2.6, 8.1] and 8.2 [6.0, 10.3] g m⁻². This enhanced post-silking N uptake in P1197 was well reflected in the grains (Fig. 3I) and, to a lower extent, in the stover net accumulation (Fig. 3J, K, and L). At high N supply, the improved grain N accumulation was predominantly a consequence of more N mobilized from stover tissues (Fig. 3E). Our results indicate that leaves were the primary sources of endogenous-N for the grains, contributing on average 3.0 [1.6, 4.3] g m⁻² under zero-N and 6.2 [4.9, 7.6] g m⁻² under full-N (Fig. 3G). Notably, the larger discrepancies in endogenous-N between genotypes were also seen in the amount contributed by their leaf tissues, in an increment of 0.79 [0.77, 0.82] g m⁻² for P1197 under full N (i.e. relative to 3394). This shows that, at high N availability, the additional exogenous-N accumulated in leaves in P1197 allowed for a larger amount of extractable N mobilized to grains. In contrast, under low N treatment, the increase in exogenous-N to leaves (and for stem and cob-husks) translated to little improvement in endogenous-N. Such patterns suggest dissimilar effects of N fertilization on post-silking N allocation and translocation dynamics for these two maize genotypes.

Exogenous-N allocation was further analyzed in proportional terms (over the total N accumulated) to account for the differences in biomass and N uptake between genotypes and fertilization levels. The summary of posterior distributions was depicted against the posteriors

for post-silking C accumulation (Fig. 4), reflecting how variations in the within-plant N demand was related to crop growth and C assimilation. Results show that hybrid P1197 showed a greater proportion of N allocated to leaves during this period relative to the older genotype (comparatively for 3394 and P1197, 0.16 and 0.23 g g⁻¹ [zero-N] and 0.22 and 0.27 g g⁻¹ [full-N]). In contrast, 3394 exhibited proportionally higher allocation towards the grains of the N derived from post-silking uptake (0.51 and 0.41 g g⁻¹ [zero-N] and 0.47 and 0.39 g g⁻¹ [full-N], respectively for 3394 and P1197). Allocation to stem and cob-husks varied little between genotypes, with expected magnitudes of 0.20 [0.18, 0.23] g g⁻¹ and 0.13 [0.10, 0.16] g g⁻¹ averaged across N levels (respectively for both fractions). Collectively, these outcomes evidence that, per unit of N absorbed, P1197 had an improved partitioning to the photosynthetic organs. In 84% of posterior predictive samples, this was related to a better C assimilation of the crop, with an expected C difference between genotypes of 99 g m⁻² (zero N) and of 103 g m⁻² (full N).

As shown in Fig. 3I, expected grain N accumulation at maturity was 5.3 and 6.2 g m⁻² under zero N (respectively for 3394 and P1197), and increased to 11.9 and 13.9 g m⁻² under full N treatment. Grain N sources were assessed using the posterior samples for the N derived from exogenous-N (i.e. direct allocation from post-silking uptake) and endogenous-N mobilized from leaves, stem, and cob-husks (i.e. originated from pre- or post-silking N allocated to the stover) (Fig. 5A). Overall, genotypic differences in grain N sources at both N supply conditions were negligible and showed a considerable level of uncertainty (reflected by their 95% credible intervals). Regardless of the genotype and N condition, leaves were the main N sources for grain-filling, contributing with 0.47 [0.33, 0.62] g per g of N in the grains at maturity. Particularly under full-N, stem and cob-husks had a relatively important contribution with expected values of 0.16 [0.09, 0.23] g g⁻¹ (stems) and 0.12 [0.06, 0.18] g g⁻¹ (cob-husks). In

addition, the expected proportion derived from exogenous-N was around 0.28 [0.19, 0.47] g g⁻¹ (averaged for both N conditions).

Given the observed variations in grain N sources (Fig. 5A), the relationship between grain weight and N content (at a per kernel basis) was re-explored in terms of exogenous- and endogenous-N quantities (Fig. 5B). The slope between exogenous-N accumulation and dry weight increase per grain varied little between genotypes and N supply levels from 3.0 to 3.8 mg N g⁻¹. Thus, the improvement in exogenous-N allocated to grains in P1197 was essentially a consequence of the sink size (grain number and weight). Under zero-N, average grain number was 2309 and 3125 grains m⁻² (3394 and P1197, respectively) and grain weight was 219 and 211 mg. On a similar trend under full-N, grain number averaged 3611 and 4259 grains m⁻² (3394 and P1197, respectively) and grain weight 276 and 283 mg.

Discussion

A key scientific pursuit with clear societal and ecological benefits has been the identification of morphological and physiological traits associated with a better N utilization in crops (Hirel et al., 2007). Conceptually, the efficiency in which maize plants use N for seed production has been traditionally associated with manipulations related to N absorption and the N conversion ratio in the reproductive organs (Moll et al., 1982). The ¹⁵N multi-stage labelling and posterior two-way N fluxes model developed are useful to quantify the complexity for a larger set of genotypes and a broader range of environmental conditions. Parameterization of the internal N allocation and cycling within plant crop models may improve the understanding of the critical components associated in the N pathway and the identification of future targets of breeding manipulations to enhance N utilization efficiency.

Coordination between exogenous- and endogenous-N dynamics with N use efficiency

Improvements in exogenous-N absorption in P1197 relative to 3394 were magnified under high-N fertilization. Under these conditions, nitrate and ammonium absorption are expected to occur at a rate closely determined by the plant growth process (Cooper and Clarkson, 1989; Lee et al., 1992). Indeed, greater N uptake in P1197 was accompanied by increments in biomass accumulation [Chapter 3, Fernandez et al. (2021)]. This is in line with a number of studies confirming the association between improvements in N uptake and plant growth in newer hybrids, in particular during the post-silking period (Chen et al., 2016; Ciampitti and Vyn, 2012; Fernandez et al., 2020a; Mueller and Vyn, 2016; Tollenaar and Lee, 2006). Considering kernels are the main growing sinks during this period, the larger grain set in P1197 appears to be the main driver for the greater post-silking growth, which subsequently led to increased root N absorption. Even more, the demand rate per kernel of exogenous-N remains stable, even under N-deficiency where other morpho-physiological root traits are recognized as additional determinants of plant N uptake (Liu et al., 2009; Presterl et al., 2002; Wang et al., 2005). This is in line with studies demonstrating the strong relationship between N uptake and grain development (Ciampitti and Vyn, 2011; Coque and Gallais, 2007; Fageria and Baligar, 2005; Worku et al., 2007). Most importantly, these results highlight the demand-driven regulation exercised by grains over reproductive N uptake in maize plants.

The N framework used here demonstrates that the improvement in exogenous-N uptake was induced by a greater sink size in P1197, but also by an enhanced circulation of post-silking N through the leaves. The greater post-silking N assimilated in P1197 translated to more N

allocated to the leaves rather than to the grains. Increasing the proportional N allocation to leaves has been identified as a plausible mechanism for N-efficient plants in other plant species (Laungani and Knops, 2009; Perchlik and Tegeder, 2018). In the present study, the increased amount of N allocated to leaves was re-translocated (as endogenous-N) to the grains as they developed, especially under high N treatment. This pattern explains why most of the N imported to the grain at maturity was originated from the leaves/stem N pool and recognizes N mobilization as a key trait in N-efficient genotypes (Chen and Mi, 2018; Masclaux-Daubresse et al., 2010; Tian et al., 2015). Despite the improvements in N uptake capacity, the P1197 hybrid also had an enhanced internal utilization of N for grain production. This was achieved by lowering the grain N requirements which predominantly alleviated the demand for endogenous-N per grain. This strategy allowed a more efficient utilization of the endogenous-N pool to sustain optimal growth in a greater number of grains in this genotype. These findings underscore the necessity to consider the internal N efficiency in crops by considering both exogenous- and endogenous-N as sources for the grain N requirement (Schiltz et al., 2005).

Carbon fixation as affected by adjustments in leaf N allocation and mobilization

A consistent increase in the proportion of exogenous-N allocated to leaves was observed in the modern hybrid P1197. Regardless of whether N uptake was increased or not, P1197 showed an improved mobilization of new N absorbed through the photosynthetic organs linked to an increase in post-silking C gain. The increment in post-silking C fixation with the greater leaf N allocation raise up the question if the N allocation to leaf has been modified. Leaf N can be categorized as N associated with photosynthetic enzymes and thylakoid N, and the soluble- and insoluble-N pool constituent of cell walls, membranes, and other structures (Mu et al., 2016).

In *Arabidopsis* mutants with greater leaf N allocation but unchanged content per unit leaf area, enhanced C fixation was a consequence of an improved investment of N into the synthesis of the photosynthetic components (Perchlik and Tegeder, 2018). Studies in maize (although from a distinct genetic background from the ones used here), showed higher leaf C exchange rates in newer hybrids but only under N-deficiency, by means of improved chlorophyll content and thylakoid electron transport (Echarte et al., 2008). Considering the correlation between leaf N and Rubisco (ribulose-1,5-bisphosphate carboxylase) content, electron transport, and photosynthesis (Dwyer et al., 1995; Eichelmann et al., 2009; Evans, 1989; Meinzer and Zhu, 1998), these outcomes seem to confirm that selection and breeding in maize hybrid development have improved leaf N status under N stress conditions (Boomsma et al., 2009; McCullough et al., 1994). While the specific impacts on the light and dark photosynthetic reactions remains to be determined, the small differences between 3394 and P1197 in green leaf biomass and leaf area under low N [Chapter 3, Fernandez et al. (2021)] suggest that the enhanced post-silking C fixation may result from adjustments in the leaf N balance induced by an optimized exogenous-N supply.

When maize plants were grown under favorable N conditions and the optimum specific leaf N (SLN) content for growth was attained (Sinclair and Horie, 1989), modifications in the chlorophyll and soluble protein content [among which are Rubisco and phosphoenolpyruvate carboxylase (PEPC)] per unit of leaf N hardly affects the net photosynthetic rates (Mu et al., 2016). These findings suggest that the modern hybrid P1197 increased C fixation under high-N by means of a greater total leaf area and a longer retention of green leaves. It therefore seems likely that the enhanced leaf N allocation in P1197 may have been triggered by a greater leaf/shoot ratio (Mueller et al., 2019a) and an improved exogenous N supply to preserve the

photosynthetic machinery during late grain development (Mu et al., 2018). Furthermore, both genotypes used in this research showed similar SLN content under high N supply [Chapter 3, Fernandez et al. (2021)]. This would imply that the optimized plant N distribution also resulted in a better C fixation efficiency per unit of leaf N, as seen in other species (Atkin et al., 2015; Perchlik and Tegeder, 2018). These results establish that direct selection for yield have indirectly favored N allocation to leaves in modern maize hybrids resulting in an improved post-silking C fixation under high- and low-N availability.

Potential implications of N dynamics on the respiratory metabolism

An increase in the endogenous-N recycling to grains, mainly from leaves, was caused by higher N supply for both genotypes, but to a greater extent for P1197. Accounting for the underlying implications of the within-plant N balance on photosynthesis and growth requires a parallel analysis of the metabolic efficiencies of the respiratory system. The two-component functional model introduced in a seminal work by McCree (1970) and extended by Thornley (1970) contemplates that plant respiration costs results from losses derived from both maintenance and growth processes. When the functioning of mature plant organs was analyzed, particularly for mature leaves, it is important to place a greater emphasis on the metabolic processes involved in the maintenance of cellular structures and intracellular ion-gradients (Penning de Vries, 1975). Fundamental maintenance processes in protein metabolism and senescence are the protein breakdown and re-synthesis (i.e. protein turnover) and active transport of ions across cell membranes (Amthor, 2000). Essentially, we can relate the endogenous-N pool with the organic N compounds, mainly amino acids, redistributed through cellular turnover (Lehmeier et al., 2013). The superior endogenous-N redistributed to the grains in P1197 could

possibly imply an increase in protein turnover and active translocation of amino acids. Furthermore, protein breakdown and synthesis reactions are energy-consuming processes catalyzed by proteases with consumption of ATP (Amthor, 2000; Zerihun et al., 1998). This cost is supported by a fraction of the respiratory process with release of CO₂, in what is termed ‘maintenance respiration’. Although not explicitly evaluated here, an increased N recycling and preservation of the photosynthetic system in P1197, mediated by more N absorbed and allocated to leaves, may attach a higher respiratory demand for ATP (Azcón-Bieto et al., 1983). In 3394, it is possible that respiration rates were reduced due to lower photosynthetic C supply (O’Leary et al., 2019) by adjusting protein turnover and redistribution rates (Earl and Tollenaar, 1998), which lead to less endogenous-N translocated to grains. Still, the scale at which respiration was affected remains to be determined because the decreases in the stem non-structural carbohydrates close to physiological maturity may also be indicative of respiration losses to support energy needs during late senescence [Chapter 3, Fernandez et al. (2021)].

Understanding the supply-demand relationship of endogenous-N at a whole-plant scale requires additional consideration on the variation pattern of grain N requirements. In this sense, a lower target of N per grain in P1197 was observed only under high N, which would imply a greater accumulation of starch and therefore lower growth costs per grain (Penning de Vries et al., 1974; Van Iersel, 2003). Although the energetic balance in the plant has not been formally quantified, P1197 showed a superior whole-plant endogenous-N mobilization suggesting altered rates of protein turnover and re-allocation of N (Irving et al., 2010). While recognizing the complexity of reactions involved, it can be argued that further work needs to be conducted evaluating the plant respiratory kinetics across different maize genotypes. Moreover, integrating this information within the two-way flux framework of exogenous-N absorbed and pre-existing

endogenous-N may bring an opportunity for models that can account for the protein turnover rates across organs in crops (Loomis and Amthor, 1999).

Conclusions

The present study presents a novel approach to study post-silking N allocation and translocation processes for two historical maize genotypes as affected by N availability. By using a dynamic framework of N fluxes considering the external N supply (exogenous-N) and the pre-existing internal N (endogenous-N) in the plant, this research advances our understanding in the adaptive changes in N use with genetic selection over time in these hybrids. Results revealed that the improvement in exogenous-N uptake during post-silking in the newer genotype was induced by both a greater number of grains and an enhanced supply of N to the leaves. Indeed, in proportional terms, hybrid P1197 had a larger partitioning of absorbed N to the photosynthetic organs relative to the older genotype which lead to a better C assimilation. This greater amount of N into leaves was re-translocated as endogenous-N to the grains and signified a critical N source for final grain N content, especially under high N. These findings establish that direct selection for yield have indirectly favored N allocation to leaves in modern maize hybrids resulting in an improved post-silking C fixation under high- and low-N availability. Moreover, we propose further investigation of the underlying implications on photosynthesis and respiratory system as involved in plant growth. Ultimately, the ^{15}N multi-stage labelling allows for the opportunity to develop meaningful crop models characterizing the internal allocation and recycling of N, and informs selection strategies towards N-efficient genotypes.

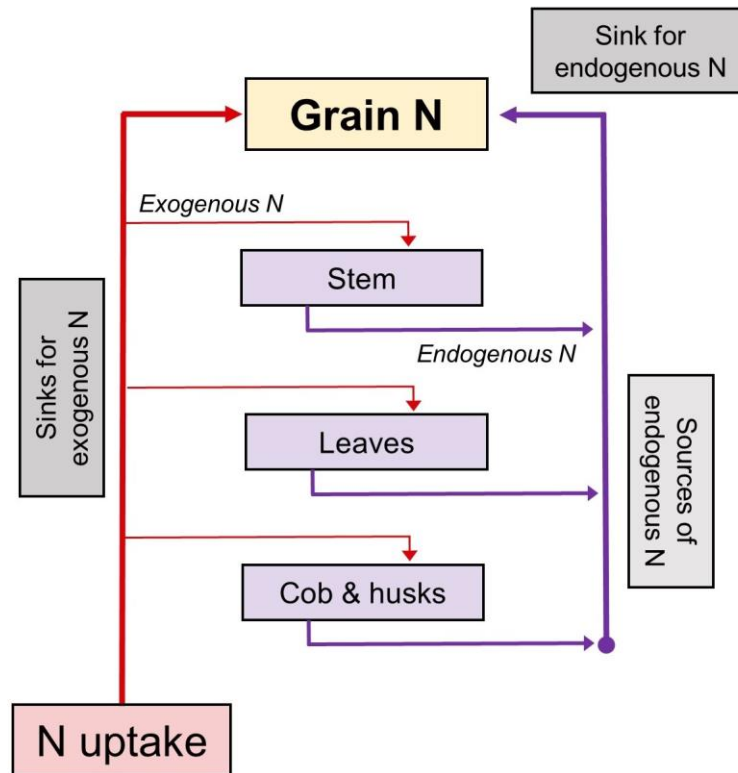


Figure 4.1. Framework to investigate post-silking N dynamics and grain N sources in maize. At a given time, N is absorbed and distributed across all stover and grain fractions (exogenous-N). Simultaneously, a fraction of N stored in these organs is remobilized and transported to the developing tissues (endogenous-N). This two-way flux model considers that grains are then sinks of (1) exogenous-N absorbed and directly allocated to grains and (2) endogenous-N translocated from stover, which derives from pre- and post-silking N initially allocated to stems, leaves, and cob-husks.

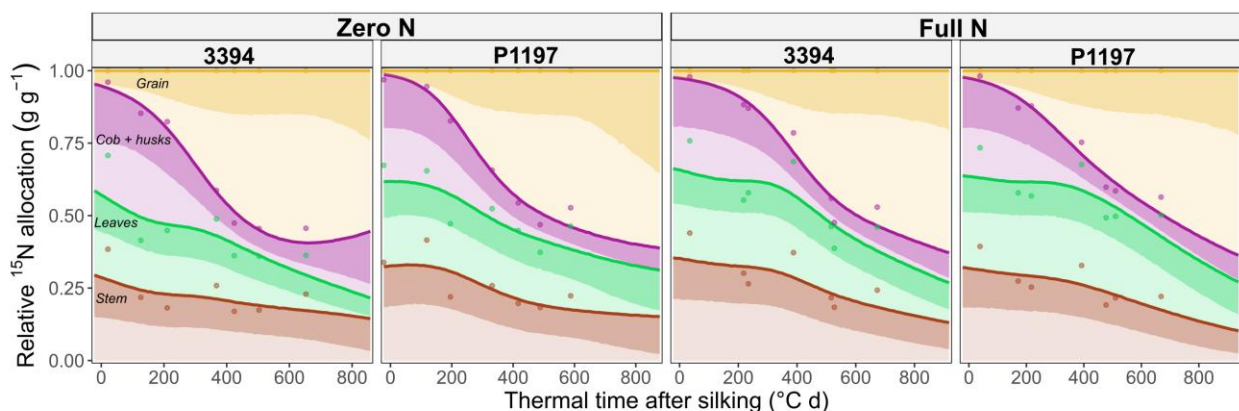


Figure 4.2. Relative allocation of ^{15}N (RA^{15}N) across plant organs throughout the post-silking period, across two maize hybrids (3394 and P1197) and two N fertilization levels (zero and full N). Solid lines represent medians from samples of the posterior predictive distribution, their corresponding shaded areas represent the 2.5% quantile (i.e. representing half of the 95%

credible interval), and symbols show the mean of three replications for each plant fraction \times sampling \times site.

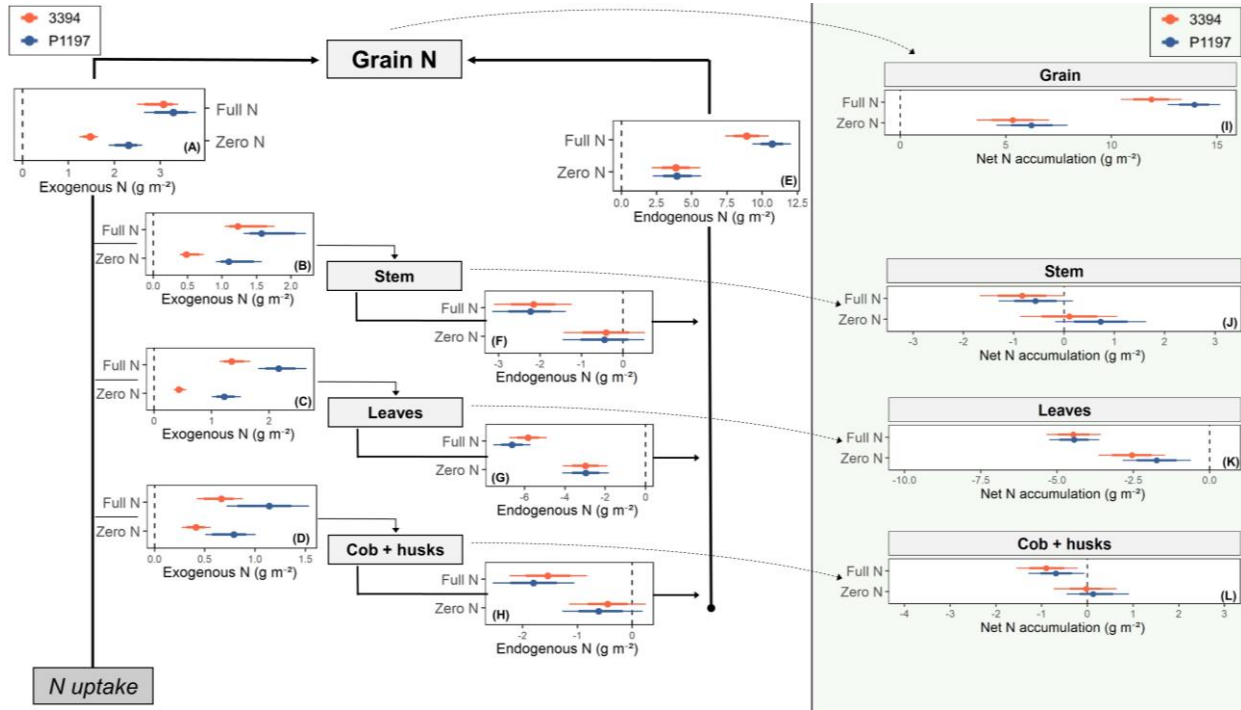


Figure 4.3. Summary of posterior predictive distributions for post-silking N fluxes in leaves, stem, cob-husks, and grain fractions for two maize hybrids (3394, orange symbols; and P1197, blue symbols) under two N fertilization levels (zero and full N). Points represent the median of the posterior distributions and whiskers their 95% credible intervals. Values on the left side of the zero-line (dashed line) indicates an export of N from the organ, while to the right, an import of N. Exogenous-N (A, B, C, and D) represents the amount of N absorbed from soil and directly allocated to each organ. Endogenous-N (E, F, G, and H) represents the N translocated from/to other tissues. Net N accumulation (I, J, K and L) represents the difference between N content at R1 and R6. All values represent the cumulative balance over the R1-R6 period. Seasonal posterior predictive estimates expressed in thermal time after silking are depicted in Supplementary Figure S4.

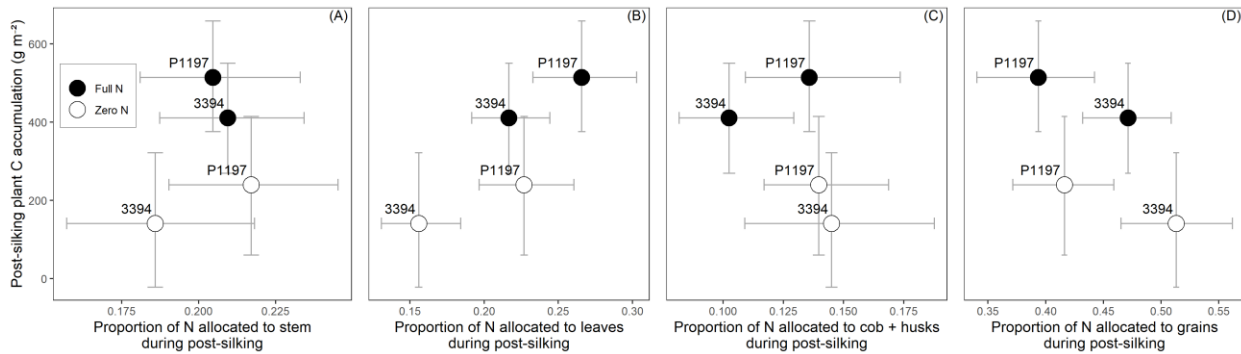


Figure 4.4. Summary of the posterior distributions for post-silking plant C accumulation (*y*-axis) and the proportion of exogenous-N (*x*-axis) allocated to (A) stem, (B) leaves, (C) cob-husks, and

(D) grains during the post-silking period. Means and credible intervals are depicted for two maize hybrids (3394 and P1197) under two N fertilization levels (zero and full N – open and closed symbols, respectively).

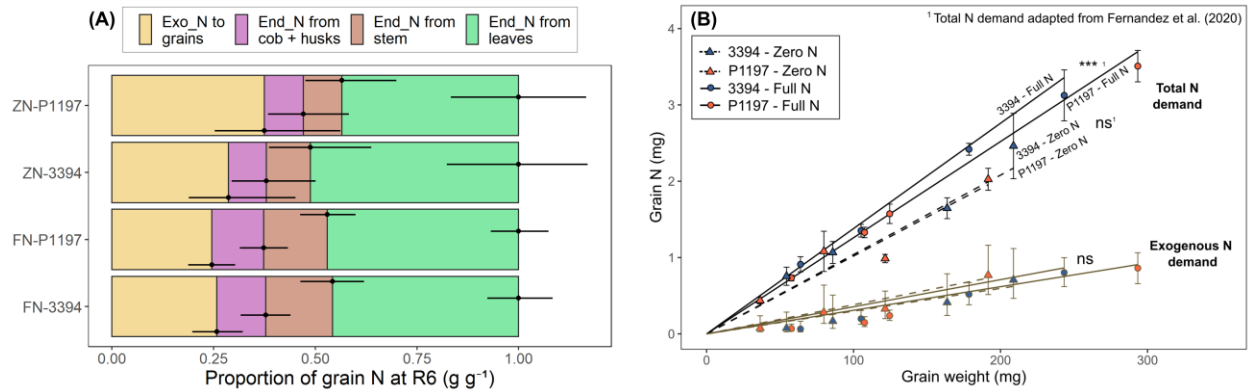


Figure 4.5. (A) Sources of grain N at maturity for two maize hybrids (3394 and P1197) under two N fertilization levels (zero and full N - ZN and FN, respectively). The four sources considered are: 1) exogenous-N to grains, which denotes N absorbed and directly allocated to grains during post-silking, and 2-4) Endogenous-N from leaves, stem, and cob-husks, which represents the N translocated respectively from each organ to grains (originated from pre-silking N or post-silking N allocated to the stover). Bars and solid points represent the median from samples of the posterior predictive distribution, and horizontal lines to the right of each bar denotes their corresponding 95% credible interval. (B) Relationship between grain N content and grain weight, throughout the grain filling period, for 3394 and P1197 under zero and full N treatments. Solid line represents the total grain N content [adapted from Chapter 3, Fernandez et al. (2021)], for which the slope represents the grain N concentration for each hybrid by N condition. Dashed lines denotes the expected exogenous grain N content calculated in the present study.

Table 4.1. Environmental and agronomic description of three experimental sites used in the study.*

Experiment	Site	Year	Irrigation	Genotype	N rate (kg ha ⁻¹)	Planting date	Planting density (plants ha ⁻¹)	¹⁵ N labelling stages	pH	Organic matter (mg kg ⁻¹)	NO ₃ -N (mg kg ⁻¹)	NH ₄ -N (mg kg ⁻¹)
1	Ashland Bottoms, KS	2017	Rainfed	3394 - P1197	0 – 137	May 5, 2017	61,000	R1 – R4	6.1	16	2.4	5.0
2	Ashland Bottoms, KS	2017	Irrigated	3394 - P1197	0 – 218	May 5, 2017	76,000	R1 – R4	6.1	13	3.2	6.1
3	Ashland Bottoms, KS	2018	Irrigated	3394 - P1197	0 – 218	April 24, 2018	76,000	R1 – R2 – R5	6.3	15	4.4	3.2

* Soil parameters were measured at pre-planting

Chapter 5 - Kernel weight contribution to genetic gain of maize: A global review and US case studies

Abstract

Over the past century of maize (*Zea mays* L.) breeding, direct selection for grain yield resulted in favorable improvements in several other related physiological and morphological traits. While the number of kernels per area has been recognized as the main driver for yield gains, the effect of breeding selection on kernel weight (KW) and its contribution to yield gains has not been yet thoroughly described for US hybrids. In this study, we propose to (i) review the contribution of KW on grain yield improvements during the last century across multiple agronomic settings and breeding programs, (ii) determine the physiological bases for improvements in KW and kernel-filling parameters for the set of Pioneer Hi-Bred ERA hybrids in the United States. A global scale literature review concludes that rates of KW improvement in US hybrids were comparatively similar to those of other commercial breeding programs but extended over a longer period of time. There is room for a continued increase of kernel size in maize for most of the genetic materials analyzed, but the trade-off between KN and KW poses a challenge to translate it into yield progress. Through multiple field experiments on the set of hybrids from Pioneer ERA breeding program, we determine that KW significantly contributed to yield gains in maize for the last century. Improvements in KW have been predominantly related to an extended kernel-filling duration. Likewise, crop improvement has conferred modern hybrids with greater KW plasticity, expressed as a better ability to respond to changes in assimilate availability. Our analysis of past trends and the current state of development identifies candidate targets for future improvements in maize.

Introduction

Over the past century, maize (*Zea mays* L.) grain yields have seen remarkable increases owing to the combination of breeding and agronomic management improvements. Because yield is an extremely complex trait, the determination of yield components has been a widely adopted strategy to rationalize this progress in kernel number per unit area (KN) and individual kernel weight (KW). In this sense, the major contribution to yield improvements has been attributed to the ability to set a greater KN via tolerance to higher plant density (Tollenaar and Lee, 2002; Duvick, 2005b). Although genotypic variation in kernel size can be responsible for important variations in maize yield, much less attention has been directed to the relative contribution of KW to yield improvements. Knowledge of the progress of KW along breeding improvement becomes even more relevant in light of the existing trade-off between the two yield components, upon which KW is often compensated by an adjustment in KN (Sadras, 2007; Gambín and Borrás, 2010). Certainly, one question to be addressed is whether KW improvements are necessary to overcome the reciprocity between both components and achieve future yield increases in these scenarios (Quintero et al., 2018).

Kernel weight is a complex trait involving several morphological and physiological processes under the combined influence of genetic and environmental factors. Typically, KW has been interpreted as the result of dry matter accumulation during the length of the kernel-filling period. After ovary fertilization, there is a short period of endosperm cellularization (Leroux et al., 2014), usually referred to as lag phase, when the potential storage capacity of the kernel is largely determined (Johnson and Tanner, 1972; Reddy and Daynard, 1983). In overall, kernel sink capacity is defined by the number of endosperm cells (Jones et al., 1985, 1996).

Nonetheless, kernel filling potential has been associated with genetic and environmental factors

also affecting the floret development and carpel growth before ovary fertilization (Scott et al., 1983; Millet and Pinthus, 1984; Calderini et al., 2001; Yang et al., 2009) and the kernel expansion via water uptake during the linear phase (Martinez-Carrasco and Thorne, 1979; Kiniry, 1988; Borrás et al., 2004). After lag phase, a period of rapid water uptake and dry matter accumulation defines the initiation of the linear kernel-filling phase (Ouattar et al., 1987b). Once the maximum water content is achieved, maximum kernel volume is largely determined (Borrás et al., 2003). However, further increases in kernel volume during the last part of linear phase may result at the expense of biomass deposition (Gambín et al., 2007; Sala et al., 2007). Water content continues to drop during this final phase reflected by the progression of the milk line towards the tip, and kernels are considered physiologically mature when they achieve their maximum dry weight (Fernandez and Ciampitti, 2018, 2019, 2021). Although variations in these kernel-filling characteristics are known to be associated with the agronomic conditions and genotype, their relative contribution to past yield improvements has not been quantified. Understanding the effect of breeding progress on kernel filling patterns under a variety of conditions is of fundamental interest to identify candidate breeding selection mechanisms for future crop improvement.

For US maize germplasms, the long-term genetic gain in yield has been successfully investigated in past retrospective studies on Pioneer Hi-Bred International (Corteva Agriscience) hybrids from the past century (Duvick et al., 2004; Campos et al., 2006; Cooper et al., 2014a; Reyes et al., 2015; DeBruin et al., 2017). Although these hybrids (usually referred to as Pioneer ERA hybrids) have been subjected to extensive evaluations of agronomic traits across multiple US production systems, changes over time in KW and underlying physiological parameters have received little attention. The objectives of the current study were to (i) review the contribution of

KW on grain yield improvements during the last century across multiple agronomic settings and breeding programs, (ii) determine the physiological bases for improvements in KW and kernel-filling parameters for the set of Pioneer Hi-Bred ERA hybrids in the US.

Materials and methods

Systematic review

The article screening procedure is summarized in Fig. S1. Briefly, a literature search was conducted using the Web of Science, Scopus, and Google Scholar databases (last search on 08/03/2021) using the following keywords: (grain OR kernel) AND weight AND (historical OR era OR decades) AND (maize OR corn). A total of 346 research articles were retrieved, and assessment of duplicates, titles, abstracts, and full-texts were conducted based on (i) experiments carried under field conditions; (ii) at a given study, two or more maize cultivars from different decades of commercial release evaluated; (iii) variable of interest KW and year of release (YOR) of hybrids provided; (iv) management information, in particular, planting density, row spacing, N fertilization, water condition, and source-sink restrictions reported; and (v) written in English language. After assessment, a total of 29 published studies were considered eligible, in addition to the five US Pioneer ERA experimental studies described in detail below (Table S1). In addition to KW, grain yield and KN variables were extracted when reported. The entire database includes 838 data points of KW (of which 751 and 763 reported grain yield and KN, respectively) along with the metadata describing management practices.

Case studies I – 2017 and 2018 field experiments

Experiments in 2017 and 2018 were performed to study the influence of rates and timing of N fertilization, water condition, and source-sink relationships on a smaller subset of three historical hybrids from the US Pioneer ERA set (Corteva Agriscience, Johnston, IA, US). All experiments (Ashland Bottoms KS, USA) were described in detail in Chapter 4 (Fernandez et al., *under review*) and main characteristics of the sites are presented in Table S1. Briefly, experiments were planted on 5 May (2017) and 24 April (2018) with plant density adjusted for irrigated (76,000 plants ha⁻¹) and rainfed (61,000 plants ha⁻¹) sites. Treatments were assigned to plots of 64 m² size (4 rows at 0.76 m between rows × 21 m length).

In 2017, both an irrigated and rainfed site were conducted as split-plot designs with three replicates. Pioneer hybrids (Corteva Agriscience) 3394 (1991), P1151 (2011), and P1197 (2014) were assigned to the whole-plots and N treatments as subplots. N treatments consisted of a low N (with no N applied) and two high + late N treatments [differing in the timing of the last N application, either at flowering (R₁, Ritchie et al., 1997) or blister stage (R₂)]. For the high + late N, rates were adjusted for N demand based on yield target for each condition: 56 kg N ha⁻¹ at planting; 56 (rainfed) and 112 kg N ha⁻¹ (irrigated) at sixth-leaf (V₆); and 25 (rainfed) and 50 kg N ha⁻¹ (irrigated) as late N at R₁ or R₂.

The experiment in 2018 was carried out in a split-plot design with three replicates under irrigated conditions. Hybrids 3394 (1991) and P1197 (2014) were assigned to the whole-plots, and combinations of N fertilization and source-sink treatments (plus a low N negative control) to the subplots. For N levels, two fertilization approaches were tested maintaining the final N rate as the preceding year for irrigated conditions (218 kg N ha⁻¹): high N, split in two applications (50% planting and 50% V₆); and high + late N, split in three applications (50% at planting, 20%

at V₆, and 30% at twelfth-leaf (V₁₂). Three levels of source-sink ratio were tested: a control without any intervention; a high source-sink ratio with reduced sink; and a low ratio with reduced source. Reduced sink treatments were achieved by means of a partially restricted pollination, covering the ears with a bag when the silks were 2.5 cm long (Rajcan and Tollenaar, 1999a). Reduced source was achieved through partial defoliation, removing all leaves above the first node from the ear position two weeks after silking. Lastly, a low N (with no N applied) treatment with normal pollination was added as a negative control.

Case studies II – 2019 and 2020 field experiments

Field experiments were conducted in 2019 at Manhattan KS, USA and in 2019-2020 at Viluco, Chile to characterize changes in KW across the last century of the Pioneer ERA maize-breeding program. Both locations were Corteva Agriscience research stations for which information on agronomic management is provided in Table S1. Seeds were planted on 5 May (2019) with a plant density of 65,200 plants ha⁻¹ (Manhattan) and on 28 Oct (2019) with a plant density of 100,000 plants ha⁻¹ (Viluco). Experiments were conducted under rainfed (Manhattan) and full-irrigated (Viluco) conditions. Nitrogen fertilizer was applied at levels to avoid N being a limiting factor and adjusted for yield target for each condition. The experimental area was kept free of weeds, pests, and diseases during the growing season.

Twenty hybrids released from 1920 to 2017 were grown in a split-plot in randomized complete block design with three replications at both locations. Hybrids were assigned to whole-plots of eight rows, 76 cm apart, and a size of 6 m wide by 5 m long. Subplots consisted of three micro-plots of 10 adjacent plants (within two rows) delimited to carry out source-sink manipulation treatments. The three levels of source-sink ratio were applied following the same

procedures described for case studies I: a control without any intervention; a high source-sink ratio with reduced sink; and a low ratio with reduced source.

Phenotypic measurements and calculations

In all experiments, phenotypic descriptors for the reproductive phase were quantified for plants within experimental units (i.e. above 60 tagged plants per plot). Key developmental stages anthesis (V_T) and silking (R_1) dates were recorded daily for all plants within experimental units. At silking date for each plot (i.e. at least 50% of the plants had exposed silks) and physiological maturity (i.e. black layer visible), shoot biomass samples were taken from an area between 0.5 m² (3 plants, 2017-2018) and 0.75 m² (6 plants, 2019-2020). Plants were cut at the ground level and separated in leaves (green leaf blades), stover (stems + leaf sheaths + attached dead leaves + tassels), ear (cobs + husks), and grains. All samples were dried at 65 °C until constant weight. Post-flowering biomass accumulation was calculated as the difference between shoot biomass at R_6 and R_1 . Since only biomass at R_1 was available for all experiments, an estimate for the post-flowering source-sink ratio was obtained here as the quotient between the post-flowering biomass accumulation and KN.

From biomass harvested at physiological maturity, numerical yield components KN and KW were determined. In 2017-2018 experiments, a subsample of 500 kernels was counted and weighed separately to estimate final KW. The KN was estimated as the ratio between total grain biomass harvested at R_6 sampling and individual KW. Yield was determined with a plot combine from the two center rows; harvest area was corrected in rows where biomass samples were taken. In 2019 and 2020 experiments, grain yield and KN were obtained using the ear-photometry (EP) imaging system from Corteva Agriscience on ears harvested at maturity (Hausmann et al., 2011).

The sampled ears were dried and shelled, and 500 individual kernels were separated to record individual KW. All grain yield values reported in this study were adjusted to a standard 150 g kg⁻¹ moisture.

For kernel filling determination, the primary ear of a previously tagged plant was collected every week per plot, from R₂ until harvest maturity, and immediately placed in an airtight plastic bag. In the laboratory, ears were transferred to a humid chamber at saturating vapor pressure for the subsequent separation of kernels. Ten (2017-2018) to fifteen kernels (2019-2020) from the central portion of the ear were excised to track changes in kernel water and dry matter content during the kernel-filling period. Fresh and, after drying in an oven at 70 °C, dried kernels were weighed with an Ohaus analytical balance (Ohaus Scale Corp. Florham Park, NJ, USA) with an error index of 0.1 mg, except for Viluco experiments for which only dried kernels were weighed. Water content was calculated as the difference between kernel fresh weight and dry weight.

Statistical analysis

All analyses were conducted using R software version 4.1.1 (R Core Team, 2021) in RStudio interface (RStudio Team, 2016). A meta-regression with mixed-effects model was used to estimate the genetic gain in KW, KN, and grain yield across hybrids' year of release (function *lme* in *nlme* package; Pinheiro and Bates (2000)). Standardized response variables (%) were used in the meta-analysis to objectively compare genetic gain (% year⁻¹) across variables and environments (Curin et al., 2020):

$$\text{Standardized value} = \frac{\text{Actual value} - \text{Environmental index}}{\text{Environmental Index}},$$

Equation 5.1

where the environmental index represents the mean value for a particular environment \times management ($E \times M$) combination. Studies and combinations of $E \times M$ were modeled as random effects to account for differences between the site-years. Because variance measures information was available for less than 25% of our dataset, individual data were weighted by the number of replicates. Non-parametric bootstrapping with replacement ($n = 5000$) was used to estimate 95% confidence intervals (95% CI) of the effect sizes for genetic gain using the *boot* package (Canty and Ripley, 2021). Genetic gains were considered significant if the 95% CI did not include zero, while differences between groups were assessed based on the 95% CI of their differences. Between-group heterogeneity was determined based on the 5000 resampling procedure using the I^2 statistic and was considered significant when tests yielded P values < 0.05 . Lastly, yield genetic gain isolines were represented in a contour plot using a generalized additive mixed model with KW and KN genetic gains as predictors and with observations weighted by the number of replicates [function *gamm* in *mgcv* package; Wood (2017)].

Subgroup meta-regression analyses were conducted to assess the effect of water regimes, N management, plant density, and source-sink relationship on the genetic progress of US Pioneer ERA hybrids relative to other global programs. Based on the treatments tested in US case trials and reviewed studies, three subgroups were established for water condition (rainfed, partially- and full-irrigated), nitrogen (low N $< 100 \text{ kg ha}^{-1}$, high N $> 100 \text{ kg ha}^{-1}$, and high + late N including a post- V_{12} application), and source-sink ratios (control, low, and high), and four subgroups for plant density (< 5 , 5 to 7.5, 7.6 to 8.9, and $> 9 \text{ pl. m}^{-2}$). Subsets were analyzed separately following the same procedure described for the pooled data.

For the description of kernel dry matter accumulation, an expolinear-plateau model was used on the case studies' data. The expolinear model developed by Goudriaan and Monteith

(1990) provides an opportunity to simultaneously model the lag (exponential) and early linear phases of kernel growth in crops (Mueller et al., 2019b). We combine here the expolinear model with a final plateau of maximum KW into a three-phase model, that is, into an expolinear-plateau model defined as:

$$W = \left(\frac{Cm}{Rm}\right) \ln(1 + e^{Rm(x-tb)}) \quad \text{for } x < x_s, \quad \text{Equation 5.2}$$

$$W = \left(\frac{Cm}{Rm}\right) \ln(1 + e^{Rm(xs-tb)}) \quad \text{for } x \geq x_s, \quad \text{Equation 5.3}$$

where W is kernel dry weight (mg kernel⁻¹), Cm is maximum absolute kernel growth rate during the linear phase (mg kernel⁻¹ d⁻¹), Rm is the maximum relative growth rate during the exponential phase (mg mg⁻¹ d⁻¹), tb is days where the extrapolated Cm slope crosses the x -axis (d), x_s is days at which the plateau of maximum KW is achieved (d), and x is the explanatory variable in days (d). The expolinear-plateau function was fit to the data using non-linear mixed-effects models with the *nlme* package. The nonlinear model was first fitted for each replication using *nlsList* function [see Meade et al. (2013)]. A self-starting function was developed for the expolinear-plateau model and used to determine starting values. The R script for the self-starting function is presented in Appendix A1. Obtained parameters for all replications were averaged to determine starting values for the non-linear mixed effect model using *nlme* function. Residuals were modeled as a power function of days to account for the heteroscedasticity due to the increased sample variance over time. The best random effects structure of non-linear models (with/without site and block effects) was assessed based on the lowest AIC (Akaike's information criterion).

Similarly, a third-order polynomial model was fitted to the kernel water content along the kernel-filling period:

$$KWC = a + b * x + c * x^2 + d * x^3 , \quad \text{Equation 5.4}$$

where KWC is kernel water content (mg kernel^{-1}), a is the y-axis intercept (mg kernel^{-1}), b , c and d are the linear, quadratic, and cubic empirical coefficients of the model, respectively, and x is the explanatory variable in days (d). Days at kernel maximum water content (KMWC, d) was estimated solving for x when the first derivative of the equation was equal to zero.

A Partial Least Squares (PLS) regression was used to model the variation in KW explained by the kernel-filling parameters extracted from kernel dry matter and water content dynamics [function *mvr* in *pls* package; Mevik et al. (2020)]. The use of PLS was based on its reliability and ability to overcome multicollinearity between a high number of explanatory variables. Variables were scaled to their unit variances and mean-centered to standardize across units. The relative importance of variables was assessed by the absolute value of their regression coefficients over the sum of all coefficients, expressed in percentage.

Results

Descriptive summary of historical changes in kernel weight

Our analysis included retrospective studies performed on a total of 7 countries, with Argentina (67), USA (38), and China (15) as leading countries in terms of number of collected sites (i.e. $E \times M$ combinations, Fig. 1a). Categorized by the number of observations, the USA was the top country comprising records of ERA hybrids from Pioneer Hi-Bred ($n = 397$) and other breeding programs ($n = 46$). Genetic gain research in this country covered the largest range of genotypes' years of introduction from 1920-2017 (Pioneer Hi-Bred) and 1930-2005 (Other programs). For other countries, the oldest genotypes recorded were developed in the 1950s and, therefore, the period of years covered in our dataset was smaller relative to the USA (Fig. 1a).

Hybrids from different ERAs were subjected to a wide range of agronomic management practices across studies. The USA presented the most balanced and exhaustive research in KW genetic gain across nitrogen, planting density, water regimes, source-sink levels, and most of their interactions (Fig. 1a). In Argentina and China, most of the studies tested genotypic variations across density, nitrogen \times density, and water condition levels. The remaining countries analyzed genotypes across two or less levels of treatments (Brazil and Canada) or a unique agronomic setting (Serbia and Nigeria) (Fig. 1a).

Meta-regression results showed positive genetic progress for grain yield across the wide range of countries and agronomic conditions explored in our database. In the USA, Pioneer Hi-Bred showed a genetic gain rate of 0.7% yr⁻¹ whereas other US hybrids followed closely with a rate near 0.6% yr⁻¹ (Fig. 1b). Rates for yield improvement in Argentina and China were comparatively higher with values of around 1.1 and 1.2% yr⁻¹, respectively, although with larger confidence intervals. Likewise, and despite the smaller sample sizes, other countries included in our database revealed similar yield increases in the range of 0.5-1% yr⁻¹. Overall, the global estimated progress was around 0.9% yr⁻¹ (Fig. 1b).

Improvements in KW were much modest than those for yield, a pattern that was repeated across all countries. KW improved at a rate of 0.3 and 0.4% yr⁻¹ in US hybrids over the last century (Fig. 1c). Genetic progress in China for the same trait was higher in the order of 0.7% yr⁻¹, although covering a narrower and more recent historical range of decades than the USA. For countries such as Argentina, Brazil, and Nigeria, our data showed non-significant improvement in KW associated with breeding over time, with mean values in the range of 0.1-0.2% yr⁻¹ (Fig. 1c). Overall, the global rate of genetic gain in maize KW was significantly positive and estimated close to 0.5% yr⁻¹.

Genetic gains in grain yield were largely driven by improvements in KN per area for hybrids both from USA Pioneer Hi-Bred and from other global institutions. Most of the records (70%) evidenced yield increases in the range of 3.8 to 16.9 g m⁻² yr⁻¹ supported predominantly by improvements in KN of between 6.1 and 68.8 kernels m⁻² year⁻¹ (Fig. 2a). Same studies, on the other hand, showed less pronounced KW improvements between -1.2 and 1.3 mg kernel⁻¹ year⁻¹. Among components, the trade-off was evident as the contribution of KW improvements to yield gain decreased when there were strong increments in KN (Fig. 2a). Our analysis showed that genetic gain in KN explained around 63% of the yield increases in the dataset, whereas KW explained a roughly 7% of the yield variation (Fig. 2b). Interestingly, the estimated 95% CI reflected large uncertainty on the potential contribution of KW improvements across genotype × environment combinations, up to even 35% of contribution to yield gain.

Effect of crop growth conditions on maize genetic gain

Agronomic management influenced genetic gains in grain yield and KN but in a different manner across breeding programs. For USA – Pioneer ERA hybrids, grain yield improvements were significantly affected by planting density and nitrogen levels (Table 1). Yield improvement was greater under high planting density (>76K pl ha⁻¹) up to 0.92% yr⁻¹. This was essentially driven by large improvements in KN (0.66% yr⁻¹) rather than in KW (0.33% yr⁻¹). Nitrogen supply did not trigger significant variations in the relative rate of gain for both yield and KN, yet it did influence the actual environmental index. Thus, when increases were expressed in their ‘actual’ units (i.e. g m⁻² yr⁻¹ for yield and kernels m⁻² yr⁻¹ for KN), rates of gain were greater under high N (7 g m⁻² yr⁻¹ and 14 kernels m⁻² yr⁻¹) than under low N supply (4 g m⁻² yr⁻¹ and 12 kernels ha⁻¹ yr⁻¹).

For other global breeding programs, the rate of gain in grain yield and KN was largely affected by all management practices evaluated but with large heterogeneity in the estimations (I^2) (Table 1). Because multiple and distinct breeding programs were combined in this analysis, significant variations within individual subgroups were expected and reflected by large I^2 values ($I^2 > 75\%$). However, our analysis evidenced predominant effects of both water and nitrogen supply motivating greater rates of improvement.

KW relative increments for Pioneer ERA hybrids were similar across most of the agronomic settings comprised in our database, except for nitrogen supply levels. Genetic progress was higher under high N ($0.37\% \text{ yr}^{-1}$) than under low N ($0.22\% \text{ yr}^{-1}$) (Table 1). Actual rates of improvements (non-standardized) can be expected to differ even more considering levels of environmental index achieved at each N condition (211 mg for low N and 272 mg for high N). A similar pattern was observed for hybrids with different genetic backgrounds, for which rates of KW gain over time were greater under high N ($0.55\% \text{ yr}^{-1}$, Table 1). In addition, better improvements in KW were observed in irrigated conditions ($0.69\% \text{ yr}^{-1}$) relative to rainfed ($0.43\% \text{ yr}^{-1}$) although, here, the large heterogeneity underpins variation in the magnitude of the water effect ($I^2 > 93\%$). Lastly, manipulations in the post-flowering source-sink levels generally affected more of the overall mean of KW in the environment (KW ranged from 190 to 319 mg) than the relative rate of gain.

Physiological traits underpinning kernel weight genetic progress of USA – Pioneer ERA hybrids

Following analysis of literature data across years and countries, hybrids from the ERA set of USA – Pioneer Hi-Bred were further examined at multiple field trials during 2017 to 2020

growing seasons. The rate of yield gain was influenced by the management combination of water regime and planting density (Fig. 3a). Yield increased from 6.0 Mg ha⁻¹ in 1920 to 14.5 Mg ha⁻¹ in 2017 under irrigation and high-density (88 kg ha⁻¹ y⁻¹), whereas from 6.9 Mg ha⁻¹ in 1920 to 12.1 Mg ha⁻¹ in 2017 in rainfed and low-density environments (54 kg ha⁻¹ y⁻¹). A similar G x M interaction effect was observed for the rate of gain in KN across years of hybrids' introduction (Fig. 3b). The rate of increase in KN was 29 kernels m⁻² yr⁻¹ under irrigation and high density, and 9.3 kernels m⁻² yr⁻¹ under rainfed and low density. These results evidence the strong influence of the improved tolerance to high plant densities of modern US hybrids.

The KW of ERA hybrids from USA – Pioneer Hi-Bred showed a linear increase over time, but without significant interactions across water x planting density levels (Fig. 3c). Kernel mass increased from 187 mg kernel⁻¹ in 1920 to 288 mg kernel⁻¹ in 2017, signifying a rate of increment of about 1.04 mg kernel⁻¹ yr⁻¹. This suggests that contrary to what was reported for yield and KN, the G x M (water regime and plant density) component was less important in the improvements achieved in KW. More importantly, and although KN was the predominant component supporting yield increases, our findings suggest that KW had a significant contribution to yield gain in Pioneer Hi-Bred ERA hybrids.

The expolinear-plateau model proved adequate to described KW as the result of dry matter accumulation during the kernel-filling period. Furthermore, parameters of such model were reasonably interpreted in useful biological terms (Fig. 4a): *cm* described the linear kernel-filling rate, *xs* represented the kernel-filling duration, *tb* described the duration of the lag phase, and the kernel growth during lag phase was obtained solving for *y* when *x* = *tb*. The linear rate of kernel growth significantly increased with years of hybrids release since the 1920s, but it has remained relatively stable over the past 40 years (Fig. 4c). Kernel filling rate increased 0.02 mg

kernel⁻¹ d⁻¹ yr⁻¹ until a plateau was achieved near 1982 at 9.11 mg kernel⁻¹ d⁻¹. Instead, the duration of kernel-filling evidenced a steady genetic gain, with a linear rate of 0.06 d yr⁻¹ (Fig. 4d). These results demonstrate that, for the last four decades, KW genetic gain has been predominantly driven by improvements in kernel-filling duration (48% of KW variation, Fig. 5a-b).

The duration of the lag phase has remained constant during the last century of maize breeding improvement (Fig. 4e). The average duration among the twenty hybrids evaluated was of 12 days, indicating that the extension of the kernel-filling period over years was driven by a prolonged linear phase. Interestingly, and although dry matter accumulation is slow during the lag phase, kernel growth during this initial period significantly increased with years of hybrids release, at a rate of 0.02 mg yr⁻¹ (Fig. 4f). While these increments contribute little to the total increase in KW (5.3%, Fig. 5 a-b), they denote a better transition through which kernels enter the rapid phase of dry matter accumulation.

Kernel water and dry matter accumulation are two tightly connected processes that determine kernel-filling growth patterns (Fig. 4b). In this sense, the definition of maximum kernel water content (MKWC) was delayed with the year of hybrid release at a rate of 0.07 d yr⁻¹ (Fig. 4g). Coupled with the lack of changes in lag phase duration, our results imply that most of the genetic progress in kernel-filling duration can be attributed to an extended lag-to-MKWC period. The MKWC value also increased linearly over time at a rate of 0.19 mg yr⁻¹ (data not shown), likely suggesting an aligned rate of improvement in kernel volume.

Phenotypic plasticity of KW (i.e. to conditions of high and low resource availability) showed a linear increase over the last century for the US Pioneer ERA hybrids. KW plasticity increased from 0.27 in 1920 to 0.36 in 2017 (Fig. 4h). This was the second most important factor

explaining changes in KW over decades (14.1%, Fig. 5 a-b). This trend in KW plasticity was essentially supported by both (i) a higher reduction in KW under conditions of low post-flowering source-sink ratio (i.e. defoliation treatments) ($p < 0.01$, not shown), and (ii) a better response in KW to increases in source-sink ratio (i.e. restricted pollination treatments) ($p < 0.05$, not shown).

Lastly, for control treatments without manipulation, we analyzed variations in the post-flowering source-sink ratio over time to quantify how the source capacity has been improved to support more kernels with greater size in modern hybrids. The post-flowering source-sink ratio increased from 192 mg kernel⁻¹ in 1920 to 302 mg kernel⁻¹ in 2017, which translates into a rate of 1.13 mg kernel⁻¹ yr⁻¹ (not shown). As can be expected, these increases were positively correlated with KW improvements explaining part of the variation (8.9%, Fig. 5 a-b). These results demonstrate that increases in reproductive biomass accumulation were comparable and even exceeded those in KN, resulting in an improved supply of assimilates per kernel during the post-flowering period.

Discussion

A large and diverse dataset on KW in historical hybrids was assembled to compare genetic improvements in this trait across commercial breeding programs. Our study, for the first time, describes the physiological characteristics underlying improvements in maize KW during the last century for US Pioneer ERA hybrids. Rates of improvement in KW of US hybrids were relatively similar to those of other commercial breeding programs around the globe but documented over a longer period of time. Our findings extend those obtained in previous decades (Crosbie and Mock, 1981; Meghji et al., 1984; Cavalieri and Smith, 1985; Russell,

1985) and further describe the $G \times M$ interaction as a critical element in the genetic improvement of KW. This analysis provides foundational knowledge to propose candidate targets for future selection gains in maize.

The contribution of KW improvements to yield genetic gain was smaller (but substantial) relative to the KN, although governed by the trade-off between KW-KN. While the negative association between KN and KW has received much of the attention in maize and other species (Sadras, 2007; Gambín and Borrás, 2010), the evolution of this trade-off through historical improvements in both components has been little investigated. Here, we demonstrated a simultaneous consideration of both components is necessary to analyze past and predict future genetic gains. Potential improvements in individual KW remain unexploited in breeding programs for which KN was the fundamental target trait to increase grain yield (e.g. Argentinean hybrids for our dataset) relative to those of the highest KW gains (e.g. Chinese hybrids in our dataset). Genetic progress in Pioneer ERA hybrids was also principally associated with increased KN but with more balanced increments in KW. These results are in agreement with what was well established in the literature for maize (Duvick et al., 2004) and other cereals (Donmez et al., 2001; Demarco et al., 2020). Still, there is a significant gap between current and maximum KW described for US hybrids that warrants a path to further increase kernel size. However, yield progress driven by increments in KW in the future will be feasible only if the reciprocity between both components is overcome through the identification of independent genetic loci for kernel size (Alvarez Prado et al., 2014a; Chen et al., 2016; Calderini et al., 2021). Considering that both kernel set and size depends on growth, it is also important to recognize the necessity to accommodate the source capacity of the crop to overcome the KW-KN trade-off and achieve further genetic gains for yield. A parallel enhancement of either radiation use efficiency (RUE)

or carbon partitioning to the grains are required for translating the larger sink capacity from KW into productivity improvements (Messina et al., 2021).

Relative increments in KW over decades showed considerable variability across management scenarios, but nitrogen supply was identified as one of the principal factors influencing KW improvements over time. Nitrogen influences the endosperm cell number and kernel sink capacity during the lag phase (Lemcoff and Loomis, 1994; Olmedo Pico et al., 2021). Hence, the higher kernel-filling rate of modern hybrids presumably demonstrates an improved response to nitrogen supply on the endosperm cell division cycle. A similar pattern of N response was repeated on genetic materials from other regions of the globe. The practice of selecting and evaluating hybrids under a high nitrogen supply has improved the ability of modern hybrids to respond to N-fertilizer (Ciampitti and Vyn, 2012; Haegele et al., 2013). Different physiological mechanisms are responsible for high grain yields under low- and high-N (Bänziger et al., 1997). Therefore, the lower genetic progress under nitrogen stress environments for KW highlights the need to explore specific adaptation to low-N environments in order to put this yield component close to its observed potential under high-N (Lafitte & Edmeades, 1994).

KW genetic gain has been predominantly related to an extended kernel-filling duration given a prolonged kernel water uptake period. These results relate to those of Yang et al. (2010) in sorghum for which genotypic differences in kernel-filling duration were established during early stages of kernel development. A number of studies have shown that the accumulation and status of water in the kernel play a pivotal role in the determination of potential kernel volume and size (Borrás et al., 2003; Gambín et al., 2007). The accumulation of water regulates cell expansion and metabolic processes in the kernel and, subsequently, the cessation of dry matter accumulation (Egli, 1990). Here, we show that breeding selection has increased the duration of

kernel filling by delaying the timing when net water uptake stops, but without major modifications in the lag- nor the late phases of development. In fact, the contribution of changes in growth during the lag phase was negligible compared to those regarding metabolic events during the determination of the potential kernel size. Furthermore, the higher filling rates showed for modern hybrids suggest that a delayed realization of MKWC also influences the determination of the maximum granule number (Jones et al., 1996; Borrás et al., 2003). It is reasonable to conclude that the variations in water content for modern hybrids reflect an improvement in the number of granule numbers with long-term genetic improvement. Our results confirm that the effects of genetic improvement in maize have exerted fundamental changes in KW through the alteration of metabolic dynamics during the early stages of kernel development.

The amount to which a trait is contingent on the environment [i.e. phenotypic plasticity, Bradshaw, (1965)] has been an often-overlooked component in past retrospective studies describing phenotypic changes associated with breeding selection in maize and other crops (Peltonen-Sainio et al., 2011; Sadras and Lawson, 2011; de Felipe and Alvarez Prado, 2021). A focus on KW plasticity allows for a valuable consideration of the reaction of the genotype-by-environment interaction to crop improvement. Here, we demonstrate a continued increase in KW plasticity with selection for yield in maize, upon which modern hybrids express a better plastic response to the assimilate availability during kernel-filling. High KW plasticity resulted from a better ability of modern hybrids to respond to favorable conditions (high resource availability) but also from a higher susceptibility to poor conditions during kernel-filling (low resource availability). Reductions in KW under assimilate constraints were usually larger in newer genotypes of our dataset, consistent with what has been reported in other cereals (Fischer and

HilleRisLambers, 1978; Kruk et al., 1997). More importantly, we also observed that crop improvement has conferred modern hybrids better responsiveness to increments in assimilate availability. This reinforces the concept of phenotypic plasticity being associated with greater productivity of agronomic traits (Calderini and Slafer, 1999; Peltonen-Sainio et al., 2011). A remaining challenge is to investigate to which extent the expression of an improved KW plasticity during kernel-filling can partially compensate for reductions in KN as an adaptive strategy to stresses at flowering. Furthermore, these results and the knowledge that genetic control of KW and its physiological characteristics are independent of the genetic control of the KW plasticity (Alvarez Prado et al., 2014b) highlights the opportunity to exploit this trait further in breeding programs and provide a better adaptation of hybrids to future environments.

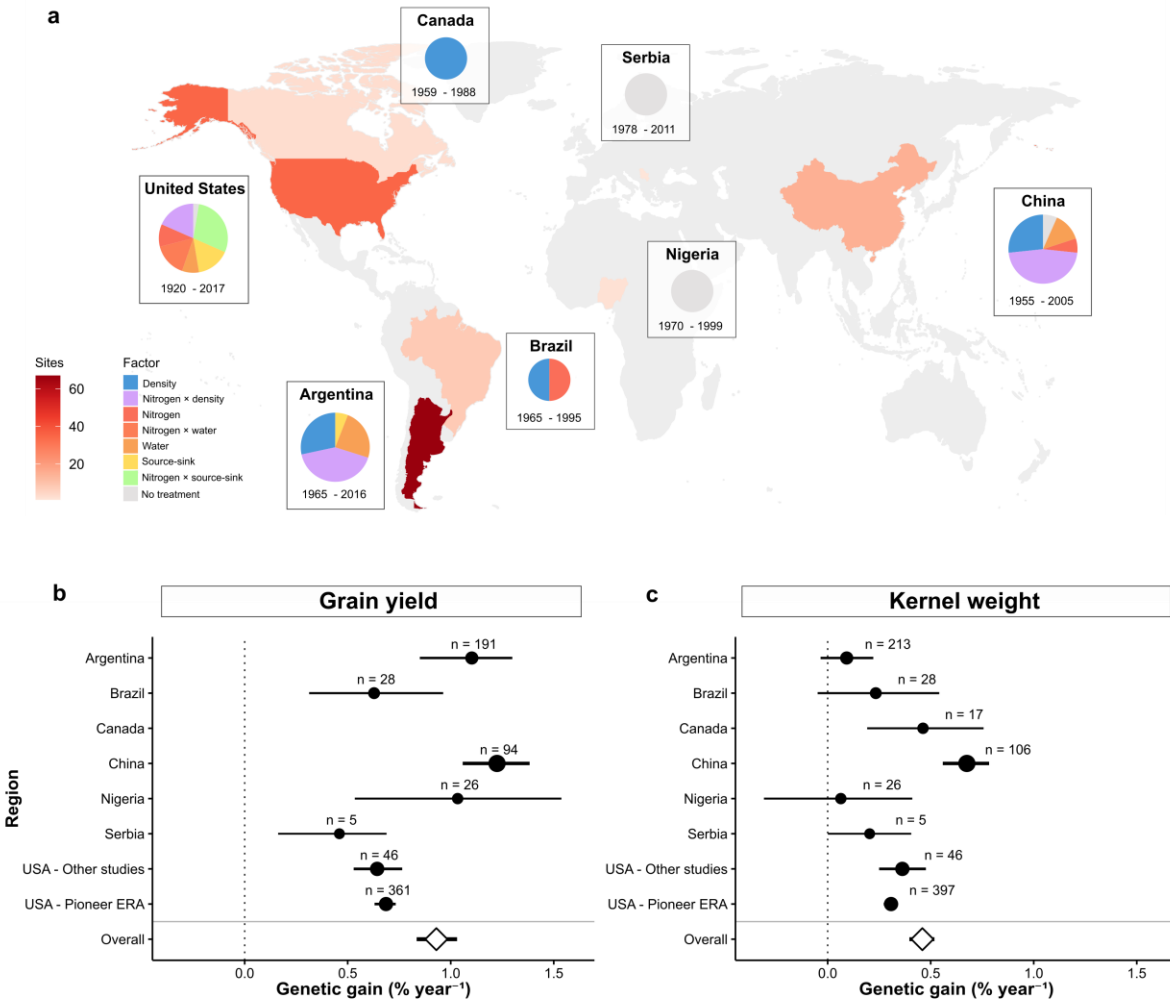


Figure 5.1. General information of the sites ($n = 134$) included in the review analysis. (A) Number of studies, management factors, and years of release of hybrids evaluated across locations. Comparison of rates of genetic progress across regions (and breeding programs for the USA) for (B), grain yield and (C), kernel weight. Size of symbols represents their weight in the global meta-regression estimate across all regions, influenced by both number of observations (n) and sites within the individual region.

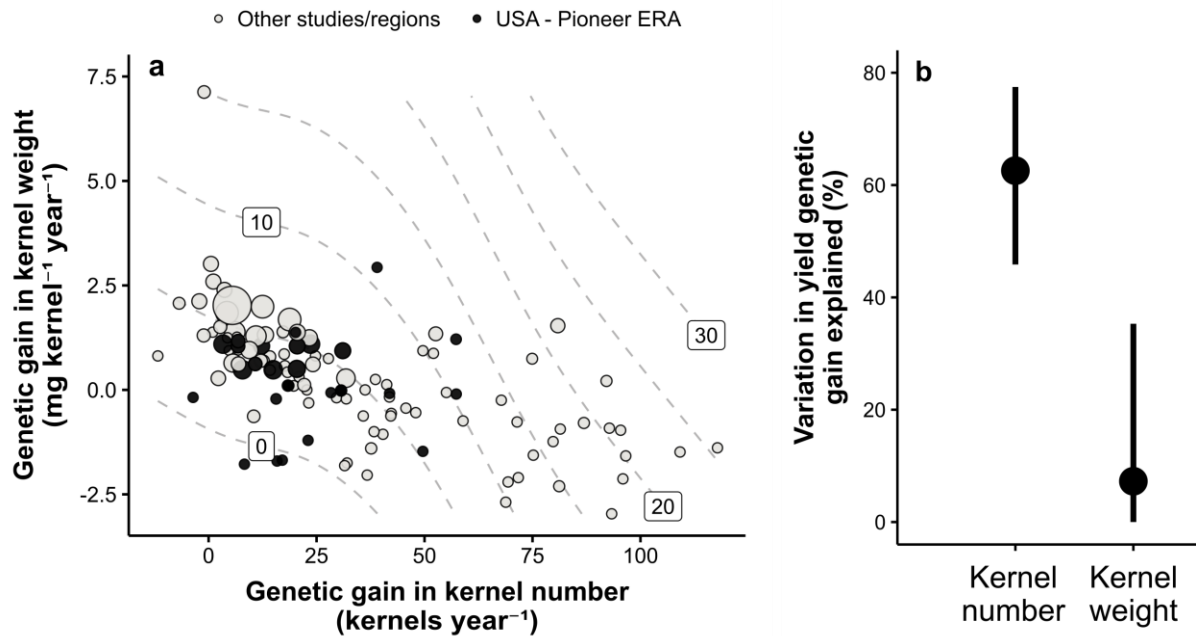


Figure 5.2. Contribution of kernel weight to the genetic gain in maize. (A) Genetic gain in kernel number and kernel weight across sites ($n = 134$) included in the review analysis. Isolines represent levels of yield genetic gain from 0 to 30 g m⁻² year⁻¹. Size of symbols represents the number of observations within each study. Dark and white symbols represent hybrids from USA – Pioneer ERA and other global breeding programs, respectively. (B) Proportion of the variation in yield genetic gain explained by improvements in kernel number and kernel weight, calculated as the coefficient of determination (r^2) of the association between variables. Whiskers represent their 95% CI.

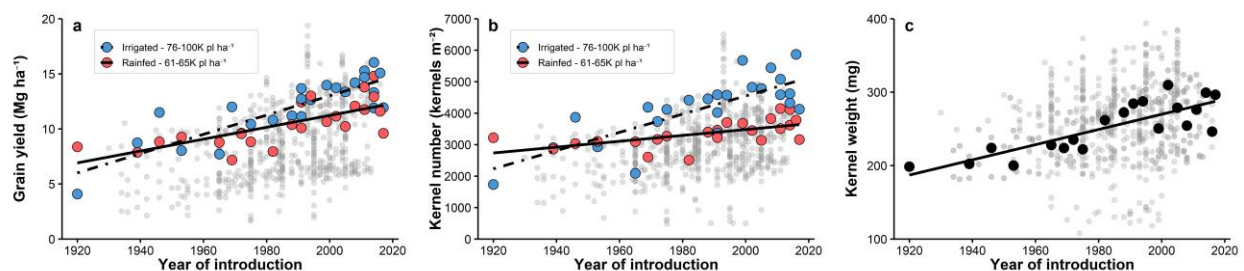


Figure 5.3. Genetic gain of USA – Pioneer ERA hybrids in multiple case studies from 2017 to 2020 growing seasons. Relationships between years of hybrid introduction and (A) grain yield, (B) kernel number, and (C) kernel weight. Symbols represent Best Linear Unbiased Estimates (BLUES) of hybrids at the group or marginal levels of inference based on 2-way interactions significance. Grey markers show observations from other studies that were included in the review analysis.

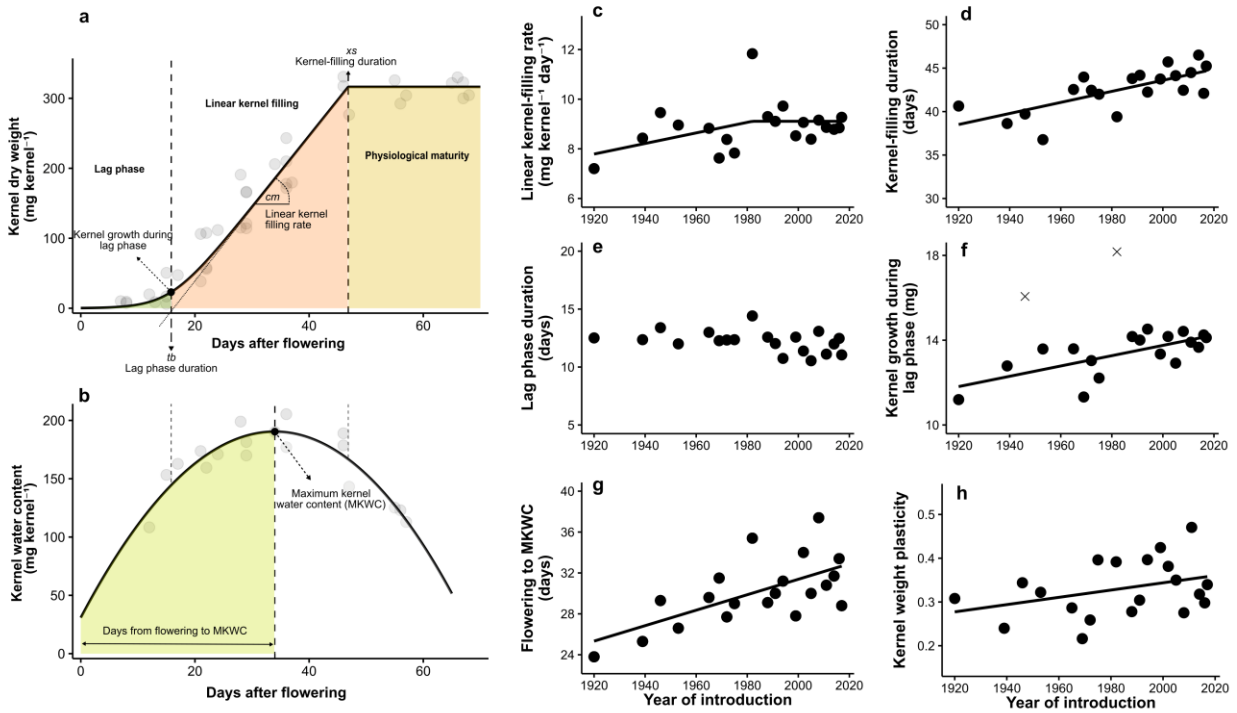


Figure 5.4. Description of analyses on kernel-filling parameters of USA – Pioneer ERA hybrids in multiple case studies from 2017 to 2020 growing seasons. Schematic diagrams of kernel-filling traits of interest and non-linear models used for (A) kernel dry matter, and (B) kernel water content dynamics. Relationships between years of hybrid introduction and (C) linear kernel-filling rate, (D) kernel-filling duration, (E) lag phase duration, (F) kernel growth during lag phase, (G) days from flowering to MKWC, and (H) kernel weight plasticity calculated as: $[(\text{Max.KW at high source-sink ratio} - \text{Min.KW at low source-sink ratio}) / (\text{Max.KW at high source-sink ratio})]$ (Valladares et al., 2006). Circles represent BLUES of hybrids, and crosses identify outliers based on studentized residuals (values > 3).

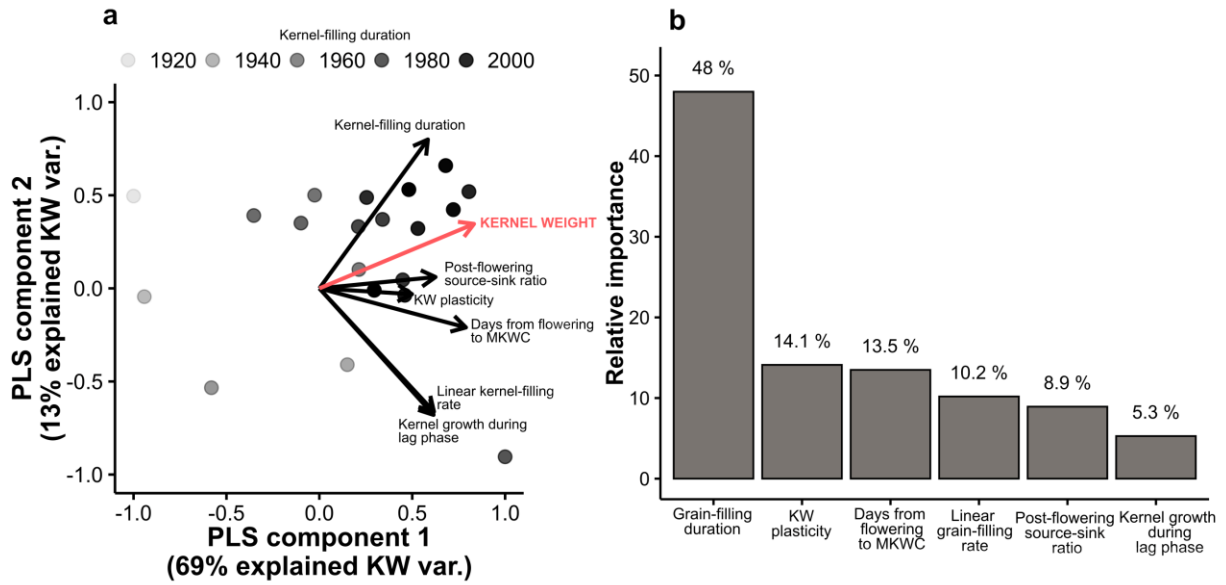


Figure 5.5. Importance of variables describing kernel weight genetic progress of USA – Pioneer ERA hybrids in multiple case studies from 2017 to 2020 growing seasons. (A) Partial least squares (PLS) regression biplot presented with two main components explaining kernel weight variance (y) based on six kernel-filling parameters as predictors (x). Arrows represent correlation loading among variables. (B) Variable importance scores for predictor variables of the PLS model.

Table 5.1. Subgroup meta-regression for the effect of crop growth conditions on the rate of genetic gain in grain yield, kernel number, and kernel weight of maize hybrids from USA – Pioneer ERA and other global breeding programs.

Condition	Range YOR	Grain yield (% year ⁻¹)				Kernel number (% year ⁻¹)				Kernel weight (% year ⁻¹)				
		df	Slope (95% CI)	EI	I ²	df	Slope (95% CI)	EI	I ²	df	Slope (95% CI)	EI	I ²	
<i>Water condition</i>														
USA – Pioneer ERA	Rainfed	1920 - 2017	10	0.7 (0.65-0.76)	8.49	98 **	10	0.42 (0.36-0.49)	2859	93 **	11	0.32 (0.28-0.36)	248	61 **
	Partially irrigated	-	-	-	-	-	-	-	-	-	-	-	-	-
	Full irrigated	1920 - 2017	12	0.59 (0.45-0.72)	9.84	63 **	12	0.62 (0.48-0.75)	3450	0	13	0.28 (0.17-0.36)	274	33
Other studies/regions	Rainfed	1930 - 2016	25	0.84 (0.73-0.94)	8.92	77 **	28	0.39 (0.27-0.5)	3036	93 **	32	0.43 (0.37-0.51)	257	96 **
	Partially irrigated	1980 - 2004	3	0.8 (0.59-1)	10.47	0	3	0.65 (0.31-1.01)	3357	0	3	0.15 (-0.08-0.35)	262	93 **
	Full irrigated	1955 - 2012	60	1.12 (0.87-1.36)	9.42	93 **	60	0.37 (0.14-0.6)	3196	77 **	64	0.69 (0.52-0.85)	258	97 **
<i>Nitrogen</i>														
USA – Pioneer ERA	Low N	1934 - 2014	5	0.72 (0.64-0.81)	5.62	98 **	5	0.53 (0.42-0.63)	2260	69 **	5	0.22 (0.18-0.27)	211	0
	High N	1920 - 2017	11	0.67 (0.6-0.74)	9.93	94 **	11	0.42 (0.34-0.5)	3261	90 **	11	0.37 (0.33-0.41)	272	92 **
	High + late N	1991 - 2014	5	0.45 (0.21-0.65)	13.29	0	5	0.76 (0.39-1.13)	3755	0	5	0.11 (-0.32-0.57)	274	0
Other studies/regions	Low N	1965 - 2012	8	0.84 (0.59-1.07)	6.45	77 **	9	0.52 (0.25-0.76)	2413	78 **	10	0.39 (0.22-0.57)	251	78 **
	High N	1930 - 2016	74	1.12 (0.96-1.29)	9.27	94 **	76	0.39 (0.26-0.53)	3117	96 **	83	0.55 (0.43-0.64)	261	88 **
	High + late N	1984 - 2000	6	1.37 (0.96-1.79)	10.79	84 **	6	1.25 (0.9-1.58)	3435	52	6	0.13 (-0.1-0.34)	271	0
<i>Planting density</i>														
USA – Pioneer ERA	< 5 pl. m ⁻²	1934 - 2013	2	0.52 (0.47-0.57)	8.27	93 **	2	0.22 (0.13-0.3)	2812	69 *	2	0.31 (0.26-0.36)	245	61
	5 – 7.5 pl. m ⁻²	1920 - 2017	5	0.43 (0.27-0.56)	9.07	88 **	5	0.28 (0.14-0.4)	3006	93 **	5	0.32 (0.23-0.39)	269	0
	7.6 – 8.9 pl. m ⁻²	1934 - 2015	12	0.92 (0.85-0.96)	8.82	96 **	12	0.62 (0.51-0.71)	2890	0	14	0.31 (0.25-0.37)	252	19
	> 9 pl. m ⁻²	1920 - 2017	3	0.66 (0.52-0.79)	9.36	94 **	3	0.66 (0.52-0.8)	3515	63 *	3	0.33 (0.23-0.43)	263	85 **
Other studies/regions	< 5 pl. m ⁻²	1955 - 2012	9	1.3 (1.05-1.53)	6.3	100 **	10	0.48 (0.26-0.72)	1932	100 **	11	0.57 (0.43-0.71)	299	100 **
	5 – 7.5 pl. m ⁻²	1930 - 2011	48	1.14 (0.87-1.4)	9.02	100 **	50	0.46 (0.29-0.6)	3097	100 **	51	0.46 (0.35-0.57)	255	99 **
	7.6 – 8.9 pl. m ⁻²	1965 - 2012	9	0.99 (0.73-1.13)	11.04	75 **	9	0.8 (0.56-0.97)	3887	83 **	10	0.16 (0.03-0.3)	242	84 **
	> 9 pl. m ⁻²	1965 - 2005	16	1.47 (1.11-1.81)	10.4	6	16	0.75 (-0.37-1.51)	3809	0	20	0.13 (-0.14-0.5)	260	0
<i>Source:sink ratio</i>														
USA – Pioneer ERA	Control	1920 - 2017	14	0.72 (0.67-0.78)	8.97	98 **	14	0.44 (0.37-0.51)	3029	88 **	16	0.32 (0.28-0.35)	252	84 **
	Low ratio	1920 - 2017	4	0.48 (0.3-0.66)	8.44	79 **	4	0.45 (0.28-0.61)	3250	77 **	4	0.25 (0.13-0.38)	213	20
	High ratio	1920 - 2017	4	0.56 (0.38-0.72)	8.29	100 **	4	0.44 (0.26-0.62)	2582	54	4	0.35 (0.22-0.47)	319	100**
Other studies/regions	Control	1930 - 2016	90	1.06 (0.91-1.2)	9.06	98 **	93	0.39 (0.27-0.5)	3057	99 **	101	0.54 (0.44-0.62)	261	100**
	Low ratio	1965 - 1993	1	0.76 (0.29-1.2)	9.2	0	1	1.91 (0.48-3.25)	4257	96 **	1	-1.21 (-2.02--0.52)	190	0
	High ratio	1965 - 1993	1	2.15 (1.06-3.09)	14.28	0	1	2.08 (0.62-3.48)	4430	0	1	0.08 (-0.7-0.71)	275	0

YOR, year of hybrid release; EI, environmental index; df, degrees of freedom; CI, confidence interval; I², heterogeneity coefficient;

* Significant at P ≤ 0.05; ** significant at P ≤ 0.01.

Chapter 6 - Final remarks

Fertilizer nitrogen (N) management is a key agronomic and environmental issue surrounding maize production, and this research has important implications for future genetic and agronomic improvements in N use. Throughout the second chapter, this dissertation suggests the existence of environmental \times management conditions where using late-N fertilization may increase grain yield. We proposed that the percentage of N uptake taking place after flowering might be used as an indicator for the type of responses in the field. This knowledge can be incorporated in remote sensing techniques that can assess crop N status in a practical and non-destructive method. From there, a remaining challenge is to certainly forecast the post-flowering N uptake in a crop earlier in the season combining crop modeling and improving weather forecasts. This approach will assist farmers in the identification of productive opportunities (and environments) for this practice.

From an environmental perspective, this research also advances in the ultimate goal of achieving tangible and sustainable improvements in food production. We have determined that fertilizer recovery efficiency was enhanced by the utilization of late N fertilization when properly adopted. This implies potentially fewer N losses into the environment from agricultural fertilizers. It is known that improving N fertilizer use efficiency can lower the carbon (C) footprints of agriculture, and therefore, this information is critical to enhancing the decision support of fertilizer recommendations to maize farmers. Investigations such as this study are required to address innovative alternatives to explore research priorities under uncertain future climate conditions.

Furthermore, this dissertation contributes significantly to our understanding of how long-term genetic improvement has modified N dynamics and their complex interaction with

management practices. The framework introduced in Chapter 3 proposes to analyze yield changes in two genotypes integrating N and C dynamics. This is a significant research contribution that helps point the way forward to future studies considering a holistic approach for the relationship between plant C and N utilization. We concluded that greater use of stem N to increase leaf area duration represents a strategy to enhance N utilization efficiency in modern hybrids. Moreover, the grain N concentration was also identified as an important trait determining N utilization in past decades. These findings provide insights into the contribution of grain and stem composition on N changes over time in maize and are of particular interest to breeders aiming to develop N-efficient hybrids.

Modern hybrids have been associated with increased post-flowering N absorption, but the physiological determinants of these increments in terms of internal N allocation and translocation have not been inspected yet. Chapter 4 of this dissertation aims to fill this gap and concludes that direct selection for yield has indirectly favored N allocation to leaves in modern maize genotypes resulting in an improved post-flowering C accumulation. This research raises further questions on the metabolic efficiencies of the photosynthetic and the respiratory systems as involved in plant growth. From a molecular physiology perspective, there is still much research needed to decode the mechanisms and functioning of N transport (and their regulatory genes) within the plant. These processes directly affect the amount and efficiency of nutrient uptake and mobilization in plants. The isotopic ^{15}N labeling method and statistical framework developed here can directly contribute in two significant aspects for future investigations:

- In crop modeling, to develop meaningful mechanistic modules characterizing the internal allocation and recycling of N in field-grown crops. This may bring an opportunity for simulation models that can account for internal N processes in field crops.

- In plant breeding, as the mapping of genes responsible for NUE requires precise and practical quantification methods that measure internal N processes. The method developed here may be applied across natural variations of maize genotypes growing in field conditions.

Finally, previous studies have predominantly focused on analyzing trends of yield increases in maize, but the main significance of the research introduced in Chapter 5 is its focus on evaluating the contribution of grain weight and its physiological characteristics. Previous studies evaluating these traits in historical maize genotypes are dated back to the 1980-decade. Therefore, these results acquire significant importance providing they include keystone phases in germplasm development in maize, defined by the increasing assistance of molecular technology in genetic selection since the 1990s. The analysis of historical trends in grain weight in Chapter 5 further describes the $G \times M$ interaction as a critical element in the breeding improvement of grain weight and offers foundational knowledge to propose candidate targets for future selection gains in maize. Finally, the reports of phenotypic plasticity linked to greater productivity of grain weight traits provide a potential avenue for yield improvement across different environments. The genetic basis of grain weight and its plasticity deserves further investigation as an opportunity to overcome the bottleneck of the trade-off between grain number and grain size in maize.

References

- Adams, D. C., Gurevitch, J., & Rosenberg, M. S. (1997). Resampling tests for meta-analysis of ecological data. *Ecology*, 78(4), 1277–1283.
- Adriaanse, F. G., & Human, J. J. (1993). Effect of time of application and nitrate: ammonium ratio on maize grain yield, grain N concentration and soil mineral N concentration in a semi-arid region. *Field Crops Research*, 34(1), 57–70. [https://doi.org/10.1016/0378-4290\(93\)90111-Y](https://doi.org/10.1016/0378-4290(93)90111-Y)
- Alvarez Prado, S., López, C. G., Senior, M. L., & Borrás, L. (2014a). The genetic architecture of maize (*Zea mays* L.) kernel weight determination. *G3 Genes|Genomes|Genetics*, 4(9), 1611–1621. <https://doi.org/10.1534/g3.114.013243>
- Alvarez Prado, S., Sadras, V. O., & Borrás, L. (2014b). Independent genetic control of maize (*Zea mays* L.) kernel weight determination and its phenotypic plasticity. *Journal of Experimental Botany*, 65(15), 4479–4487. <https://doi.org/10.1093/jxb/eru215>
- Amthor, J. (2000). The McCree–de Wit–Penning de Vries–Thornley respiration paradigms: 30 years later. *Annals of Botany*, 86(1), 1–20. <https://doi.org/10.1006/anbo.2000.1175>
- Andrade, F. H., Sadras, V. O., Vega, C. R. C., & Echarte, L. (2005). Physiological determinants of crop growth and yield in maize, sunflower and soybean. *Journal of Crop Improvement*, 14(1–2), 51–101. https://doi.org/10.1300/j411v14n01_05
- Arkoun, M., Sarda, X., Jannin, L., Laine, P., Etienne, P., Garcia-Mina, J.-M., Yvin, J.-C., & Ourry, A. (2012). Hydroponics versus field lysimeter studies of urea, ammonium and nitrate uptake by oilseed rape (*Brassica napus* L.). *Journal of Experimental Botany*, 63(14), 5245–5258. <https://doi.org/10.1093/jxb/ers183>
- Atkin, O. K., Bloomfield, K. J., Reich, P. B., Tjoelker, M. G., Asner, G. P., Bonal, D., Bönisch, G., Bradford, M. G., Cernusak, L. A., Cosio, E. G., Creek, D., Crous, K. Y., Domingues, T. F., Dukes, J. S., Egerton, J. J. G., Evans, J. R., Farquhar, G. D., Fyllas, N. M., Gauthier, P. P. G., ... Zaragoza-Castells, J. (2015). Global variability in leaf respiration in relation to climate, plant functional types and leaf traits. *New Phytologist*, 206(2), 614–636. <https://doi.org/10.1111/nph.13253>
- Avice, J. C., Ourry, A., Lemaire, G., & Boucaud, J. (1996). Nitrogen and carbon flows estimated by ¹⁵N and ¹³C pulse-chase labeling during regrowth of alfalfa. *Plant Physiology*, 112(1), 281–290. <https://doi.org/10.1104/pp.112.1.281>
- Azcón-Bieto, J., Lambers, H., & Day, D. A. (1983). Effect of photosynthesis and carbohydrate status on respiratory rates and the involvement of the alternative pathway in leaf respiration. *Plant Physiology*, 72(3), 598–603. <https://doi.org/10.1104/pp.72.3.598>

- Bänziger, M., Betrán, F. J., & Lafitte, H. R. (1997). Efficiency of high-nitrogen selection environments for improving maize for low-nitrogen target environments. *Crop Science*, 37(4), 1103–1109. <https://doi.org/10.2135/cropsci1997.0011183X003700040012x>
- Banziger, M., Feil, B., & Stamp, P. (1994). Competition between nitrogen accumulation and grain growth for carbohydrates during grain filling of wheat. *Crop Science*, 34(2), 440–446. <https://doi.org/10.2135/cropsci1994.0011183X003400020025x>
- Barker, T., Campos, H., Cooper, M., Dolan, D., Edmeades, G., Habben, J., Schussler, J., Wright, D., & Zinselmeier, C. (2005). Improving drought tolerance in maize. In *Plant Breeding Reviews* (Vol. 25, pp. 173–253).
- Bates, D., Mächler, M., Bolker, B., & Walker, S. (2015). Fitting linear mixed-effects models using lme4. *Journal of Statistical Software*, 67(1), 1–48. <https://doi.org/10.18637/jss.v067.i01>
- Below, F. E., Christensen, L. E., Reed, A. J., & Hageman, R. H. (1981). Availability of reduced N and carbohydrates for ear development of maize. *Plant Physiology*, 68(5), 1186–1190. <https://doi.org/10.1104/pp.68.5.1186>
- Bigeriego, M., Hauck, R. D., & Olson, R. A. (1979). Uptake, translocation and utilization of ¹⁵N-depleted fertilizer in irrigated corn. *Soil Science Society of America Journal*, 43(3), 528–533.
- Bihmidine, S., Hunter, C. T., Johns, C. E., Koch, K. E., & Braun, D. M. (2013). Regulation of assimilate import into sink organs: update on molecular drivers of sink strength. *Frontiers in Plant Science*, 4(June), 1–15. <https://doi.org/10.3389/fpls.2013.00177>
- Binder, D. L., Sander, D. H., & Walters, D. T. (2000). Maize response to time of nitrogen application as affected by level of nitrogen deficiency. *Agronomy Journal*, 92(6), 1228–1236. <https://doi.org/10.2134/agronj2000.9261228x>
- Boomsma, C. R., Santini, J. B., Tollenaar, M., & Vyn, T. J. (2009). Maize morphophysiological responses to intense crowding and low nitrogen availability: An analysis and review. *Agronomy Journal*, 101(6), 1426–1452. <https://doi.org/10.2134/agronj2009.0082>
- Borrás, L., Westgate, M. E., & Otegui, M. E. (2003). Control of kernel weight and kernel water relations by post-flowering source-sink ratio in maize. *Annals of Botany*, 91(7), 857–867. <https://doi.org/10.1093/aob/mcg090>
- Borrás, Lucas, Slafer, G. A., & Otegui, M. E. (2004). Seed dry weight response to source-sink manipulations in wheat, maize and soybean: A quantitative reappraisal. *Field Crops Research*, 86(2–3), 131–146. <https://doi.org/10.1016/j.fcr.2003.08.002>
- Borrell, A. K., & Hammer, G. L. (2000). Nitrogen dynamics and the physiological basis of stay-green in Sorghum. *Crop Science*, 40(5), 1295–1307. <https://doi.org/10.2135/cropsci2000.4051295x>

- Borrell, A., Hammer, G., & Van Oosterom, E. (2001). Stay-green: A consequence of the balance between supply and demand for nitrogen during grain filling? *Annals of Applied Biology*, 138(1), 91–95. <https://doi.org/10.1111/j.1744-7348.2001.tb00088.x>
- Bradshaw, A. D. (1965). Evolutionary significance of phenotypic plasticity in plants. In *Advances in Genetics* (Vol. 13, Issue C, pp. 115–155). [https://doi.org/10.1016/S0065-2660\(08\)60048-6](https://doi.org/10.1016/S0065-2660(08)60048-6)
- Bürkner, P. C. (2017). brms: An R package for Bayesian multilevel models using Stan. *Journal of Statistical Software*. <https://doi.org/10.18637/jss.v080.i01>
- Bürkner, P. C. (2018). Advanced Bayesian multilevel modeling with the R package brms. *R Journal*. <https://doi.org/10.32614/rj-2018-017>
- Cabrera, M. L., & Kissel, D. E. (1989). Review and simplification of calculations in ¹⁵N tracer studies. *Fertilizer Research*, 20(1), 11–15.
- Calderini, D. F., Savin, R., Abeledo, L. G., Reynolds, M. P., & Slafer, G. A. (2001). The importance of the period immediately preceding anthesis for grain weight determination in wheat. *Euphytica*, 119(1–2), 199–204. <https://doi.org/10.1023/A:1017597923568>
- Calderini, Daniel F., & Slafer, G. A. (1999). Has yield stability changed with genetic improvement of wheat yield? *Euphytica*, 107(1), 51–59. <https://doi.org/10.1023/A:1003579715714>
- Calderini, Daniel F., Castillo, F. M., Arenas-M, A., Molero, G., Reynolds, M. P., Craze, M., Bowden, S., Milner, M. J., Wallington, E. J., Dowle, A., Gomez, L. D., & McQueen-Mason, S. J. (2021). Overcoming the trade-off between grain weight and number in wheat by the ectopic expression of expansin in developing seeds leads to increased yield potential. *New Phytologist*, 230(2), 629–640. <https://doi.org/10.1111/nph.17048>
- Campos, H., Cooper, M., Edmeades, G. O., Löffler, C., Schussler, J. R., & Ibañez, M. (2006). Changes in drought tolerance in maize associated with fifty years of breeding for yield in the U.S. corn belt. *Maydica*, 51(2), 369–381.
- Canty, A., & Ripley, B. (2021). boot: Bootstrap R (S-Plus) functions. R package version 1.3-28.
- Cao, P., Lu, C., & Yu, Z. (2018). Historical nitrogen fertilizer use in agricultural ecosystems of the contiguous United States during 1850–2015: application rate, timing, and fertilizer types. *Earth System Science Data*, 10(2), 969–984. <https://doi.org/10.5194/essd-10-969-2018>
- Cassman, K. G., Dobermann, A., & Walters, D. T. (2002). Agroecosystems, nitrogen-use efficiency, and nitrogen management. *AMBIO: A Journal of the Human Environment*, 31(2), 132–140. <https://doi.org/10.1579/0044-7447-31.2.132>

- Cavaliere, A. J., & Smith, O. S. (1985). Grain filling and field drying of a set of maize hybrids released from 1930 to 1982. *Crop Science*, 25(5), 856–860. <https://doi.org/10.2135/cropsci1985.0011183x002500050031x>
- Chen, J., Zhang, L., Liu, S., Li, Z., Huang, R., Li, Y., Cheng, H., Li, X., Zhou, B., Wu, S., Chen, W., Wu, J., & Ding, J. (2016). The genetic basis of natural variation in kernel size and related traits using a four-way cross population in maize. *PLoS ONE*, 11(4), 1–12. <https://doi.org/10.1371/journal.pone.0153428>
- Chen, K., Camberato, J. J., Tuinstra, M. R., Kumudini, S. V., Tollenaar, M., & Vyn, T. J. (2016). Genetic improvement in density and nitrogen stress tolerance traits over 38 years of commercial maize hybrid release. *Field Crops Research*, 196, 438–451. <https://doi.org/10.1016/j.fcr.2016.07.025>
- Chen, K., Kumudini, S. V., Tollenaar, M., & Vyn, T. J. (2015). Plant biomass and nitrogen partitioning changes between silking and maturity in newer versus older maize hybrids. *Field Crops Research*, 183, 315–328. <https://doi.org/10.1016/j.fcr.2015.08.013>
- Chen, X., Zhang, F., Römheld, V., Horlacher, D., Schulz, R., Böning-Zilkens, M., Wang, P., & Claupein, W. (2006). Synchronizing N supply from soil and fertilizer and N demand of winter wheat by an improved N_{min} method. *Nutrient Cycling in Agroecosystems*, 74(2), 91–98. <https://doi.org/10.1007/s10705-005-1701-9>
- Chen, Y., & Mi, G. (2018). Physiological mechanisms underlying post-silking nitrogen use efficiency of high-yielding maize hybrids differing in nitrogen remobilization efficiency. *Journal of Plant Nutrition and Soil Science*, 181(6), 923–931. <https://doi.org/10.1002/jpln.201800161>
- Chen, Y., Zhang, J., Li, Q., He, X., Su, X., Chen, F., Yuan, L., & Mi, G. (2015). Effects of nitrogen application on post-silking root senescence and yield of maize. *Agronomy Journal*, 107(3), 835–842. <https://doi.org/10.2134/agronj14.0509>
- Chun, L., Chen, F., Zhang, F., & Mi, G. (2005). Root growth, nitrogen uptake and yield formation of hybrid maize with different N efficiency. *Plant Nutrition and Fertilizer Science*, 11(5), 615–619.
- Ciampitti, I. A., & Vyn, T. J. (2011). A comprehensive study of plant density consequences on nitrogen uptake dynamics of maize plants from vegetative to reproductive stages. *Field Crops Research*, 121(1), 2–18. <https://doi.org/10.1016/j.fcr.2010.10.009>
- Ciampitti, I. A., & Vyn, T. J. (2012). Physiological perspectives of changes over time in maize yield dependency on nitrogen uptake and associated nitrogen efficiencies: A review. *Field Crops Research*, 133, 48–67. <https://doi.org/10.1016/j.fcr.2012.03.008>
- Ciampitti, I. A., & Vyn, T. J. (2013). Grain nitrogen source changes over time in maize: A review. *Crop Science*, 53(2), 366–377. <https://doi.org/10.2135/cropsci2012.07.0439>

- Ciampitti, I. A., Zhang, H., Friedemann, P., & Vyn, T. J. (2012). Potential physiological frameworks for mid-season field phenotyping of final plant nitrogen uptake, nitrogen use efficiency, and grain yield in maize. *Crop Science*, 52(6), 2728–2742. <https://doi.org/10.2135/cropsci2012.05.0305>
- Cleveland, W. S., Grosse, E., & Shyu, W. M. (1992). Local regression models. In J. M. Chambers & T. J. Hastie (Eds.), *Statistical Models in S*. Wadsworth & Brooks/Cole. <https://doi.org/10.1201/9780203738535>
- Cliquet, J.-B., Deleens, E., & Mariotti, A. (1990). C and N mobilization from stalk and leaves during kernel filling by ^{13}C and ^{15}N tracing in *Zea mays* L. *Plant Physiol*, 94, 1547–1553. <https://doi.org/10.1104/pp.94.4.1547>
- Cooper, H. D., & Clarkson, D. T. (1989). Cycling of amino-nitrogen and other nutrients between shoots and roots in cereals—A possible mechanism integrating shoot and root in the regulation of nutrient uptake. *Journal of Experimental Botany*, 40(7), 753–762. <https://doi.org/10.1093/jxb/40.7.753>
- Cooper, M., Gho, C., Leafgren, R., Tang, T., & Messina, C. (2014a). Breeding drought-tolerant maize hybrids for the US corn-belt: Discovery to product. *Journal of Experimental Botany*, 65(21), 6191–6194. <https://doi.org/10.1093/jxb/eru064>
- Cooper, M., Messina, C. D., Podlich, D., Totir, L. R., Baumgarten, A., Hausmann, N. J., Wright, D., & Graham, G. (2014b). Predicting the future of plant breeding: complementing empirical evaluation with genetic prediction. *Crop and Pasture Science*, 65(4), 311–336. <https://doi.org/10.1071/cp14007>
- Cooper, M., Tang, T., Gho, C., Hart, T., Hammer, G., & Messina, C. (2020). Integrating genetic gain and gap analysis to predict improvements in crop productivity. *Crop Science*, January, 1–23. <https://doi.org/10.1002/csc2.20109>
- Coque, M., & Gallais, A. (2007). Genetic variation for nitrogen remobilization and postsilking nitrogen uptake in maize recombinant inbred lines: heritabilities and correlations among traits. *Crop Science*, 47(5), 1787–1796.
- Coque, M., Martin, A., Veyrieras, J. B., Hirel, B., & Gallais, A. (2008). Genetic variation for N-remobilization and postsilking N-uptake in a set of maize recombinant inbred lines. 3. QTL detection and coincidences. *Theoretical and Applied Genetics*, 117(5), 729–747. <https://doi.org/10.1007/s00122-008-0815-2>
- Crawford, T. W., Rendig, V. V., & Broadbent, F. E. (1982). Sources, fluxes, and sinks of nitrogen during early reproductive growth of maize (*Zea mays* L.). *Plant Physiology*, 70(6), 1654–1660. <https://doi.org/10.1104/pp.70.6.1654>
- Crosbie, T. M., & Mock, J. J. (1981). Changes in physiological traits associated with grain yield improvement in three maize breeding programs. *Crop Science*, 21(2), 255–259. <https://doi.org/10.2135/cropsci1981.0011183X002100020013x>

- Crozier, C. R., Gehl, R. J., Hardy, D. H., & Heiniger, R. W. (2014). Nitrogen management for high population corn production in wide and narrow rows. *Agronomy Journal*, 106(1), 66–72. <https://doi.org/10.2134/agronj2013.0280>
- Curin, F., Severini, A. D., Gonzalez, F. G., & Otegui, M. E. (2020). Water and radiation use efficiencies in maize: breeding effects on single-cross Argentine hybrids released between 1980 and 2012. *Field Crops Research*, 246, 107683.
- Davison, A. C., & Hinkley, D. V. (1997). *Bootstrap methods and their applications*. Cambridge University Press, Cambridge. ISBN 0-521-57391-2.
- Daynard, T. B., Tanner, J. W., & Hume, D. J. (1969). Contribution of stalk soluble carbohydrates to grain yield in corn (*Zea mays* L.)1. *Crop Science*, 9(1966), 831. <https://doi.org/10.2135/cropsci1969.0011183X000900060050x>
- de Felipe, M., & Alvarez Prado, S. (2021). Has yield plasticity already been exploited by soybean breeding programmes in Argentina? *Journal of Experimental Botany*. <https://doi.org/10.1093/jxb/erab347>
- de Oliveira Silva, A., Camberato, J. J., Coram, T., Filley, T., & Vyn, T. J. (2017). Applicability of a “multi-stage pulse labeling” ¹⁵N approach to phenotype N dynamics in maize plant components during the growing season. *Frontiers in Plant Science*, 8(August), 1–17. <https://doi.org/10.3389/fpls.2017.01360>
- DeBruin, J. L., Schussler, J. R., Mo, H., & Cooper, M. (2017). Grain yield and nitrogen accumulation in maize hybrids released during 1934 to 2013 in the US Midwest. *Crop Science*, 57(3), 1431–1446. <https://doi.org/10.2135/cropsci2016.08.0704>
- Demarco, P. A., Mayor, L., Tamagno, S., Fernandez, J., Vara, P. V., Prasad, J. L., ... & Ciampitti, I. A. (2020). Physiological changes across historical sorghum hybrids released during the last six decades. *Kansas Agricultural Experiment Station Research Reports*, 55.
- Donmez, E., Sears, R. G., Shroyer, J. P., & Paulsen, G. M. (2001). Genetic gain in yield attributes of winter wheat in the Great Plains. *Crop science*, 41(5), 1412-1419.
- Douma, J. C., & Weedon, J. T. (2019). Analysing continuous proportions in ecology and evolution: A practical introduction to beta and Dirichlet regression. *Methods in Ecology and Evolution*, 10(9), 1412–1430. <https://doi.org/10.1111/2041-210X.13234>
- Dreccer, M. F., Schapendonk, A. H. C. M., Slafer, G. A., & Rabbinge, R. (2000). Comparative response of wheat and oilseed rape to nitrogen supply: Absorption and utilisation efficiency of radiation and nitrogen during the reproductive stages determining yield. *Plant and Soil*, 220(1–2), 189–205. <https://doi.org/10.1023/a:1004757124939>
- Duvick, D. N. (2005a). Genetic progress in yield of United States maize (*Zea mays* L.). *Maydica*, 50, 193–202.

- Duvick, D. N. (2005b). The contribution of breeding to yield advances in maize (*Zea mays* L.). In *Advance in Agronomy* (Vol. 86, pp. 83–145). [https://doi.org/10.1016/S0065-2113\(05\)86002-X](https://doi.org/10.1016/S0065-2113(05)86002-X)
- Duvick, D. N., & Cassman, K. G. (1999). Post-green revolution trends in yield potential of temperate maize in the north-central United States. *Crop Science*, 39(6), 1622–1630. <https://doi.org/10.2135/cropsci1999.3961622x>
- Duvick, D., Smith, J., & Cooper, M. (2004). Long-term selection in a commercial hybrid maize breeding program. *Plant Breeding Reviews*, 24(2), 109–152.
- Dwyer, L. M., Anderson, A. M., Stewart, D. W., Ma, B. L., & Tollenaar, M. (1995). Changes in maize hybrid photosynthetic response to leaf nitrogen, from pre-anthesis to grain fill. *Agronomy Journal*, 87(6), 1221–1225. <https://doi.org/10.2134/agronj1995.00021962008700060031x>
- Earl, H. J., & Tollenaar, M. (1998). Differences among commercial maize (*Zea mays* L.) hybrids in respiration rates of mature leaves. *Field Crops Research*, 59(1), 9–19. [https://doi.org/10.1016/S0378-4290\(98\)00098-7](https://doi.org/10.1016/S0378-4290(98)00098-7)
- Eathington, S. R., Crosbie, T. M., Edwards, M. D., Reiter, R. S., & Bull, J. K. (2007). Molecular markers in a commercial breeding program. *Crop Science*, 47(SUPPL. DEC.), S-154-S-163. <https://doi.org/10.2135/cropsci2007.04.0015IPBS>
- Echarte, L., Andrade, F. H., Vega, C. R. C., & Tollenaar, M. (2004). Kernel number determination in argentinean maize hybrids released between 1965 and 1993. *Crop Science*, 44(5), 1654–1661. <https://doi.org/10.2135/cropsci2004.1654>
- Echarte, L., Rothstein, S., & Tollenaar, M. (2008). The response of leaf photosynthesis and dry matter accumulation to nitrogen supply in an older and a newer maize hybrid. *Crop Science*, 48(2), 656–665. <https://doi.org/10.2135/cropsci2007.06.0366>
- Efron, B., & Tibshirani, R. (1993). *An introduction to the bootstrap*. Chapman & Hall.
- Egli, D. B. (1990). Seed water relations and the regulation of the duration of seed growth in soybean. *Journal of Experimental Botany*, 41(2), 243–248. <https://doi.org/10.1093/jxb/41.2.243>
- Egli, D. B. (2015). Is there a role for sink size in understanding maize population–yield relationships? *Crop Science*, 55(6), 2453–2462. <https://doi.org/10.2135/cropsci2015.04.0227>
- Eichelmann, H., Talts, E., Oja, V., Padu, E., & Laisk, A. (2009). Rubisco *in planta* k_{cat} is regulated in balance with photosynthetic electron transport. *Journal of Experimental Botany*, 60(14), 4077–4088. <https://doi.org/10.1093/jxb/erp242>
- Ellison, A. M. (2004). Bayesian inference in ecology. *Ecology Letters*, 7(6), 509–520. <https://doi.org/10.1111/j.1461-0248.2004.00603.x>

- Evans, J. R. (1989). Photosynthesis and nitrogen relationships in leaves of C₃ plants. *Oecologia*, 78(1), 9–19.
- Fageria, N. K., & Baligar, V. C. (2005). Enhancing nitrogen use efficiency in crop plants. *Advances in Agronomy*, 88(05), 97–185. [https://doi.org/10.1016/S0065-2113\(05\)88004-6](https://doi.org/10.1016/S0065-2113(05)88004-6)
- Fairey, N. A., & Daynard, T. B. (1978). Assimilate distribution and utilization in maize. *Canadian Journal of Plant Science*, 58(3), 719–730.
- Feng, G., Zhang, Y., Chen, Y., Li, Q., Chen, F., Gao, Q., & Mi, G. (2016). Effects of nitrogen application on root length and grain yield of rain-fed maize under different soil types. *Agronomy Journal*, 108(4), 1656–1665. <https://doi.org/10.2134/agronj2015.0367>
- Fernandez, J. A., & Ciampitti, I. A. (2018). Effect of late nitrogen applications on grain filling in corn. *Kansas Agricultural Experiment Station Research Reports*, 4(7). <https://doi.org/10.4148/2378-5977.7603>
- Fernandez, J. A., & Ciampitti, I. A. (2019). Effect of late nitrogen fertilization on grain yield and grain filling in corn. *Kansas Agricultural Experiment Station Research Reports*, 5(6). <https://doi.org/10.4148/2378-5977.7776>
- Fernandez, J. A., & Ciampitti, I. A. (2021). Corn grain weight: dependence upon nitrogen supply and source-sink relations. *Kansas Agricultural Experiment Station Research Reports*, 7(5). <https://doi.org/10.4148/2378-5977.8073>
- Fernandez, J. A., DeBruin, J., Messina, C. D., & Ciampitti, I. A. (2020a). Late-season nitrogen fertilization on maize yield: A meta-analysis. *Field Crops Research*, 247, 107586. <https://doi.org/10.1016/j.fcr.2019.107586>
- Fernandez, J. A., Nippert, J. B., & Ciampitti, I. A. (2020b). Dynamics of post-flowering nitrogen uptake and nitrogen recovery efficiency using ¹⁵N isotope labeling in corn. *Kansas Agricultural Experiment Station Research Reports*, 28.
- Fernandez, J. A., Messina, C. D., Rotundo, J. L., & Ciampitti, I. A. (2021). Integrating nitrogen and water-soluble carbohydrates dynamics in maize: a comparison of hybrids from different decades. *Crop Science*, 61(2), 1360–1373. <https://doi.org/10.1002/csc2.20338>
- Fernandez, J. A., Nippert, J. B., Prasad, P. V. V., Messina, C. D., & Ciampitti, I. A. Post-silking ¹⁵N labelling reveals an enhanced nitrogen allocation to leaves in modern maize (*Zea mays*) genotypes. –Under review.
- Fischer, R. A., & HilleRisLambers, D. (1978). Effect of environment and cultivar on source limitation to grain weight in wheat. *Australian Journal of Agricultural Research*, 29(3), 443–458. <https://doi.org/10.1071/AR9780443>
- Foulkes, M. J., Hawkesford, M. J., Barraclough, P. B., Holdsworth, M. J., Kerr, S., Kightley, S., & Shewry, P. R. (2009). Identifying traits to improve the nitrogen economy of wheat:

- Recent advances and future prospects. *Field Crops Research*, 114(3), 329–342.
<https://doi.org/10.1016/j.fcr.2009.09.005>
- Foyer, C. H., Valadier, M.-H., Migge, A., & Becker, T. W. (1998). Drought-induced effects on nitrate reductase activity and mRNA and on the coordination of nitrogen and carbon metabolism in maize leaves. *Plant Physiology*, 117(1), 283–292.
<https://doi.org/10.1104/pp.117.1.283>
- Friedrich, J. W., & Schrader, L. E. (1979). N deprivation in maize during grain-filling. II. Remobilization of ¹⁵N and ³⁵S and the relationship between N and S accumulation. *Agronomy Journal*, 71(3), 466–472.
<https://doi.org/10.2134/agronj1979.00021962007100030021x>
- Galicia, L., Nurit, E., Rosales, A., & Palacios-Rojas, N. (2009). Laboratory protocols 2008: Maize nutrition quality and plant tissue analysis laboratory. CIMMYT.
- Gallais, A., & Coque, M. (2005). Genetic variation and selection for nitrogen use efficiency in maize: a synthesis. *Maydica*, 50(3/4), 531–547.
- Gallais, A., Coque, M., Quillére, I., Prioul, J. L., & Hirel, B. (2006). Modelling postsilking nitrogen fluxes in maize (*Zea mays*) using ¹⁵N-labelling field experiments. *New Phytologist*, 172(4), 696–707. <https://doi.org/10.1111/j.1469-8137.2006.01890.x>
- Gambín, B. L., & Borrás, L. (2010). Resource distribution and the trade-off between seed number and seed weight: A comparison across crop species. *Annals of Applied Biology*, 156(1), 91–102. <https://doi.org/10.1111/j.1744-7348.2009.00367.x>
- Gambín, Brenda L., Borrás, L., & Otegui, M. E. (2007). Kernel water relations and duration of grain filling in maize temperate hybrids. *Field Crops Research*, 101(1), 1–9.
<https://doi.org/10.1016/j.fcr.2006.09.001>
- Gao, J., Shi, J., Dong, S., Liu, P., Zhao, B., & Zhang, J. (2017). Grain yield and root characteristics of summer maize (*Zea mays* L.) under shade stress conditions. *Journal of Agronomy and Crop Science*, 203(6), 562–573. <https://doi.org/10.1111/jac.12210>
- Gastal, F., Lemaire, G., Durand, J. L., & Louarn, G. (2014). Quantifying crop responses to nitrogen and avenues to improve nitrogen-use efficiency. In *Crop Physiology: Applications for Genetic Improvement and Agronomy: Second Edition* (Second Edition, Issue December, pp. 161–206). Elsevier. <https://doi.org/10.1016/B978-0-12-417104-6.00008-X>
- Gelman, A., & Rubin, D. B. (1992). Inference from iterative simulation using multiple sequences. *Statistical Science*, 7(4), 457–472. <https://doi.org/10.1214/ss/1177011136>
- Goudriaan, J., & Monteith, J. L. (1990). A mathematical function for crop growth based on light interception and leaf area expansion. *Annals of Botany*, 66(6), 695–701.
<https://doi.org/10.1093/oxfordjournals.aob.a088084>

- Greenwood, D. J., Lemaire, G., Gosse, G., Cruz, P., Draycott, A., & Neeteson, J. J. (1990). Decline in percentage N of C3 and C4 crops with increasing plant mass. *Annals of Botany*, 66(4), 425–436. <https://doi.org/10.1093/oxfordjournals.aob.a088044>
- Haegerle, J. W., Cook, K. A., Nichols, D. M., & Below, F. E. (2013). Changes in nitrogen use traits associated with genetic improvement for grain yield of maize hybrids released in different decades. *Crop Science*, 53(4), 1256–1268. <https://doi.org/10.2135/cropsci2012.07.0429>
- Hammer, G. L., Dong, Z., McLean, G., Doherty, A., Messina, C., Schussler, J., Zinselmeier, C., Paszkiewicz, S., & Cooper, M. (2009). Can changes in canopy and/or root system architecture explain historical maize yield trends in the U.S. corn belt? *Crop Science*, 49(1), 299–312. <https://doi.org/10.2135/cropsci2008.03.0152>
- Hausmann, J. N., Abadie, T. E., Cooper, M., Lafitte, H. R., & Schussler, J. R. (2011). Method and system for digital image analysis of ear traits.
- Hedges, L. V., Gurevitch, J., & Curtis, P. S. (1999). The meta-analysis of response ratios in ecology. *Ecology*, 80(4), 1150–1156.
- Hirel, B., Le Gouis, J., Ney, B., & Gallais, A. (2007). The challenge of improving nitrogen use efficiency in crop plants: towards a more central role for genetic variability and quantitative genetics within integrated approaches. *Journal of Experimental Botany*, 58(9), 2369–2387. <https://doi.org/10.1093/jxb/erm097>
- Hirose, T., & Werger, M. J. A. (1987). Maximizing daily canopy photosynthesis with respect to the leaf nitrogen allocation pattern in the canopy. *Oecologia*, 72(4), 520–526. <https://doi.org/10.1007/BF00378977>
- Högberg, P. (1997). Tansley Review No. 95 ¹⁵N natural abundance in soil–plant systems. *The New Phytologist*, 137(2), 179–203.
- Hollinger, D. Y. (1996). Optimality and nitrogen allocation in a tree canopy. *Tree Physiology*, 16(7), 627–634. <https://doi.org/10.1093/treephys/16.7.627>
- Hoogmoed, M., Neuhaus, A., Noack, S., & Sadras, V. O. (2018). Benchmarking wheat yield against crop nitrogen status. *Field Crops Research*, 222(April), 153–163. <https://doi.org/10.1016/j.fcr.2018.03.013>
- Irving, L. J., Suzuki, Y., Ishida, H., & Makino, A. (2010). Protein turnover in grass leaves. In *Advances in Botanical Research* (Vol. 54, Issue C, pp. 139–182). [https://doi.org/10.1016/S0065-2296\(10\)54004-7](https://doi.org/10.1016/S0065-2296(10)54004-7)
- Jägermeyr, J., Müller, C., Ruane, A. C., Elliott, J., Balkovic, J., Castillo, O., ... & Rosenzweig, C. (2021). Climate impacts on global agriculture emerge earlier in new generation of climate and crop models. *Nature Food*, 1-13.

- Jamieson, P. D., Zyskowski, R. F., Li, F. Y., & Semenov, M. A. (2008). Water and nitrogen uptake and responses in models of wheat, potatoes, and maize. In Quantifying and understanding plant nitrogen uptake for systems modeling (pp. 127–145). <https://doi.org/10.1201/9781420052978-6>
- Jaynes, D. B., & Colvin, T. S. (2006). Corn yield and nitrate loss in subsurface drainage from midseason nitrogen fertilizer application. *Agronomy Journal*, 98(6), 1479–1487. <https://doi.org/10.2134/agronj2006.0046>
- Jiang, G. L. (2013). Molecular markers and marker-assisted breeding in plants. In S.B. Anderson (Ed.), *Plant Breeding from Laboratories to Fields* (Vol. 3, pp. 45–83). InTech. <https://doi.org/10.5772/52583>
- Johnson, D. R., & Tanner, J. W. (1972). Calculation of the rate and duration of grain filling in corn (*Zea mays* L.). *Crop Science*, 12(4), 485–486. <https://doi.org/10.2135/cropsci1972.0011183X001200040028x>
- Jones, J., Hoogenboom, G., Porter, C., Boote, K., Batchelor, W., Hunt, L., Wilkens, P., Singh, U., Gijsman, A., & Ritchie, J. (2003). The DSSAT cropping system model. *European Journal of Agronomy*, 18, 235–265. [https://doi.org/10.1016/S1161-0301\(02\)00107-7](https://doi.org/10.1016/S1161-0301(02)00107-7)
- Jones, R. J., & Simmons, S. R. (1983). Effect of altered source-sink ratio on growth of maize kernels. *Crop Science*, 23(1), 129–134. <https://doi.org/10.2135/cropsci1983.0011183X002300010038x>
- Jones, R. J., Roessler, J., & Ouattar, S. (1985). Thermal environment during endosperm cell division in maize: effects on number of endosperm cells and starch granules. *Crop Science*, 25(5), 830–834. <https://doi.org/10.2135/cropsci1985.0011183X002500050025x>
- Jones, R. J., Schreiber, B. M. N., & Roessler, J. A. (1996). Kernel sink capacity in maize: Genotypic and maternal regulation. *Crop Science*, 36(2), 301–306. <https://doi.org/10.2135/cropsci1996.0011183X003600020015x>
- Jung, P. E., Peterson, L. A., & Schrader, L. E. (1972). Response of irrigated corn to time, rate, and source of applied N on sandy soils. *Agronomy Journal*, 64(5), 668. <https://doi.org/10.2134/agronj1972.00021962006400050035x>
- Kansas Mesonet. (2019). Historical weather. Kansas State University. <http://mesonet.k-state.edu/weather/historical/>
- Keeney, D. R. (1982). Nitrogen management for maximum efficiency and minimum pollution. *Nitrogen in Agricultural Soils*, 605–649.
- Killorn, R., & Zourarakis, D. (1992). Nitrogen fertilizer management effects on corn grain yield and nitrogen uptake. *Journal of Production Agriculture*, 5(1), 142–148. <https://doi.org/10.2134/jpa1992.0142>

- Kiniry, J. R. (1988). Kernel weight increase in response to decreased kernel number in sorghum. *Agronomy Journal*, 80(2), 221–226. <https://doi.org/10.2134/agronj1988.00021962008000020016x>
- Kinugasa, T., Sato, T., Oikawa, S., & Hirose, T. (2012). Demand and supply of N in seed production of soybean (*Glycine max*) at different N fertilization levels after flowering. *Journal of Plant Research*, 125(2), 275–281. <https://doi.org/10.1007/s10265-011-0439-5>
- Kitonyo, O. M., Sadras, V. O., Zhou, Y., & Denton, M. D. (2018). Nitrogen fertilization modifies maize yield response to tillage and stubble in a sub-humid tropical environment. *Field Crops Research*, 223(March), 113–124. <https://doi.org/10.1016/j.fcr.2018.03.024>
- Knowles, R., & Blackburn, T. H. (Eds.). (1993). *Nitrogen isotope techniques*. Academic Press, Inc.
- Kosgey, J. R., Moot, D. J., Fletcher, A. L., & McKenzie, B. A. (2013). Dry matter accumulation and post-silking N economy of “stay-green” maize (*Zea mays* L.) hybrids. *European Journal of Agronomy*, 51, 43–52. <https://doi.org/10.1016/j.eja.2013.07.001>
- Kovács, P., Van Scoyoc, G. E., Doerge, T. A., Camberato, J. J., & Vyn, T. J. (2015). Anhydrous ammonia timing and rate effects on maize nitrogen use efficiencies. *Agronomy Journal*, 107, 1205–1214. <https://doi.org/10.2134/agronj14.0350>
- Kruk, B. C., Calderini, D. F., & Slafer, G. A. (1997). Grain weight in wheat cultivars released from 1920 to 1990 as affected by post-anthesis defoliation. *Journal of Agricultural Science*, 128(3), 273–281. <https://doi.org/10.1017/S0021859696004133>
- Kunrath, T. R., Lemaire, G., Sadras, V. O., & Gastal, F. (2018). Water use efficiency in perennial forage species: Interactions between nitrogen nutrition and water deficit. *Field Crops Research*, 222(March), 1–11. <https://doi.org/10.1016/j.fcr.2018.02.031>
- Kunrath, T. R., Lemaire, G., Teixeira, E., Brown, H. E., Ciampitti, I. A., & Sadras, V. O. (2020). Allometric relationships between nitrogen uptake and transpiration to untangle interactions between nitrogen supply and drought in maize and sorghum. *European Journal of Agronomy*, 120(April), 126145. <https://doi.org/10.1016/j.eja.2020.126145>
- Ladha, J. K., Pathak, H., Krupnik, T. J., Six, J., & van Kessel, C. (2005). Efficiency of fertilizer nitrogen in cereal production: Retrospects and prospects. *Advances in Agronomy*, 87(05), 85–156. [https://doi.org/10.1016/S0065-2113\(05\)87003-8](https://doi.org/10.1016/S0065-2113(05)87003-8)
- Ladha, J. K., Tirol-Padre, A., Reddy, C. K., Cassman, K. G., Verma, S., Powlson, D. S., Van Kessel, C., De Richter, D. B., Chakraborty, D., & Pathak, H. (2016). Global nitrogen budgets in cereals: A 50-year assessment for maize, rice, and wheat production systems. *Scientific Reports*, 6(January), 1–9. <https://doi.org/10.1038/srep19355>
- Lafitte, H. R., & Edmeades, G. O. (1994). Improvement for tolerance to low soil nitrogen in tropical maize I. Selection criteria. *Field Crops Research*, 39(1), 1–14. [https://doi.org/10.1016/0378-4290\(94\)90066-3](https://doi.org/10.1016/0378-4290(94)90066-3)

- Lambers, H., Chapin, F. S., & Pons, T. L. (2008). Plant physiological ecology. In *Plant Physiological Ecology* (Second Edi). Springer New York. <https://doi.org/10.1007/978-0-387-78341-3>
- Laungani, R., & Knops, J. M. H. (2009). Species-driven changes in nitrogen cycling can provide a mechanism for plant invasions. *Proceedings of the National Academy of Sciences of the United States of America*, 106(30), 12400–12405. <https://doi.org/10.1073/pnas.0900921106>
- Lawlor, D. W. (2002). Carbon and nitrogen assimilation in relation to yield: Mechanisms are the key to understanding production systems. *Journal of Experimental Botany*, 53(370), 773–787. <https://doi.org/10.1093/jxb/53.370.773>
- Lee, R. B., Purves, J. V., Ratcliffe, R. G., & Saker, L. R. (1992). Nitrogen assimilation and the control of ammonium and nitrate absorption by maize roots. *Journal of Experimental Botany*, 43(256), 1385–1396. <https://doi.org/https://doi.org/10.1093/jxb/43.11.1385>
- Lehmeier, C. A., Wild, M., & Schnyder, H. (2013). Nitrogen stress affects the turnover and size of nitrogen pools supplying leaf growth in a grass. *Plant Physiology*, 162(4), 2095–2105. <https://doi.org/10.1104/pp.113.219311>
- Lemaire, G., & Gastal, F. (1997). N uptake and distribution in plant canopies. In *Diagnosis of the nitrogen status in crops* (pp. 3–43). Springer Berlin Heidelberg. https://doi.org/10.1007/978-3-642-60684-7_1
- Lemaire, G., Oosterom, E. van, Sheehy, J., Jeuffroy, M. H., Massignam, A., & Rossato, L. (2007). Is crop N demand more closely related to dry matter accumulation or leaf area expansion during vegetative growth? *Field Crops Research*, 100(1), 91–106. <https://doi.org/10.1016/j.fcr.2006.05.009>
- Lemcoff, J. H., & Loomis, R. S. (1994). Nitrogen and density influences on silk emergence, endosperm development, and grain yield in maize (*Zea mays* L.). *Field Crops Research*, 38(2), 63–72. [https://doi.org/10.1016/0378-4290\(94\)90001-9](https://doi.org/10.1016/0378-4290(94)90001-9)
- Leroux, B. M., Goodyke, A. J., Schumacher, K. I., Abbott, C. P., Clore, A. M., Yadegari, R., Larkins, B. A., & Dannenhoffer, J. M. (2014). Maize early endosperm growth and development: From fertilization through cell type differentiation. *American Journal of Botany*, 101(8), 1259–1274. <https://doi.org/10.3732/ajb.1400083>
- Lewis, S., & Clarke, M. (2001). Forest plots : trying to see the wood and the trees. *British Medical Journal*, 322(7300), 1479–1480.
- Li, L. J., Han, X. Z., You, M. Y., Yuan, Y. R., Ding, X. L., & Qiao, Y. F. (2013). Carbon and nitrogen mineralization patterns of two contrasting crop residues in a Mollisol: Effects of residue type and placement in soils. *European Journal of Soil Biology*, 54, 1–6. <https://doi.org/10.1016/j.ejsobi.2012.11.002>

- Liang, H., Li, F., & Nong, M. (2013). Effects of alternate partial root-zone irrigation on yield and water use of sticky maize with fertigation. *Agricultural Water Management*, 116(3), 242–247. <https://doi.org/10.1016/j.agwat.2012.08.003>
- LI-COR Biosciences Inc., Lincoln, N. (n.d.). LAI-2200 Plant canopy analyzer. Retrieved July 23, 2020, from https://www.licor.com/env/products/leaf_area/LAI-2200C/
- Lillo, C. (2008). Signalling cascades integrating light-enhanced nitrate metabolism. *Biochemical Journal*, 415(1), 11–19. <https://doi.org/10.1042/BJ20081115>
- Liu, J., Chen, F., Olokhnuud, C., Glass, A. D. M., Tong, Y., Zhang, F., & Mi, G. (2009). Root size and nitrogen-uptake activity in two maize (*Zea mays*) inbred lines differing in nitrogen-use efficiency. *Journal of Plant Nutrition and Soil Science*, 172(2), 230–236. <https://doi.org/10.1002/jpln.200800028>
- Liu, Z., Zhu, K., Dong, S., Liu, P., Zhao, B., & Zhang, J. (2017). Effects of integrated agronomic practices management on root growth and development of summer maize. *European Journal of Agronomy*, 84, 140–151. <https://doi.org/10.1016/j.eja.2016.12.006>
- Loomis, R. S., & Amthor, J. S. (1999). Yield potential, plant assimilatory capacity, and metabolic efficiencies. *Crop Science*, 39(6), 1584–1596. <https://doi.org/10.2135/cropsci1999.3961584x>
- Lü, P., Zhang, J. W., Jin, L. B., Liu, W., Dong, S. T., & Liu, P. (2012). Effects of nitrogen application stage on grain yield and nitrogen use efficiency of high-yield summer maize. *2012(2009)*, 211–216.
- Ma, B. L., & Dwyer, L. M. (1998). Nitrogen uptake and use of two contrasting maize hybrids differing in leaf senescence. *Plant and Soil*, 199, 283–291. <https://doi.org/10.1023/A:1004397219723>
- Malagoli, P., Laine, P., Rossato, L., & Ourry, A. (2005). Dynamics of nitrogen uptake and mobilization in field-grown winter oilseed rape (*Brassica napus*) from stem extension to harvest. II. An ¹⁵N-labelling-based simulation model of N partitioning between vegetative and reproductive tissues. *Annals of Botany*, 95(7), 1187–1198. <https://doi.org/10.1093/aob/mci131>
- Martinez-Carrasco, R., & Thorne, G. N. (1979). Physiological factors limiting grain size in wheat. *Journal of Experimental Botany*, 30(4), 669–679. <https://doi.org/10.1093/jxb/30.4.669>
- Masclaux-Daubresse, C., Daniel-Vedele, F., Dechorgnat, J., Chardon, F., Gaufichon, L., & Suzuki, A. (2010). Nitrogen uptake, assimilation and remobilization in plants: Challenges for sustainable and productive agriculture. *Annals of Botany*, 105(7), 1141–1157. <https://doi.org/10.1093/aob/mcq028>
- Matejovic, I. (1995). Total nitrogen in plant material determined by means of dry combustion: A possible alternative to determination by kjeldahl digestion. *Communications in Soil*

- Science and Plant Analysis, 26(13–14), 2217–2229.
<https://doi.org/10.1080/00103629509369441>
- McCree, K. J. (1970). An equation for the rate of respiration of white clover plants grown under controlled conditions. Prediction and Measurement of Photosynthetic Productivity (Proc. IBP/PP Technical Meeting, Trebon), 221–229.
- McCullough, D. E., Girardin, P., Mihajlovic, M., Aguilera, A., & Tollenaar, M. (1994). Influence of N supply on development and dry matter accumulation of an old and a new maize hybrid. Canadian Journal of Plant Science, 74(3), 471–477.
<https://doi.org/10.4141/cjps94-087>
- Meade, K. A., Cooper, M., & Beavis, W. D. (2013). Modeling biomass accumulation in maize kernels. Field Crops Research, 151, 92–100. <https://doi.org/10.1016/j.fcr.2013.07.014>
- Meghji, M. R., Dudley, J. W., Lambert, R. J., & Sprague, G. F. (1984). Inbreeding depression, inbred and hybrid grain yields, and other traits of maize genotypes representing three eras. Crop Science, 24(3), 545–549.
<https://doi.org/10.2135/cropsci1984.0011183x002400030028x>
- Meinzer, F. C., & Zhu, J. (1998). Nitrogen stress reduces the efficiency of the C₄CO₂ concentrating system, and therefore quantum yield, in *Saccharum* (sugarcane) species. Journal of Experimental Botany, 49(324), 1227–1234.
<https://doi.org/10.1093/jxb/49.324.1227>
- Messina, C. D., Hammer, G. L., McLean, G., Cooper, M., van Oosterom, E. J., Tardieu, F., Chapman, S. C., Doherty, A., & Gho, C. (2019). On the dynamic determinants of reproductive failure under drought in maize. In Silico Plants, 1(1), diz003.
<https://doi.org/10.1093/insilicoplants/diz003>
- Messina, C., Hammer, G., Dong, Z., Podlich, D., & Cooper, M. (2009). Modelling crop improvement in a G×E×M framework via gene–trait–phenotype relationships. In V. Sadras & D. F. Calderini (Eds.), Crop Physiology: Applications for Genetic Improvement and Agronomy (pp. 235–265). Academic Press, Elsevier. <https://doi.org/10.1016/B978-0-12-374431-9.00010-4>
- Messina, C. D., Rotundo, J., Hammer, G. L., Gho, C., Reyes, A., Fang, Y., van Oosterom, E., Borrás, L., Cooper, M. (2021). Radiation use efficiency increased over a century of maize (*Zea mays* L.) breeding in the US corn belt. Journal of Experimental Botany.
- Mevik, B.-H., Wehrens, R., & Liland, K. H. (2020). pls: Partial least squares and principal component regression. R package version 2.7-3. <https://cran.r-project.org/package=pls>
- Millet, E., & Pinthus, M. J. (1984). Effects of removing floral organs, light penetration and physical constraint on the development of wheat grains. Annals of Botany, 53(2), 261–269.

- Moll, R. H., Kamprath, E. J., & Jackson, W. A. (1982). Analysis and interpretation of factors which contribute to efficiency of nitrogen utilization. In *Agronomy Journal* (Vol. 74, Issue 3, p. 562). <https://doi.org/10.2134/agronj1982.00021962007400030037x>
- Moser, S. B., Feil, B., Jampatong, S., & Stamp, P. (2006). Effects of pre-anthesis drought, nitrogen fertilizer rate, and variety on grain yield, yield components, and harvest index of tropical maize. *Agricultural Water Management*, 81(1–2), 41–58. <https://doi.org/10.1016/j.agwat.2005.04.005>
- Mu, X., Chen, Q., Chen, F., Yuan, L., & Mi, G. (2016). Within-leaf nitrogen allocation in adaptation to low nitrogen supply in maize during grain-filling stage. *Frontiers in Plant Science*, 7, 699. <https://doi.org/10.3389/fpls.2016.00699>
- Mu, X., Chen, Q., Chen, F., Yuan, L., & Mi, G. (2018). Dynamic remobilization of leaf nitrogen components in relation to photosynthetic rate during grain filling in maize. *Plant Physiology and Biochemistry*, 129(May), 27–34. <https://doi.org/https://doi.org/10.1016/j.plaphy.2018.05.020>
- Muchow, R. C. (1998). Nitrogen utilization efficiency in maize and grain sorghum. *Field Crops Research*, 56, 209–216.
- Muchow, R. C., & Sinclair, T. R. (1994). Nitrogen response of leaf photosynthesis and canopy radiation use efficiency in field-grown maize and sorghum. *Crop Science*, 34(3), 721–727. <https://doi.org/10.2135/cropsci1994.0011183X003400030022x>
- Mueller, S. M., & Vyn, T. J. (2016). Maize plant resilience to N stress and post-silking N capacity changes over time: a review. *Frontiers in Plant Science*, 7(February), 1–14. <https://doi.org/10.3389/fpls.2016.00053>
- Mueller, S. M., & Vyn, T. J. (2018). Physiological constraints to realizing maize grain yield recovery with silking-stage nitrogen fertilizer applications. *Field Crops Research*, 228(June), 102–109. <https://doi.org/10.1016/j.fcr.2018.08.025>
- Mueller, S. M., Camberato, J. J., Messina, C., Shanahan, J., Zhang, H., & Vyn, T. J. (2017). Late-split nitrogen applications increased maize plant nitrogen recovery but not yield under moderate to high nitrogen rates. *Agronomy Journal*, 109(6), 2689–2699. <https://doi.org/10.2134/agronj2017.05.0282>
- Mueller, S. M., Messina, C. D., & Vyn, T. J. (2019a). Simultaneous gains in grain yield and nitrogen efficiency over 70 years of maize genetic improvement. *Scientific Reports*, 9, 9095. <https://doi.org/10.1038/s41598-019-45485-5>
- Mueller, S. M., Messina, C. D., & Vyn, T. J. (2019b). The role of the exponential and linear phases of maize (*Zea mays* L.) ear growth for determination of kernel number and kernel weight. *European Journal of Agronomy*, 111(August), 125939. <https://doi.org/10.1016/j.eja.2019.125939>

- Nasielski, J., Earl, H., & Deen, B. (2019). Luxury vegetative nitrogen uptake in maize buffers grain yield under post-silking water and nitrogen stress: A mechanistic understanding. *Frontiers in Plant Science*, 10(March), 1–14. <https://doi.org/10.3389/fpls.2019.00318>
- Ning, P., Fritschi, F. B., & Li, C. (2017). Temporal dynamics of post-silking nitrogen fluxes and their effects on grain yield in maize under low to high nitrogen inputs. *Field Crops Research*, 204, 249–259. <https://doi.org/10.1016/j.fcr.2017.01.022>
- Ning, P., Yang, L., Li, C., & Fritschi, F. B. (2018). Post-silking carbon partitioning under nitrogen deficiency revealed sink limitation of grain yield in maize. *Journal of Experimental Botany*, 69(7), 1707–1719. <https://doi.org/10.1093/jxb/erx496>
- O’Leary, B. M., Asao, S., Millar, A. H., & Atkin, O. K. (2019). Core principles which explain variation in respiration across biological scales. *New Phytologist*, 222(2), 670–686. <https://doi.org/10.1111/nph.15576>
- Oikeh, S. O., Kling, J. G., Horst, W. J., Chude, V. O., & Carsky, R. J. (1999). Growth and distribution of maize roots under nitrogen fertilization in plinthite soil. *Field Crops Research*, 62(1), 1–13. [https://doi.org/10.1016/S0378-4290\(98\)00169-5](https://doi.org/10.1016/S0378-4290(98)00169-5)
- Olmedo Pico, L. B., Zhang, C., & Vyn, T. J. (2021). The central role of ear nitrogen uptake in maize endosperm cell and kernel weight determination during the lag period. *Field Crops Research*, 273(March), 108285. <https://doi.org/10.1016/j.fcr.2021.108285>
- Osenberg, C. W., Sarnelle, O., Cooper, S. D., & Holt, R. D. (1999). Resolving ecological questions through meta-analysis: Goals, metrics, and models. *Ecology*, 80(4), 1105–1117.
- Ouattar, S., Jones, R. J., Crookston, R. K., & Kajeiou, M. (1987a). Effect of drought on water relations of developing maize kernels. *Crop Science*, 27, 730–735. <https://doi.org/10.2135/cropsci1987.0011183X002700040026x>
- Ouattar, S., Jones, R. J., & Crookston, R. K. (1987b). Effect of water deficit during grain filling on the pattern of maize kernel growth and development1. *Crop Science*, 27(4), 726. <https://doi.org/10.2135/cropsci1987.0011183x002700040025x>
- Palmer, A. F. E., Heichel, G. H., & Musgrave, R. B. (1973). Patterns of translocation, respiratory loss, and redistribution of ¹⁴C in maize labeled after flowering 1. *Crop Science*, 13(3), 371–376. <https://doi.org/10.2135/cropsci1973.0011183x001300030025x>
- Pan, W. L., Camberato, J. J., Moll, R. H., Kamprath, E. J., & Jackson, W. A. (1995). Altering source-sink relationships in prolific maize hybrids: Consequences for nitrogen uptake and remobilization. *Crop Science*, 35(3), 836–845. <https://doi.org/10.2135/cropsci1995.0011183X003500030034x>
- Pan, W. L., Jackson, W. A., & Moll, R. H. (1985). Nitrate uptake and partitioning by corn (*Zea mays* L.) root systems and associated morphological differences among genotypes and

- stages of root development. *Journal of Experimental Botany*, 36(9), 1341–1351.
<https://doi.org/10.1093/jxb/36.9.1341>
- Pandey, R. K., Maranville, J. W., & Admou, A. (2000). Deficit irrigation and nitrogen effects on maize in a Sahelian environment: I. Grain yield and yield components. *Agricultural Water Management*, 46(1), 1–13. [https://doi.org/10.1016/S0378-3774\(00\)00073-1](https://doi.org/10.1016/S0378-3774(00)00073-1)
- Paponov, I. A., & Engels, C. (2005). Effect of nitrogen supply on carbon and nitrogen partitioning after flowering in maize. *Journal of Plant Nutrition and Soil Science*, 168(4), 447–453. <https://doi.org/10.1002/jpln.200520505>
- Paponov, I. A., Sambo, P., Schulte Auf'm Erley, G., Presterl, T., Geiger, H. H., & Engels, C. (2005). Grain yield and kernel weight of two maize genotypes differing in nitrogen use efficiency at various levels of nitrogen and carbohydrate availability during flowering and grain filling. *Plant and Soil*, 272(1–2), 111–123. <https://doi.org/10.1007/s11104-004-4211-7>
- Peltonen-Sainio, P., Jauhiainen, L., & Sadras, V. O. (2011). Phenotypic plasticity of yield and agronomic traits in cereals and rapeseed at high latitudes. *Field Crops Research*, 124(2), 261–269. <https://doi.org/10.1016/j.fcr.2011.06.016>
- Peng, Y., Li, C., & Fritschi, F. B. (2013). Apoplastic infusion of sucrose into stem internodes during female flowering does not increase grain yield in maize plants grown under nitrogen-limiting conditions. *Physiologia Plantarum*, 148(4), 470–480.
<https://doi.org/10.1111/j.1399-3054.2012.01711.x>
- Penning de Vries, F. W. T. (1975). The cost of maintenance processes in plant cells. *Annals of Botany*, 39, 77–92. <http://edepot.wur.nl/218532>
- Penning de Vries, F. W. T., Brunsting, A. H. M., & Van Laar, H. H. (1974). Products, requirements and efficiency of biosynthesis a quantitative approach. *Journal of Theoretical Biology*, 45(2), 339–377. [https://doi.org/10.1016/0022-5193\(74\)90119-2](https://doi.org/10.1016/0022-5193(74)90119-2)
- Perchlik, M., & Tegeder, M. (2018). Leaf amino acid supply affects photosynthetic and plant nitrogen use efficiency under nitrogen stress. *Plant Physiology*, 178(1), 174–188.
<https://doi.org/10.1104/pp.18.00597>
- Philibert, A., Loyce, C., & Makowski, D. (2012). Assessment of the quality of meta-analysis in agronomy. *Agriculture, Ecosystems and Environment*, 148, 72–82.
<https://doi.org/10.1016/j.agee.2011.12.003>
- Pinheiro, J. C., & Bates, D. M. (2000). Linear mixed-effects models: basic concepts and examples. In *Mixed-effects models in S and S-Plus* (pp. 3–56).
- Pinheiro, J., Bates, D., DebRoy, S., Sarkar, D., & R, C. T. (2018). *nlme: Linear and nonlinear mixed effects models (R package version 3.1-137)*. <https://cran.r-project.org/package=nlme>

- Plénet, D., & Lemaire, G. (2000). Relationships between dynamics of nitrogen uptake and dry matter accumulation in maize crops. Determination of critical N concentration. *Plant and Soil*, 216(ii), 65–82. <https://doi.org/10.1023/A:1004783431055>
- Presterl, T., Groh, S., Landbeck, M., Seitz, G., Schmidt, W., & Geiger, H. H. (2002). Nitrogen uptake and utilization efficiency of European maize hybrids developed under conditions of low and high nitrogen input. *Plant Breeding*, 121(6), 480–486. <https://doi.org/10.1046/j.1439-0523.2002.00770.x>
- Pykälä, J., Luoto, M., Heikkinen, R. K., & Kontula, T. (2005). Plant species richness and persistence of rare plants in abandoned semi-natural grasslands in northern Europe. *Basic and Applied Ecology*, 6(1), 25–33. <https://doi.org/10.1016/j.baae.2004.10.002>
- Quintero, A., Molero, G., Reynolds, M. P., & Calderini, D. F. (2018). Trade-off between grain weight and grain number in wheat depends on GxE interaction: A case study of an elite CIMMYT panel (CIMCOG). *European Journal of Agronomy*, 92(March 2017), 17–29. <https://doi.org/10.1016/j.eja.2017.09.007>
- Rajcan, I., & Tollenaar, M. (1999a). Source : sink ratio and leaf senescence in maize: II. Nitrogen metabolism during grain filling. *Field Crops Research*, 60(3), 255–265. [https://doi.org/10.1016/S0378-4290\(98\)00143-9](https://doi.org/10.1016/S0378-4290(98)00143-9)
- Rajcan, I., & Tollenaar, M. (1999b). Source:sink ratio and leaf senescence in maize: I. Dry matter accumulation and partitioning during grain filling. *Field Crops Research*, 60(3), 245–253. [https://doi.org/10.1016/S0378-4290\(98\)00142-7](https://doi.org/10.1016/S0378-4290(98)00142-7)
- Randall, G. W., Iragavarapu, T. K., & Bock, B. R. (1997). Nitrogen application methods and timing for corn after soybean in a ridge-tillage system. *Journal of Production Agriculture*, 10(2), 300. <https://doi.org/10.2134/jpa1997.0300>
- Randall, G., & Schmitt, M. (2004). Strategies for split N applications in 2004. In *Proc. Wis. Fert. Aglime and Pest Mgmt. Conf*, 43, 60–67.
- Randall, Gyles W., & Vetsch, J. A. (2005). Corn production on a subsurface-drained mollisol as affected by fall versus spring application of nitrogen and nitrapyrin. *Agronomy Journal*, 97(2), 472–478. <https://doi.org/10.2134/agronj2005.0472>
- Raun, W. R., & Johnson, G. V. (1999). Improving nitrogen use efficiency for cereal production. *Agronomy Journal*, 91(3), 357. <https://doi.org/10.2134/agronj1999.00021962009100030001x>
- Reddy, V. M., & Daynard, T. B. (1983). Endosperm characteristics associated with rate of grain filling and kernel size in corn. *Maydica*, 28, 339–355.
- Ren, B., Dong, S., Zhao, B., Liu, P., & Zhang, J. (2017). Responses of nitrogen metabolism, uptake and translocation of maize to waterlogging at different growth stages. *Frontiers in Plant Science*, 8(July), 1–9. <https://doi.org/10.3389/fpls.2017.01216>

- Reyes, A., Messina, C. D., Hammer, G. L., Liu, L., Oosterom, E. Van, Lafitte, R., & Cooper, M. (2015). Soil water capture trends over 50 years of single-cross maize (*Zea mays* L.) breeding in the US corn-belt. *Journal of Experimental Botany*, 66(22), 7339–7346. <https://doi.org/10.1093/jxb/erv430>
- Ritchie, S. W., Hanway, J. J., & Benson, G. O. (1997). How a corn plant develops. Spec. Rep. No. 48. Iowa State University of Science and Technology Cooperative Extension Service, Ames, IA.
- Roberts, T. L., Slaton, N. A., Kelley, J. P., Greub, C. E., & Fulford, A. M. (2016). Fertilizer nitrogen recovery efficiency of furrow-irrigated corn. *Agronomy Journal*, 108(5), 2123–2128. <https://doi.org/10.2134/agronj2016.02.0092>
- Rossato, L., Lainé, P., & Ourry, A. (2001). Nitrogen storage and remobilization in *Brassica napus* L. during the growth cycle: Nitrogen fluxes within the plant and changes in soluble protein patterns. *Journal of Experimental Botany*, 52(361), 1655–1663. <https://doi.org/10.1093/jxb/52.361.1655>
- RStudio Team. (2016). RStudio: Integrated development for R. RStudio, Inc. Boston, MA. <http://www.rstudio.com/>
- Ruiz Diaz, D. A., Hawkins, J. A., Sawyer, J. E., & Lundvall, J. P. (2008). Evaluation of in-season nitrogen management strategies for corn production. *Agronomy Journal*, 100(6), 1711–1719. <https://doi.org/10.2134/agronj2008.0175>
- Russell, W. A. (1985). Evaluations for plant, ear, and grain traits of maize cultivars representing seven eras of breeding. *Maydica*, 30(1), 85–96.
- Russelle, M. P., Hauck, R. D., & Olson, R. A. (1983). Nitrogen accumulation rates of irrigated maize. *Agronomy Journal*, 75(4), 593. <https://doi.org/10.2134/agronj1983.00021962007500040006x>
- Sadras, V. O. (2007). Evolutionary aspects of the trade-off between seed size and number in crops. *Field Crops Research*, 100(2–3), 125–138. <https://doi.org/10.1016/j.fcr.2006.07.004>
- Sadras, V. O., & Lawson, C. (2011). Genetic gain in yield and associated changes in phenotype, trait plasticity and competitive ability of South Australian wheat varieties released between 1958 and 2007. *Crop and Pasture Science*, 62(7), 533–549. <https://doi.org/10.1071/CP11060>
- Sadras, V. O., & Lemaire, G. (2014). Quantifying crop nitrogen status for comparisons of agronomic practices and genotypes. *Field Crops Research*, 164, 54–64. <https://doi.org/10.1016/j.fcr.2014.05.006>
- Sainz Rozas, H. R., Echeverría, H. E., & Barbieri, P. A. (2004). Nitrogen balance as affected by application time and nitrogen fertilizer rate in irrigated no-tillage maize. *Agronomy Journal*, 96(6), 1622–1631. <https://doi.org/10.2134/agronj2004.1622>

- Sainz Rozas, H., Echeverría, H. E., Studdert, G. A., & Andrade, F. H. (1999). No-till maize nitrogen uptake and yield: Effect of urease inhibitor and application time. *Agronomy Journal*, 91(6), 950–955. <https://doi.org/10.2134/agronj1999.916950x>
- Sala, R. G., Westgate, M. E., & Andrade, F. H. (2007). Source/sink ratio and the relationship between maximum water content, maximum volume, and final dry weight of maize kernels. *Field Crops Research*, 101(1), 19–25. <https://doi.org/10.1016/j.fcr.2006.09.004>
- Salon, C., Munier-Jolain, N. G., Duc, G. G., Voisin, A.-S., Grandgirard, D., Larmure, A., Emery, R. J. N., & Ney, B. (2001). Grain legume seed filling in relation to nitrogen acquisition: A review and prospects with particular reference to pea. *Agronomie*, 21(6–7), 539–552. <https://doi.org/10.1051/agro:2001143>
- Scharf, P., Wiebold, W., & Lory, J. (2002). Corn yield response to nitrogen fertilizer timing and deficiency level. *Agronomy Journal*, 1972, 435–441. <https://doi.org/10.2134/agronj2002.0435>
- Schiltz, S., Munier-Jolain, N., Jeudy, C., Burstin, J., & Salon, C. (2005). Dynamics of exogenous nitrogen partitioning and nitrogen remobilization from vegetative organs in pea revealed by ¹⁵N in vivo labeling throughout seed filling. *Plant Physiology*, 137(4), 1463–1473. <https://doi.org/10.1104/pp.104.056713>
- Scott, W. R., Appleyard, M., Fellowes, G., & Kirby, E. J. M. (1983). Effect of genotype and position in the ear on carpel and grain growth and mature grain weight of spring barley. *The Journal of Agricultural Science*, 100(2), 383–391. <https://doi.org/10.1017/S0021859600033530>
- Sekhon, R. S., Breitzman, M. W., Silva, R. R., Santoro, N., Rooney, W. L., de Leon, N., & Kaeppler, S. M. (2016). Stover composition in maize and sorghum reveals remarkable genetic variation and plasticity for carbohydrate accumulation. *Frontiers in Plant Science*, 7(June), 1–12. <https://doi.org/10.3389/fpls.2016.00822>
- Setter, T. I. M. L., & Meller, V. H. (1984). Reserve carbohydrate in maize stem. *Plant Physiol.*, 75, 617–622.
- Silva, P. R. F. da, Strieder, M. L., Coser, R. P. da S., Rambo, L., Sangoi, L., Argenta, G., Forsthofer, E. L., & Silva, A. A. da. (2005). Grain yield and kernel crude protein content increases of maize hybrids with late nitrogen side-dressing. *Scientia Agricola*, 62(5), 487–492. <https://doi.org/10.1590/S0103-90162005000500014>
- Simmons, S. R., & Jones, R. J. (1985). Contributions of pre-silking assimilate to grain yield in maize. *Crop Science*, 25(6), 1004–1006. <https://doi.org/10.2135/cropsci1985.0011183X002500060025x>
- Sinclair, T. R., & Horie, T. (1989). Leaf nitrogen, photosynthesis, and crop radiation use efficiency: A review. *Crop Science*, 29(1), 90–98. <https://doi.org/10.2135/cropsci1989.0011183X002900010023x>

- Sinclair, T. R., & Rufty, T. W. (2015). Genetic improvement of water and nitrogen use to increase crop yields: A whole plant physiological perspective. In P. Drechsel, P. Heffer, H. Magen, R. Mikkelsen, & D. Wichelns (Eds.), *Managing Water and Fertilizer for Sustainable Agricultural Intensification* (First edit, pp. 87–108). International Fertilizer Industry Association (IFA), International Water Management Institute (IWMI), International Plant Nutrition Institute (IPNI), and International Potash Institute (IPI). www.ipipotash.org
- Sitthaphanit, S., Limpinuntana, V., Toomsan, B., Panchaban, S., & Bell, R. W. (2009). Fertiliser strategies for improved nutrient use efficiency on sandy soils in high rainfall regimes. *Nutrient Cycling in Agroecosystems*, 85(2), 123–139. <https://doi.org/10.1007/s10705-009-9253-z>
- Soufizadeh, S., Munaro, E., McLean, G., Massignam, A., van Oosterom, E. J., Chapman, S. C., Messina, C., Cooper, M., & Hammer, G. L. (2018). Modelling the nitrogen dynamics of maize crops – Enhancing the APSIM maize model. *European Journal of Agronomy*, 100, 118–131. <https://doi.org/10.1016/j.eja.2017.12.007>
- Swank, J. C., Below, F. E., Lambert, R. J., & Hageman, R. H. (1982). Interaction of carbon and nitrogen metabolism in the productivity of maize. *Plant Physiology*, 70(4), 1185–1190. <https://doi.org/10.1104/pp.70.4.1185>
- Ta, C. T., & Weiland, R. T. (1992). Nitrogen partitioning in maize during ear development. *Crop Science*, 32(2), 443–451. <https://doi.org/10.2135/cropsci1992.0011183x003200020032x>
- Tanemura, R., Kurashima, H., Ohtake, N., Sueyoshi, K., & Ohyama, T. (2008). Absorption and translocation of nitrogen in cucumber (*Cucumis sativus* L.) plants using the ¹⁵N tracer technique. *Soil Science and Plant Nutrition*, 54(1), 108–117. <https://doi.org/10.1111/j.1747-0765.2007.00213.x>
- Tegeder, M., & Masclaux-Daubresse, C. (2018). Source and sink mechanisms of nitrogen transport and use. *New Phytologist*, 217(1), 35–53. <https://doi.org/10.1111/nph.14876>
- Thornley, J. H. M. (1970). Respiration, growth and maintenance in plants. *Nature*, 227, 304–305. <https://doi.org/10.1038/227304b0>
- Tian, H., Fu, J., Drijber, R. A., & Gao, Y. (2015). Expression patterns of five genes involved in nitrogen metabolism in two winter wheat (*Triticum aestivum* L.) genotypes with high and low nitrogen utilization efficiencies. *Journal of Cereal Science*, 61, 48–54. <https://doi.org/10.1016/j.jcs.2014.09.007>
- Tilman, D., Cassman, K. G., Matson, P. A., Naylor, R., & Polasky, S. (2002). Agricultural sustainability and intensive production practices. *Nature*, 418(6898), 671–677. <https://doi.org/10.1038/nature01014>
- Tollenaar, M., & Lee, E. A. (2002). Yield potential, yield stability and stress tolerance in maize. *Field Crops Research*, 75(2–3), 161–169. [https://doi.org/10.1016/S0378-4290\(02\)00024-2](https://doi.org/10.1016/S0378-4290(02)00024-2)

- Tollenaar, M., & Lee, E. A. (2006). Dissection of physiological processes underlying grain yield in maize by examining genetic improvement and heterosis. *51*(2), 399–408.
- Tremblay, N., Bouroubi, Y. M., Bélec, C., Mullen, R. W., Kitchen, N. R., Thomason, W. E., Ebelhar, S., Mengel, D. B., Raun, W. R., Francis, D. D., Vories, E. D., & Ortiz-Monasterio, I. (2012). Corn response to nitrogen is influenced by soil texture and weather. *Agronomy Journal*, *104*(6), 1658–1671. <https://doi.org/10.2134/agronj2012.0184>
- Triboi, E., & Triboi-Blondel, A. M. (2002). Productivity and grain or seed composition: A new approach to an old problem - Invited paper. *European Journal of Agronomy*, *16*(3), 163–186. [https://doi.org/10.1016/S1161-0301\(01\)00146-0](https://doi.org/10.1016/S1161-0301(01)00146-0)
- Triboi, E., Martre, P., Girousse, C., Ravel, C., & Triboi-Blondel, A. M. (2006). Unravelling environmental and genetic relationships between grain yield and nitrogen concentration for wheat. *European Journal of Agronomy*, *25*(2), 108–118. <https://doi.org/10.1016/j.eja.2006.04.004>
- Uhart, S. A., & Andrade, F. H. (1995). Nitrogen and carbon accumulation and remobilization during grain filling in maize under different source/sink ratios. *Crop Science*, *35*(1), 183–190. <https://doi.org/10.2135/cropsci1995.0011183X003500010034x>
- Valentinuz, O. R., & Tollenaar, M. (2004). Vertical profile of leaf senescence during the grain-filling period in older and newer maize hybrids. *Crop Science*, *44*(3), 827–834. <https://doi.org/10.2135/cropsci2004.0827>
- Valladares, F., Sanchez Gomez, D. A. V. I. D., & Zavala, M. A. (2006). Quantitative estimation of phenotypic plasticity: bridging the gap between the evolutionary concept and its ecological applications. *Journal of Ecology*, *94*(6), 1103–1116.
- Valluru, R., Link, J., & Claupein, W. (2011). Natural variation and morpho-physiological traits associated with water-soluble carbohydrate concentration in wheat under different nitrogen levels. *Field Crops Research*, *124*(1), 104–113. <https://doi.org/10.1016/j.fcr.2011.06.008>
- Van Den Noortgate, W., & Onghena, P. (2005). Parametric and nonparametric bootstrap methods for meta-analysis. *Behavior Research Methods*, *37*(1), 11–22.
- Van Iersel, M. W. (2003). Carbon use efficiency depends on growth respiration, maintenance respiration, and relative growth rate. A case study with lettuce. *Plant, Cell & Environment*, *26*(9), 1441–1449. <https://doi.org/10.1046/j.0016-8025.2003.01067.x>
- Van Oosterom, E. J., Chapman, S. C., Borrell, A. K., Broad, I. J., & Hammer, G. L. (2010). Functional dynamics of the nitrogen balance of sorghum. II. Grain filling period. *Field Crops Research*, *115*(1), 29–38. <https://doi.org/10.1016/j.fcr.2009.09.019>

- Veen, B. W., van Noordwijk, M., de Willigen, P., Boone, F. R., & Kooistra, M. J. (1992). Root-soil contact of maize, as measured by a thin-section technique. *Plant and Soil*, 139(1), 131–138. <https://doi.org/10.1007/BF00012848>
- Viechtbauer, W. (2010). Conducting meta-analyses in R with the metafor package. *Journal of Statistical Software*, 36(3).
- Vos, J. (1981). Effects of temperature and nitrogen supply on post-floral growth of wheat; measurements and simulations. *Agricultural Research Reports*, 911, 164.
- Vos, J., Van Der Putten, P. E. L., & Birch, C. J. (2005). Effect of nitrogen supply on leaf appearance, leaf growth, leaf nitrogen economy and photosynthetic capacity in maize (*Zea mays* L.). *Field Crops Research*, 93(1), 64–73. <https://doi.org/10.1016/j.fcr.2004.09.013>
- Walsh, O., Raun, W., Klatt, A., & Solie, J. (2012). Effect of delayed nitrogen fertilization on maize (*Zea mays* L.) grain yields and nitrogen use efficiency. *Journal of Plant Nutrition*, 35(4), 538–555. <https://doi.org/10.1080/01904167.2012.644373>
- Wang, Q. X., Wang, P., Yang, X. Y., Zhai, Z. X., Wang, X. L., & Shen, L. X. (2003). Effects of nitrogen application time on root distribution and its activity in maize (*Zea mays* L.). *Scientia Agricultura Sinica*, 36(12), 1469-1475 (in Chinese with English abstract).
- Wang, S., Luo, S., Yue, S., Shen, Y., & Li, S. (2016). Fate of ¹⁵N fertilizer under different nitrogen split applications to plastic mulched maize in semiarid farmland. *Nutrient Cycling in Agroecosystems*, 105(2), 129–140. <https://doi.org/10.1007/s10705-016-9780-3>
- Wang, Y., & Wahba, G. (1995). Bootstrap confidence intervals for smoothing splines and their comparison to bayesian confidence intervals. *Journal of Statistical Computation and Simulation*, 51(2–4), 263–279. <https://doi.org/10.1080/00949659508811637>
- Wang, Y., Mi, G., Chen, F., Zhang, J., & Zhang, F. (2005). Response of root morphology to nitrate supply and its contribution to nitrogen accumulation in maize. *Journal of Plant Nutrition*, 27(12), 2189–2202. <https://doi.org/10.1081/PLN-200034683>
- Weiland, R., & Ta, T. (1992). Allocation and retranslocation of ¹⁵N by maize (*Zea mays* L.) hybrids under field conditions of low and high N fertility. *Functional Plant Biology*, 19(1), 77. <https://doi.org/10.1071/PP9920077>
- Wood, C. W., Reeves, D. W., & Himelrick, D. G. (1993). Relationships between chlorophyll meter readings and leaf chlorophyll concentration, N status, and crop yield: A review. *Proceedings of the Agronomy Society of New Zealand*, 23, 1–9.
- Wood, S. N. (2017). *Generalized additive models: An introduction with R* (2nd editio). Chapman and Hall/CRC.

- Worku, M., Bänziger, M., Erley, G. S. A. m., Friesen, D., Diallo, A. O., & Horst, W. J. (2007). Nitrogen uptake and utilization in contrasting nitrogen efficient tropical maize hybrids. *Crop Science*, 47(2), 519–528. <https://doi.org/10.2135/cropsci2005.05.0070>
- Yan, P., Yue, S., Qiu, M., Chen, X., Cui, Z., & Chen, F. (2014). Using maize hybrids and in-season nitrogen management to improve grain yield and grain nitrogen concentrations. *Field Crops Research*, 166, 38–45. <https://doi.org/10.1016/j.fcr.2014.06.012>
- Yan, P., Zhang, Q., Shuai, X. F., Pan, J. X., Zhang, W. J., Shi, J. F., Wang, M., Chen, X. P., & Cui, Z. L. (2016). Interaction between plant density and nitrogen management strategy in improving maize grain yield and nitrogen use efficiency on the North China Plain. *Journal of Agricultural Science*, 154(6), 978–988. <https://doi.org/10.1017/S0021859615000854>
- Yang, L., Guo, S., Chen, Q., Chen, F., Yuan, L., & Mi, G. (2016). Use of the stable nitrogen isotope to reveal the source-sink regulation of nitrogen uptake and remobilization during grain filling phase in maize. *PLoS ONE*, 11(9), 1–16. <https://doi.org/10.1371/journal.pone.0162201>
- Yang, Z., van Oosterom, E. J., Jordan, D. R., & Hammer, G. L. (2009). Pre-anthesis ovary development determines genotypic differences in potential kernel weight in sorghum. *Journal of Experimental Botany*, 60(4), 1399–1408. <https://doi.org/10.1093/jxb/erp019>
- Yee, T. W., & Mackenzie, M. (2002). Vector generalized additive models in plant ecology. *Ecological Modelling*, 157(2–3), 141–156. [https://doi.org/10.1016/S0304-3800\(02\)00192-8](https://doi.org/10.1016/S0304-3800(02)00192-8)
- Yoneyama, T., Ito, O., & Engelaar, W. M. H. G. (2003). Uptake, metabolism and distribution of nitrogen in crop plants traced by enriched and natural ¹⁵N: Progress over the last 30 years. *Phytochemistry Reviews*, 2(1–2), 121–132. <https://doi.org/10.1023/B:PHYT.0000004198.95836.ad>
- Zerihun, A., McKenzie, B. A., & Morton, J. D. (1998). Photosynthate costs associated with the utilization of different nitrogen-forms: influence on the carbon balance of plants and shoot-root biomass partitioning. *New Phytologist*, 138, 1–11. <https://doi.org/10.1046/j.1469-8137.1998.00893.x>
- Zhou, G., & Wang, Q. (2018). A new nonlinear method for calculating growing degree days. *Scientific Reports*, 8(1), 1–14. <https://doi.org/10.1038/s41598-018-28392-z>
- Ziadi, N., Brassard, M., Bélanger, G., Cambouris, A. N., Tremblay, N., Nolin, M. C., Claessens, A., & Parent, L.-étienne. (2008). Critical nitrogen curve and nitrogen nutrition index for corn in eastern Canada. *Agronomy Journal*, 100(2), 271–276. <https://doi.org/10.2134/agronj2007.0059>
- Ziadi, N., Brassard, M., Bélanger, G., Claessens, A., Tremblay, N., Cambouris, A. N., Nolin, M. C., & Parent, L. É. (2008). Chlorophyll measurements and nitrogen nutrition index for

the evaluation of corn nitrogen status. *Agronomy Journal*, 100(5), 1264–1273.
<https://doi.org/10.2134/agronj2008.0016>

Appendix A - Chapter 2 - Figures and tables

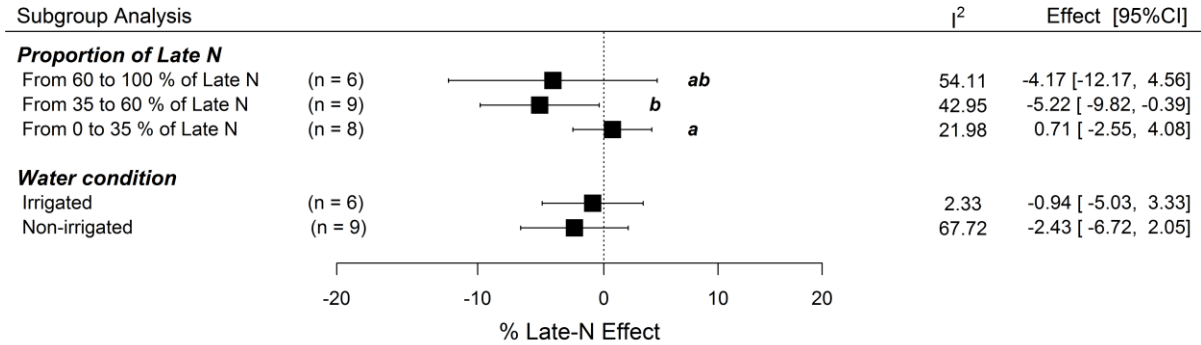


Figure A.1. Forest plot for subgroup analysis on late season N effect on yield across different proportion of late N applied (late N less than 35%, between 35 and 60%, and more than 60% of final N rate) and water regimes (irrigated and non-irrigated). Effect sizes and 95 % confidence intervals (CI) are expressed as a late-N effect ratio (percentage of grain yield variation in L_N / E_N) calculated as (6). Square symbols represent point estimates and whiskers depict their respective 95% CI. Heterogeneity of the results is described through I^2 (I-square statistic). n = number of studies within subgroup. Different letters indicate significant differences between pooled effect sizes at $P \leq 0.05$.

Table A.1. Sensitivity analysis for determination of late N proportion for subgrouping meta-analysis. Values (*i, j, k*) within each combination of thresholds represent number of studies allocated in the upper, middle, and lower late N subgroups, respectively. In bold, the selected combination based on the balance of studies and the range within intervals (difference between maximum and minimum limits).

Lower Threshold in %	Upper Threshold in %								
	50	55	60	65	70	75	80	85	90
5	8, 9, 0	6, 13, 0	6, 13, 0	5, 13, 0	4, 13, 0	4, 13, 0	4, 13, 0	4, 13, 0	4, 13, 0
10	8, 9, 0	6, 13, 0	6, 13, 0	5, 13, 0	4, 13, 0	4, 13, 0	4, 13, 0	4, 13, 0	4, 13, 0
15	8, 9, 1	6, 13, 1	6, 13, 1	5, 13, 1	4, 13, 1	4, 13, 1	4, 13, 1	4, 13, 1	4, 13, 1
20	8, 9, 3	6, 13, 3	6, 13, 3	5, 13, 3	4, 13, 3	4, 13, 3	4, 13, 3	4, 13, 3	4, 13, 3
25	8, 8, 4	6, 12, 4	6, 12, 4	5, 12, 4	4, 12, 4	4, 12, 4	4, 12, 4	4, 12, 4	4, 12, 4
30	8, 8, 5	6, 12, 5	6, 12, 5	5, 12, 5	4, 12, 5	4, 12, 5	4, 12, 5	4, 12, 5	4, 12, 5
35	8, 4, 8	6, 9, 8	<u>6, 9, 8</u>	5, 9, 8	4, 9, 8	4, 9, 8	4, 9, 8	4, 9, 8	4, 9, 8
40	8, 4, 8	6, 9, 8	6, 9, 8	5, 9, 8	4, 9, 8	4, 9, 8	4, 9, 8	4, 9, 8	4, 9, 8
45	8, 3, 9	6, 8, 9	6, 8, 9	5, 8, 9	4, 8, 9	4, 8, 9	4, 8, 9	4, 8, 9	4, 8, 9

Table A.2. Subset of the overall dataset with reported values on plant N content at silking and at maturity ($n_1=98$). Mean \pm standard deviation (SD) for each N-timing group of plant N uptake at physiological maturity per unit area (PNU_{PM}), plant N uptake at silking per unit area (PNU_{SILK}), and percentage of total PNU that occurs from the period that goes from silking until physiological maturity ($NU_{Post-Silking}$). When biomass at silking was reported, the N Nutrition Index at silking ($NNI_{SILKING}$) was calculated ($n_2=66$).

No	Reference	Zero-N (Z_N)			Early-N (E_N)			Late-N (L_N)		
		PNU_{PM} kg ha ⁻¹	PNU_{SILK} kg ha ⁻¹	$NU_{Post-silking}$ %	PNU_{PM} kg ha ⁻¹	PNU_{SILK} kg ha ⁻¹	$NU_{Post-silking}$ %	PNU_{PM} kg ha ⁻¹	PNU_{SILK} kg ha ⁻¹	$NU_{Post-silking}$ %
1	Mueller et al., 2017	108.16 \pm 5.22	81.28 \pm 3.89	24.85 \pm 0.03	208.88 \pm 28.63	151.67 \pm 36.01	28.22 \pm 9.01	227.13 \pm 16.74	157.99 \pm 35.08	30.97 \pm 11.82
2 [†]	Randall et al., 1997	88.17 \pm 14.24	74.91 \pm 0.00	13.38 \pm 15.42	140.15 \pm 15.95	125.20 \pm 8.70	9.90 \pm 8.54	136.00 \pm 11.22	110.64 \pm 0.96	18.19 \pm 6.76
3* [†]	Yan et al., 2014	-	-	-	-	-	-	175.76 \pm 17.54	145.32 \pm 8.61	16.88 \pm 6.58
4 [†]	Yan et al., 2016	82.31 \pm 3.29	51.61 \pm 7.44	37.26 \pm 8.98	222.07 \pm 4.39	150.53 \pm 6.33	32.22 \pm 2.31	213.47 \pm 15.36	146.71 \pm 10.45	31.19 \pm 3.46
5 [†]	Corteva Agriscience, 2011	96.20 \pm 3.21	40.76 \pm 1.03	56.25 \pm 1.50	171.61 \pm 2.31	109.58 \pm 1.78	35.97 \pm 0.68	246.87 \pm 30.32	152.82 \pm 13.67	36.81 \pm 14.07

* Nitrogen accumulation values considered as silking were reported at tasseling (VT).

[†] Studies included in the $NNI_{SILKING}$ subset analysis.

Appendix B - Chapter 3 - Figures and tables

Table B.1. Grain yield (15.5% moisture), grain number, grain weight, harvest index, total plant N uptake at maturity, post-flowering N uptake, and LAI at maturity for 3394 and P1197 hybrids under Zero and Full N conditions during 2017 and 2018. Pairwise comparisons were performed only when the global test was significant for each factor evaluated.

Nitrogen	Hybrid	Grain yield Mg ha ⁻¹	Grain number grains m ⁻²	Grain weight mg grain ⁻¹	Harvest index Dimensionless	Total N uptake kg ha ⁻¹	Post-flowering N kg ha ⁻¹	LAI at R6 m m ⁻²
2017								
Zero N		6.8 (±0.9)	b 2719 (±215)	b 210 (±8.2)	b 0.42 (±0.02)	b 109 (±11.9)	b 46 (±9.0)	b 1.7 (±0.2)
Full N		13.1 (±0.7)	a 3980 (±161)	a 283 (±6.0)	a 0.51 (±0.01)	a 219 (±9.0)	a 81 (±7.0)	a 2.7 (±0.2)
	3394	9.0 (±0.8)	3059 (±198)	b 243 (±8.4)	0.45 (±0.02)	154 (±10.5)	52 (±8.8)	2.0 (±0.2)
	P1197	10.9 (±0.8)	3640 (±198)	a 251 (±5.6)	0.49 (±0.02)	174 (±10.5)	74 (±8.8)	2.4 (±0.2)
Zero N	3394	6.0 (±1.2)	2378 (±304)	208 (±13.5)	0.41 (±0.02)	99 (±16.2)	34 (±12.7)	1.5 (±0.3)
	P1197	7.5 (±1.2)	3060 (±304)	213 (±8.8)	0.44 (±0.02)	120 (±16.2)	57 (±12.7)	2.0 (±0.3)
Full N	3394	11.9 (±0.9)	3741 (±228)	277 (±9.6)	0.49 (±0.02)	209 (±11.9)	71 (±9.9)	2.5 (±0.2)
	P1197	14.3 (±0.9)	4220 (±228)	289 (±6.4)	0.53 (±0.02)	228 (±11.9)	91 (±9.9)	2.8 (±0.2)
ANOVA[†]								
Nitrogen (N)		***	***	***	***	***	***	**
Hybrid (H)		+	*	ns	ns	ns	+	+
N * H		ns	ns	ns	ns	ns	ns	ns
2018								
Zero N		2.9 (±0.8)	1988 (±350)	149 (±47.8)	0.27 (±0.04)	51 (±10.1)	13 (±17.3)	1.8 (±0.5)
Full N		15.1 (±0.9)	3904 (±354)	335 (±47.3)	0.49 (±0.04)	270 (±11.0)	61 (±16.7)	2.6 (±0.6)
	3394	8.3 (±0.7)	2661 (±243)	237 (±36.0)	0.37 (±0.03)	143 (±8.2)	31 (±13.5)	2.2 (±0.6)
	P1197	9.7 (±0.7)	3231 (±290)	247 (±35.0)	0.38 (±0.03)	178 (±8.2)	44 (±12.0)	2.1 (±0.8)
Zero N	3394	2.9 (±0.9)	1911 (±346)	154 (±51.5)	0.26 (±0.05)	51 (±10.7)	25 (±19.7)	1.9 (±0.5)
	P1197	2.9 (±0.9)	2064 (±404)	145 (±49.7)	0.27 (±0.05)	52 (±10.7)	2 (±18.0)	1.6 (±0.5)
Full N	3394	13.6 (±1.0)	b 3410 (±341)	b 321 (±50.2)	0.49 (±0.04)	236 (±12.3)	b 38 (±18.4)	b 2.5 (±0.6)
	P1197	16.6 (±1.0)	a 4398 (±416)	a 349 (±49.4)	0.49 (±0.04)	305 (±12.3)	a 85 (±17.4)	a 2.7 (±0.6)
ANOVA								
H		**	*	ns	ns	***	ns	ns
N * H		**	*	ns	ns	***	**	ns

Different letters indicate significant differences at $P \leq 0.05$

+ significant at $P \leq 0.1$; * significant at $P \leq 0.05$; ** significant at $P \leq 0.01$; *** significant at $P \leq 0.001$, ns: non-significant.

† The effect of N timing sub-treatments within N fertilization was fit but not reported for the purpose of this study.

Table B.2. Number of parameters (k) and AIC (Akaike's Information Criteria) values for linear and linear plateau models between grain yield, grain number, grain weight, and harvest index with total N uptake (Figures 2A to 2D). A lower score of AIC indicates a better fit (bold). Respectively for each variable and type of regression, model 1 and model 2 represent the best fit to the data based on a backward selection procedure for the number of coefficients.

Variable	Hybrid	k		AIC	
		Model 1: Simple linear model	Model 2: Linear-plateau model	Model 1: Simple linear model	Model 2: Linear-plateau model
Grain yield	3394	3	-	115.43	-
	P1197	3	4	124.47	114.54
Grain number	3394	3	-	452.21	-
	P1197	3	4	477.07	472.40
Grain weight	3394 – P1197	3	4	535.66	518.26
Harvest index	3394 – P1197	3	5	-148.31	-181.51

Hyphens (-) indicate models for which convergence was not achieved.

Appendix C - Chapter 4 - Figures and tables

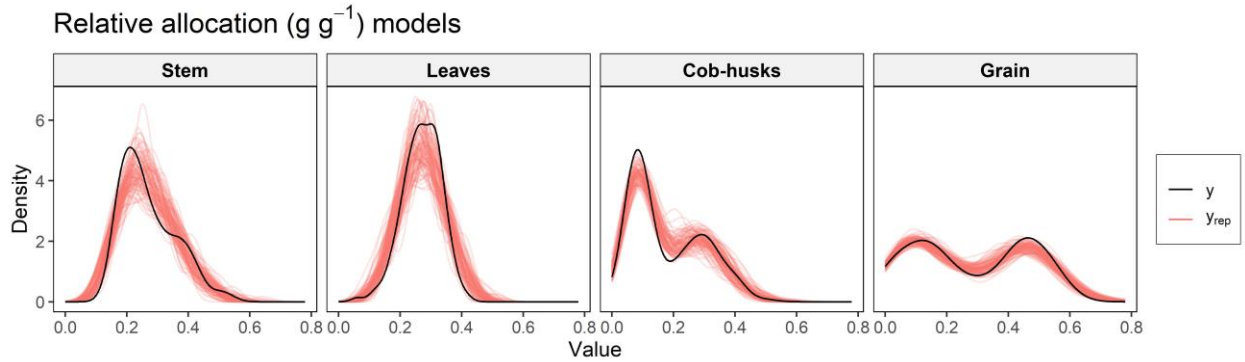


Figure C.1. Posterior predictive check for Bayesian model on the relative allocation of ^{15}N absorbed across plant organs.

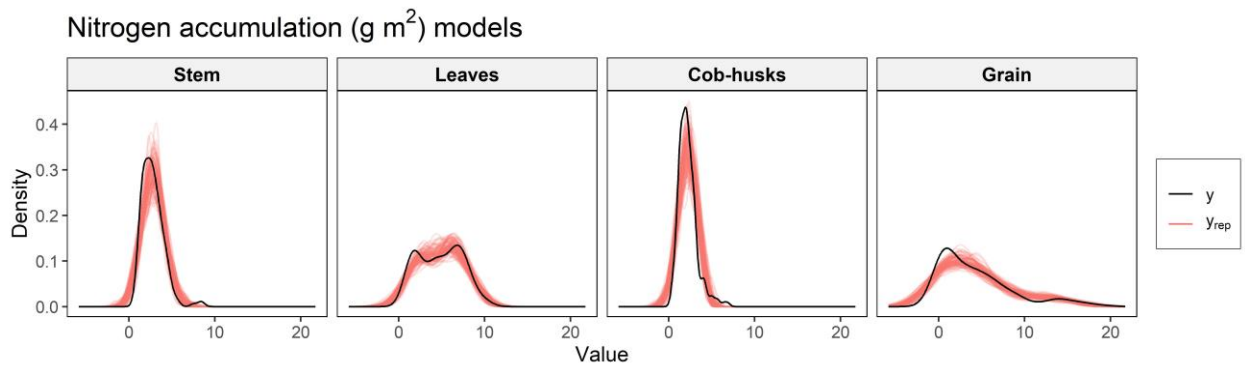


Figure C.2. Posterior predictive check for Bayesian models on stem, leaves, cob-husks, and grain N accumulation.

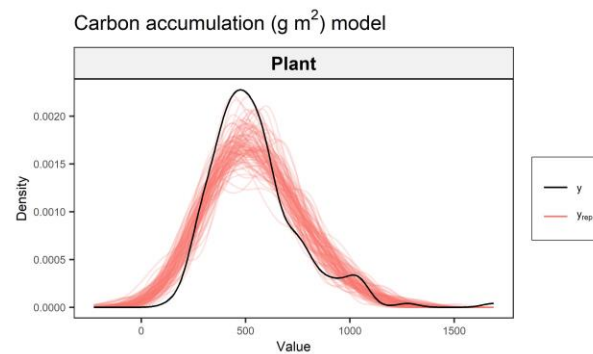


Figure C.3. Posterior predictive check for Bayesian model on plant C accumulation.

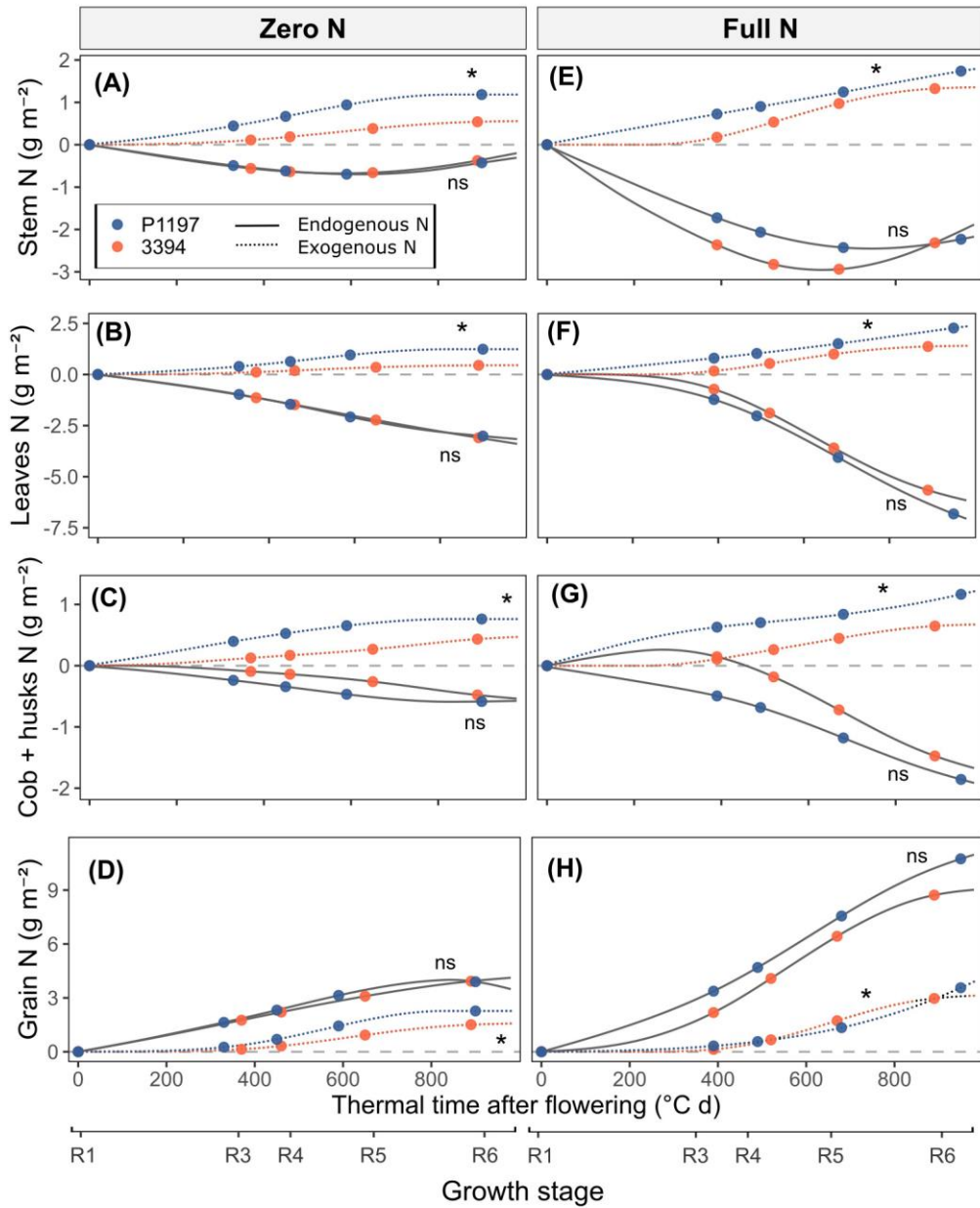


Figure C.4. Cumulative endogenous-N mobilized (solid lines) or exogenous-N absorbed (dashed lines) in stem, leaves, cob-husks, and grain fractions for 3394 (orange symbols) and P1197 (blue symbols) hybrids under zero and full N fertilization. Sections with black lines represent non-significant differences between hybrids, while colored lines and asterisks indicate significant differences ($\alpha=0.05$).

Appendix D - Chapter 5 - Figures and tables

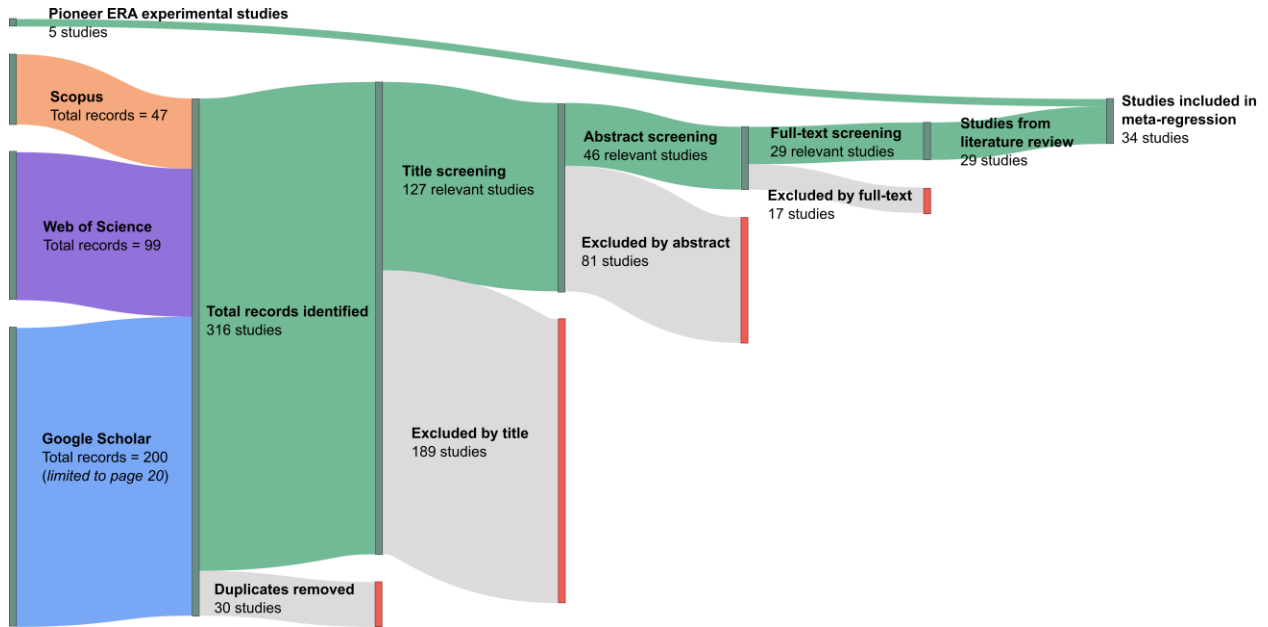


Figure D.1. Sankey diagram summarizing the literature review screening procedure. The width of each node represents the quantity of studies in the flow.

Table D.1. Publication number and reference, country, years of experiments, experimental design, range of years of hybrid release (YOR), management practices, and number of means obtained for the historical maize experiments used for the meta-regression analyses.

No	Reference	Country	Years	Design	Range of YOR	Water condition	Nitrogen rate (kg ha ⁻¹)	Planting density (pl m ⁻²)	Row spacing (m)	n
1	Abdala et al. (2018)	Argentina	2015-2016	RCBD	1965-2016	Rainfed	165	6, 10	0.52	32
2	Chazarreta et al. (2021)	Argentina	2016-2018	RCBD	1980-2016	Rainfed, irrigated	200	9	0.52, 0.7	18
3	Cirilo et al. (2011)	Argentina	2003-2005	Split-plot	1984-2000	Full irrigated	40-80, 140-180	7.5, 9	0.7	48
4	Echarte et al. (2000)	Argentina	1996-1998	Split-plot	1965-1993	Full irrigated	140-202	3, 5, 6, 8, 9, 11, 12, 14.5, 18	0.7	28
5	Echarte et al. (2003)	Argentina	1998-2000	Split-plot	1965-1993	Full irrigated	150	2, 4, 8, 16, 30	0.7	6
6	Echarte et al. (2006)	Argentina	1995-1996 2000-2001	RCBD Split-plot	1965-1993	Full irrigated	150	8.5	0.7	19
7	Luque et al. (2006)	Argentina	1996-1998	Split-plot	1965-1997	Full irrigated	222, 235	3, 6, 9, 12, 18	0.7	13
8	Nagore et al. (2017)	Argentina	2008-2013	Split-plot	1980-2004	Rainfed, partially irrigated, full irrigated	195	7.5	0.7	29
9	Parco et al. (2020)	Argentina	2015 - 2017	RCBD	1983-2012	Full irrigated	0, 270	4, 8	0.5	20
10	Sangoi et al. (2001)	Brazil	1998	Split-plot	1965-1995	Rainfed	0, 50, 100, 200	7.5	0.8	16
11	Sangoi et al. (2002)	Brazil	1999-2001	Split-plot	1975-1995	Full irrigated	110	2.5, 5, 7.5, 10	0.75	12
12	Vyn et al. (1998)	Canada	1987-1988	Split-plot	1959-1988	Rainfed	250	4, 8	0.5	18
13	Chen et al. (2013)	China	2010-2011	Split-plot	1973-2000	Rainfed	0-240	6	0.6	9
14	Chen et al. (2014)	China	2010-2011	RCBD	1989-2000	Rainfed	240	6	0.6	3
15	Ci et al. (2013)	China	2007-2009	Split-plot	1955-2005	Rainfed, irrigated	NA	1.5, 4.5, 7.5	0.6	18
16	Li et al. (2011)	China	2006-2009	Split-plot	1964-2004	Full irrigated	276	3.75, 5.25, 6.75	NA	36
17	Qian et al. (2016)	China	2009-2010	Split-split-plot	1975-2005	Rainfed	0, 150, 300, 450	3, 5.25, 7.5	NA	28
18	Sun et al. (2017)	China	2010-2011	Split-plot	1955-2005	Full irrigated, rainfed	NA	6.75	0.6	12
19	Adebo et al. (2010)	Nigeria	2005-2006	RCBD	1975-1995	Rainfed	80	2.7	0.75	6
20	Kamara et al. (2004)	Nigeria	2001-2002	RCBD	1970-1999	Rainfed	100	5.33	0.75	20
21	Mitrovic et al. (2016)	Serbia	2013-2014	RCBD	1978-2011	Rainfed	NA	5.8, 6.2, 6.5	0.75	5
22	Chen et al. (2016)	USA	2013-2014	Split-split-plot	1967-2005	Rainfed	55, 220	5.4, 7.9, 10.4	0.76	16
23	Mason et al. (2008)	USA	1999-2001	Split-plot	1950-1999	Rainfed, irrigated	246	5.56, 6.67	0.38, 0.76	8
24	Russell (1985)	USA	1982-1983	RCBD	1930-1985	Rainfed	180	5.17	0.76	7
25	Wu et al. (2019)	USA	2012	Split-split-plot	1975-2005	Rainfed	55, 220	5.4, 7.9, 10.4	0.76	3
26	Haegerle et al. (2013)	USA	2009-2010	Strip-plot	1975-2005	Rainfed	0, 67, 252	8.28	0.76	12
27	Mueller et al. (2019) ¹	USA	2016-2017	Split-plot	1946-2015	Rainfed	0, 220	7.85	0.76	7
28	DeBruin et al. (2017) ¹	USA	2013-2014	Split-plot	1934-2013	Rainfed	56, >224	3.95, 7.9	0.76	188
29	Campos et al (2004) ¹	Chile	2001-2002	RIBD	1953-2001	Full irrigated, rainfed	NA	8.5	NA	36
30	Fernandez, 2017 ¹	USA	2017	Split-plot	1991-2014	Rainfed	0, 137	6.1	0.76	9
31	Fernandez, 2017 ¹	USA	2017	Split-plot	1991-2014	Full irrigated	0, 218	7.6	0.76	9
32	Fernandez, 2018 ¹	USA	2018	Split-plot	1991-2014	Full irrigated	0, 218	7.6	0.76	14
33	Fernandez, 2019 ¹	USA	2019	Split-plot	1920-2017	Rainfed	220	6.52	0.76	60
34	Fernandez, 2019 ¹	Chile	2019-2020	Split-plot	1920-2017	Full irrigated	220	10	0.76	60

¹ Pioneer ERA hybrids were tested in the experiments.

Appendix E - Chapter 5 - References for the literature review

- Abdala, L. J., Vitantonio-Mazzini, L. N., Gerde, J. A., Martí Ribes, F., Murtagh, G., & Borrás, L. (2018). Dry milling grain quality changes in Argentinean maize genotypes released from 1965 to 2016. *Field Crops Research*, 226(April), 74–82. <https://doi.org/10.1016/j.fcr.2018.07.008>
- Adebo, F. A., & Olaoye, G. (2010). Growth indices and grain yield attributes in six maize cultivars representing two era of maize breeding in Nigeria. *Journal of Agricultural Science*, 2(3). <https://doi.org/10.5539/jas.v2n3p218>
- Campos, H., Cooper, M., Habben, J. E., Edmeades, G. O., & Schussler, J. R. (2004). Improving drought tolerance in maize: A view from industry. *Field Crops Research*, 90(1), 19–34. <https://doi.org/10.1016/j.fcr.2004.07.003>
- Chazarreta, Y. D., Amas, J. I., & Otegui, M. E. (2021). Kernel filling and desiccation in temperate maize: Breeding and environmental effects. *Field Crops Research*, 271(July). <https://doi.org/10.1016/j.fcr.2021.108243>
- Chen, K., Camberato, J. J., Tuinstra, M. R., Kumudini, S. V, Tollenaar, M., & Vyn, T. J. (2016). Genetic improvement in density and nitrogen stress tolerance traits over 38 years of commercial maize hybrid release. *Field Crops Research*, 196, 438–451. <https://doi.org/10.1016/j.fcr.2016.07.025>
- Chen, X., Chen, F., Chen, Y., Gao, Q., Yang, X., Yuan, L., Zhang, F., & Mi, G. (2013). Modern maize hybrids in Northeast China exhibit increased yield potential and resource use efficiency despite adverse climate change. *Global Change Biology*, 19(3), 923–936. <https://doi.org/10.1111/gcb.12093>
- Chen, Y., Xiao, C., Chen, X., Li, Q., Zhang, J., Chen, F., Yuan, L., & Mi, G. (2014). Characterization of the plant traits contributed to high grain yield and high grain nitrogen concentration in maize. *Field Crops Research*, 159, 1–9. <https://doi.org/10.1016/j.fcr.2014.01.002>
- Ci, X., Zhang, D., Li, X., Xu, J., Liang, X., Lu, Z., Bai, P., Ru, G., Bai, L., Hao, Z., Weng, J., Li, M., & Zhang, S. (2013). Trends in ear traits of chinese maize cultivars from the 1950s to the 2000s. *Agronomy Journal*, 105(1), 20–27. <https://doi.org/10.2134/agronj2012.0123>
- Cirilo, A. G., Actis, M., Andrade, F. H., & Valentinuz, O. R. (2011). Crop management affects dry-milling quality of flint maize kernels. *Field Crops Research*, 122(2), 140–150. <https://doi.org/10.1016/j.fcr.2011.03.007>
- DeBruin, J. L., Schussler, J. R., Mo, H., & Cooper, M. (2017). Grain yield and nitrogen accumulation in maize hybrids released during 1934 to 2013 in the US Midwest. *Crop Science*, 57(3), 1431–1446. <https://doi.org/10.2135/cropsci2016.08.0704>

- Echarte, L., & Andrade, F. H. (2003). Harvest index stability of Argentinean maize hybrids released between 1965 and 1993. *Field Crops Research*, 82(1), 1–12. [https://doi.org/10.1016/S0378-4290\(02\)00232-0](https://doi.org/10.1016/S0378-4290(02)00232-0)
- Echarte, L., Andrade, F. H., Sadras, V. O., & Abbate, P. (2006). Kernel weight and its response to source manipulations during grain filling in Argentinean maize hybrids released in different decades. *Field Crops Research*, 96(2–3), 307–312. <https://doi.org/10.1016/j.fcr.2005.07.013>
- Echarte, L., Luque, S., Andrade, F. H., Sadras, V. O., Cirilo, A., Otegui, M. E., & Vega, C. R. C. (2000). Response of maize kernel number to plant density in Argentinean hybrids released between 1965 and 1993. *Field Crops Research*, 68(1), 1–8. [https://doi.org/10.1016/S0378-4290\(00\)00101-5](https://doi.org/10.1016/S0378-4290(00)00101-5)
- Fernandez, J. A., & Ciampitti, I. A. (2018). Effect of late nitrogen applications on grain filling in corn. *Kansas Agricultural Experiment Station Research Reports*, 4(7). <https://doi.org/10.4148/2378-5977.7603>
- Fernandez, J. A., & Ciampitti, I. A. (2019). Effect of late nitrogen fertilization on grain yield and grain filling in corn. *Kansas Agricultural Experiment Station Research Reports*, 5(6). <https://doi.org/10.4148/2378-5977.7776>
- Fernandez, J. A., & Ciampitti, I. A. (2021). Corn grain weight: dependence upon nitrogen supply and source-sink relations. *Kansas Agricultural Experiment Station Research Reports*, 7(5). <https://doi.org/10.4148/2378-5977.8073>
- Haegerle, J. W., Cook, K. A., Nichols, D. M., & Below, F. E. (2013). Changes in nitrogen use traits associated with genetic improvement for grain yield of maize hybrids released in different decades. *Crop Science*, 53(4), 1256–1268. <https://doi.org/10.2135/cropsci2012.07.0429>
- Kamara, A. Y., Menkir, A., Fakorede, M. A. B., Ajala, S. O., Badu-Apraku, B., & Kureh, I. (2004). Agronomic performance of maize cultivars representing three decades of breeding in the Guinea Savannas of West and Central Africa. *Journal of Agricultural Science*, 142(5), 567–575. <https://doi.org/10.1017/S0021859604004575>
- Li, Y., Ma, X., Wang, T., Li, Y., Liu, C., Liu, Z., Sun, B., Shi, Y., Song, Y., Carlone, M., Bubeck, D., Bhardwaj, H., Whitaker, D., Wilson, W., Jones, E., Wright, K., Sun, S., Niebur, W., & Smith, S. (2011). Increasing maize productivity in China by planting hybrids with germplasm that responds favorably to higher planting densities. *Crop Science*, 51(6), 2391–2400. <https://doi.org/10.2135/cropsci2011.03.0148>
- Luque, S. F., Cirilo, A. G., & Otegui, M. E. (2006). Genetic gains in grain yield and related physiological attributes in Argentine maize hybrids. *Field Crops Research*, 95(2–3), 383–397. <https://doi.org/10.1016/j.fcr.2005.04.007>

- Mason, S. C., Kathol, D., Eskridge, K. M., & Galusha, T. D. (2008). Yield increase has been more rapid for maize than for grain sorghum. *Crop Science*, 48(4), 1560–1568. <https://doi.org/10.2135/cropsci2007.09.0529>
- Mitrović, B., Stojaković, M., Zorić, M., Stanisavljević, D., Bekavac, G., Nastasić, A., & Mladenov, V. (2016). Genetic gains in grain yield, morphological traits and yield stability of middle-late maize hybrids released in Serbia between 1978 and 2011. *Euphytica*, 211(3), 321–330. <https://doi.org/10.1007/s10681-016-1739-6>
- Nagore, M. L., Della Maggiora, A., Andrade, F. H., & Echarte, L. (2017). Water use efficiency for grain yield in an old and two more recent maize hybrids. *Field Crops Research*, 214(June), 185–193. <https://doi.org/10.1016/j.fcr.2017.09.013>
- Parco, M., Ciampitti, I. A., D'Andrea, K. E., & Maddonni, G. Á. (2020). Prolificacy and nitrogen internal efficiency in maize crops. *Field Crops Research*, 256(June). <https://doi.org/10.1016/j.fcr.2020.107912>
- Qian, C., Yu, Y., Gong, X., Jiang, Y., Zhao, Y., Yang, Z., Hao, Y., Li, L., Song, Z., & Zhang, W. (2016). Response of grain yield to plant density and nitrogen rate in spring maize hybrids released from 1970 to 2010 in Northeast China. *Crop Journal*, 4(6), 459–467. <https://doi.org/10.1016/j.cj.2016.04.004>
- Russell, W. A. (1985). Evaluations for plant, ear, and grain traits of maize cultivars representing seven eras of breeding. *Maydica*, 30(1), 85–96.
- Sangoi, L., Gracietti, M. A., Rampazzo, C., & Bianchetti, P. (2002). Response of Brazilian maize hybrids from different eras to changes in plant density. *Field Crops Research*, 79(1), 39–51. [https://doi.org/10.1016/S0378-4290\(02\)00124-7](https://doi.org/10.1016/S0378-4290(02)00124-7)
- Sangoi, Luis, Ender, M., Guidolin, A. F., De Almeida, M. L., & Konflanz, V. A. (2001). Nitrogen fertilization impact on agronomic traits of maize hybrids released at different decades. *Pesquisa Agropecuaria Brasileira*, 36(5), 757–764. <https://doi.org/10.1590/S0100-204X2001000500005>
- Sun, Q., Liang, X., Zhang, D., Li, X., Hao, Z., Weng, J., Li, M., & Zhang, S. (2017). Trends in drought tolerance in Chinese maize cultivars from the 1950s to the 2000s. *Field Crops Research*, 201, 175–183. <https://doi.org/10.1016/j.fcr.2016.10.018>
- Vyn, T. J., & Tollenaar, M. (1998). Changes in chemical and physical quality parameters of maize grain during three decades of yield improvement. *Field Crops Research*, 59(2), 135–140. [https://doi.org/10.1016/S0378-4290\(98\)00114-2](https://doi.org/10.1016/S0378-4290(98)00114-2)